Technische Universität München
TUM School of Natural Sciences

A Novel Process for Rare Earth Metal Extraction from Kaolin by Elution and Biosorption

Max Koch

Vollständiger Abdruck der von der TUM School of Natural Sciences der Technischen Universität München zur Erlangung eines

Doktors der Naturwissenschaften (Dr. rer. nat.)

genehmigten Dissertation.

Vorsitz		Prof. Dr. Klaus Köhler
Prüfer der Dissertation	1.	Prof. Dr. Tom Nilges
	2.	Prof. Dr. Thomas Brück

Die Dissertation wurde am 22.05.2024 bei der Technischen Universität München eingereicht und durch die TUM School of Natural Sciences am 21.06.2024 angenommen.

"**Science may set limits to knowledge, but should not set limits to imagination.**"

- Bertrand Russell -

Danksagung

Ich möchte meine aufrichtige Dankbarkeit gegenüber all jenen zum Ausdruck bringen, die mich während meiner Promotion mit großer Unterstützung begleitet haben.

Mein herzlicher Dank gilt Prof. Dr. Tom Nilges, der mir die einzigartige Gelegenheit gab, meine Promotion unter seiner Leitung durchzuführen. Ich danke Ihm für jede hilfreiche Unterstützung, da er sich stets Zeit genommen hat, um mir bei Problemen und offenen Fragen beizustehen. Sein Vertrauen in mich und seiner steigen Hilfestellung haben meinen akademischen Fortschritt entscheidend beeinflusst, wofür ich ihm sehr dankbar bin.

Weiterhin danke ich Prof. Dr. Thomas Brück für die tolle Kooperation im gemeinsamen Projekt MiKa und für die wissenschaftliche Betreuung als Zweitgutachter herzlich.

Außerdem möchte ich Dr. Janio Venturini meinen Dank für seine fachliche und anregende Diskussionen sowie für seine persönliche Unterstützung aussprechen.

Ein spezieller Dank gebührt Dr. Michael Paper, mit dem ich über drei Jahre hinweg im Rahmen des Projekts MiKa zusammengearbeitet habe. Unsere Zusammenarbeit war stets unkompliziert, äußerst produktiv und von einer freundlichen Atmosphäre geprägt.

Ein herzliches Dankeschön geht an die aktuellen und ehemaligen Kollegen meiner Arbeitsgruppe, deren Freundschaft und gemeinsame Erlebnisse außerhalb der Universität meine Zeit hier besonders bereichert haben.

Besonderer Dank gilt meiner Familie und meinen Freunden, die mich immer in meinem Leben motiviert und unterstützt haben. Ohne eure Unterstützung wäre ich nicht da, wo ich mich heute befinde.

Zu guter Letzt möchte ich meiner Freundin, Marie Sandvoß, meinen größten Dank aussprechen für ihre bedingungslose Liebe, ihr Verständnis und ihre unermüdliche Unterstützung in allen Lebenslagen.

Abstract

This study is a part of a project ForCycle II – MiKa funded by the Bavarian State Ministry of the Environment and Consumer Protection, where Prof. Brück and Prof. Nilges participate in collaboration. The aim of this project is to develop a combined method of inorganic and microalgae-based processes for the extraction of Rare Earth Elements (REE) from the residual kaolinite (RK) minerals. Various RKs, which belong to the phyllosilicates, obtained from different stages of kaolin production at the mining company Amberger Kaolinwerke are evaluated for their REE content. X-ray diffraction (XRD) analysis elucidates the mineral composition of the studied materials, revealing the presence of feldspar, quartz, and predominantly kaolinite phases. The first part of this study (chapter 3.1) investigates the chemical mobilization (elution) in an ion exchange mechanism of adsorbed metal ions in RK by commonly used acids (hydrochloric, sulfuric, and nitric acids) and highlights the potential importance of recycling REE through an elution process from waste soil minerals. To improve the environmental impact, the elution process is carried out under the mildest conditions possible. The ion exchange procedure for the extraction of REE can be accelerated and the availability of adsorbed metal ions improved using a microwave in a closed system. This wet chemical availability is influenced by many factors, such as acid concentrations, temperature, reaction time, pH, etc., which are further explored in this study. Optical emission spectroscopy with inductive plasma (ICP-OES) is an established quantification method used in this study for the determination of trace elements. Given the scarcity of Rare Earth raw materials, such recycling mechanisms could play a pivotal role in future high-tech applications. At lower acid concentrations, phyllosilicates exhibit a reduced recovery of metal ions compared to concentrated acids. In further experiments, the optimization of elution experiments in diluted acids by multiple elutions is performed to increase the metal concentration, especially REE. Additionally, the experiments are extended into the subject area of biosorption, specifically the interaction with cyanobacterial biomass. The conditions that pose challenges to metal adsorption on biomass are adapted and expanded through the implementation of a semi-continuous elution process. This adaptation enhances our understanding of the complexities involved in metal-biosorption interactions and contributes valuable insights for future applications in environmental and technological contexts.
The second part of our study (chapter 3.2) is conducted in collaboration with the chair of Prof. Brück. This study provides insights into metal uptake mechanisms on tested strains and suggests the potential use of cyanobacteria in future microalgae-based processes for recovering REE from residual streams. In this part we investigate the adsorption properties of twelve cyanobacterial strains. In an adsorption process,

their potential is determined to what extent Rare Earth Elements are enriched on this cyanobacterial biomass. The examined cyanobacterial strains have a significant level of genetic diversity, according to a biogenetic investigation. In a screening process for the maximum adsorption capacity for lanthanum, cerium, neodymium, and terbium, five promising algae strains are identified. The aim is to investigate how the variations in pH, metal concentration, and incubation affect the adsorption properties. The adsorption experiments show different affinities of the biomasses for certain metals, e.g., lead with higher affinity than cerium, and indicate an ion exchange mechanism at the surface of the biomass. The metal uptake at the biomass reaches the adsorption capacity after only a few minutes. In chapter 3.3 the further metal adsorption properties of the biomass, which are influenced by varying the growth parameters during biomass production, are investigated in this study. Under nitrogen-limited environmental conditions, the biomass production of extracellular polymeric substances (EPS) is stimulated. In terms of REE adsorption capacity, the isolated EPS outperform the intact biomass, demonstrating the important potential of EPS in metal absorption. Therefore, EPS can be considered as promising biosorbents for the recovery of REE-containing wastewater.

Zusammenfassung

Diese Studie ist Teil des vom Bayerischen Staatsministerium für Umwelt und Verbraucherschutz geförderten Projekts ForCycle II - MiKa, an dem Prof. Brück und Prof. Nilges mitarbeiten. Das Ziel dieses Projektes ist die Entwicklung eines kombinierten Verfahrens aus anorganischen und mikroalgenbasierten Prozessen zur Gewinnung von Seltenen Erden (engl. REE) aus den Rückständen der Kaolinitmineralien (RK). Verschiedene RKs, die zu den Schichtsilikaten gehören und aus verschiedenen Stufen der Kaolinproduktion bei den Amberger Kaolinwerken stammen, werden auf ihren REE-Gehalt untersucht. Die Röntgenbeugungsanalyse (engl. XRD) gibt Aufschluss über die mineralische Zusammensetzung der untersuchten Materialien und zeigt, dass sie aus Feldspat-, Quarz- und überwiegend Kaolinitphasen bestehen. Der erste Teil dieser Studie (Kapitel 3.1) untersucht die chemische Mobilisierung (Elution) in einem Ionenaustauschmechanismus von adsorbierten Metallionen in RK durch gängige Säuren (Salz-, Schwefel- und Salpetersäure) und unterstreicht die potenzielle Bedeutung des Recyclings von REE durch einen Elutionsprozess aus Abfalltonmineralien. Um die Umweltverträglichkeit zu verbessern, wird der Elutionsprozess unter möglichst milden Bedingungen durchgeführt. Das Ionenaustauschverfahren für die REE-Extraktion kann beschleunigt und die Verfügbarkeit der adsorbierten Metallionen durch den Einsatz einer Mikrowelle in einem geschlossenen System verbessert werden. Diese nasschemische Verfügbarkeit wird von vielen Faktoren beeinflusst, wie z. B. Säurekonzentration, Temperatur, Reaktionszeit, pH-Wert usw., die in dieser Studie näher untersucht werden. Die optische Emissionsspektroskopie mit induktivem Plasma (ICP-OES) ist eine etablierte Quantifizierungsmethode, die in dieser Studie für die Bestimmung von Spurenelementen verwendet wird. In Anbetracht der Knappheit von einigen Seltenen Erden könnten derartige Recyclingmechanismen zur Verfügbarmachung von REE und Anwendung in High-Tech-Prozessen eine entscheidende Rolle spielen. Bei niedrigeren Säurekonzentrationen weisen Schichtsilikate im Vergleich zu konzentrierten Säuren eine geringere Rückgewinnung von Metallionen auf. In weiteren Experimenten wird die Optimierung von Elutionsversuchen in verdünnten Säuren durch Mehrfachelutionen durchgeführt, um die Metallkonzentration, insbesondere der REE, zu erhöhen. Darüber hinaus werden die Experimente auf den Themenbereich der Biosorption ausgeweitet, insbesondere auf die Interaktion mit cyanobakterieller Biomasse. Die Bedingungen, die eine Herausforderung für die Metalladsorption an Biomasse darstellen, werden angepasst und durch die Implementierung eines semi-kontinuierlichen Elutionsprozesses erweitert. Diese Anpassung verbessert unser Verständnis für die Komplexität der Wechselwirkungen zwischen Metall und Biosorption und liefert wertvolle Erkenntnisse für künftige Anwendungen in Umwelt und Technik.

Der zweite Teil unserer Studie (Kapitel 3.2) wird in Zusammenarbeit mit dem Lehrstuhl von Prof. Brück durchgeführt. Diese Studie bietet Einblicke in die Mechanismen der Metallaufnahme durch die getesteten Stämme und deutet auf den potenziellen Einsatz von Cyanobakterien in künftigen mikroalgenbasierten Verfahren zur Rückgewinnung von Seltenen Erden aus Restströmen hin. In diesem Teil untersuchen wir die Adsorptionseigenschaften von zwölf Cyanobakterienstämmen. In einem Adsorptionsprozess wird deren Potenzial ermittelt, in welchem Maß Seltene Erdelemente an dieser cyanobakteriellen Biomassen angereichert werden. Eine biogenetische Analyse zeigt eine hohe genetische Vielfalt innerhalb dieser untersuchten Bakterienstämmen auf. In einem Screening-Verfahren auf die maximale Adsorptionskapazität für Lanthan, Cer, Neodym und Terbium wurden fünf aussichtsreiche Algenstämme identifiziert. Das Ziel ist es, zu untersuchen, wie sich die Variationen des pH-Werts, der Metallkonzentration und der Inkubation auf die Adsorptionseigenschaften auswirken. Die Adsorptionsversuche zeigen unterschiedliche Affinitäten der Biomassen für bestimmte Metalle, z.B. Blei höhere Affinität als Cer, und deuten auf einen Ionenaustauschmechanismus an der Oberfläche der Biomasse hin. Die Metallaufnahme an der Biomasse erreicht die Adsorptionskapazitätsgrenze bereits nach wenigen Minuten. In Kapitel 3.3 werden die weiteren Metalladsorptionseigenschaften der Biomasse, die durch die Variation der Wachstumsparameter während der Biomasseproduktion beeinflusst werden, in dieser Studie untersucht. Unter stickstofflimitierten Umweltbedingungen wird die Biomasseproduktion von extrazellulären polymeren Substanzen (EPS) angeregt. In Bezug auf die REE-Adsorptionskapazität übertreffen die isolierten EPS die intakte Biomasse, was das wichtige Potenzial der EPS bei der Metallabsorption zeigt. Daher können EPS als vielversprechende Biosorbentien für die Rückgewinnung von REE-haltigen Abwässern betrachtet werden.

Abbreviations

Å	Angstrom
AKW	Amberger Kaolinwerke
cm	centimeter
DI-H_2O	deionized water
DIC	differential interference contrast
EDTA	ethylenediaminetetraacetic acid
EPS	extracellular polymeric substances
eV	electronvolt
FT-IR	Fourier-transform infrared spectroscopy
h	hour
HREE	Heavy Rare Earth Elements
HPLC	high-performance liquid chromatography
HSAB	hard and soft acids and bases
ICP	inductively coupled plasma
ICP-OES	inductively coupled plasma optical emission spectroscopy
kV	kilovolt
L	liter
LTE	local thermal equilibrium
LREE	Light Rare Earth Elements
M	molar
mg	milligram
MΩ	megaohm
μg	microgram
nm	nanometer

OES	optical emission spectroscopy
REE	Rare Earth Elements
REO	Rare Earth Oxides
RF	radio frequency
RK	residual kaolinites
rpm	revolutions per minute
RT	room temperature
rRNA	ribosomal ribonucleic acid
sec	second
SEM	scanning electron microscopy
t	tons
UV	ultraviolet
W	watt
XRD	X-ray diffraction
XRF	X-ray fluorescence
°C	degree Celsius

Contents

1 Introduction

Rare Earth Elements (REE) are of great importance to the industrial branch in the 21st century, as they are used in many technical applications. There are few deposits worldwide that have profitable deposits. Most REE are mined in China. The extraction of this raw material is costly, environmentally damaging, dangerous, and involves high energy consumption. For this reason, great efforts are being made to find new REE sources and alternative REE extraction processes. The phyllosilicates are frequently encountered minerals and are discussed later in this study due to their high adsorption capacity. As a result of weathering, the various metals can be washed up and absorbed in the interlayer space. Developing a more sustainable REE extraction process from these minerals may prove profitable.
This study investigated the extraction of REE from kaolinite, a phyllosilicate, in more detail by combining an inorganic and microbiological process.

1.1 Rare Earth Elements

The primary focus of this thesis was the investigation of the elution process for the recovery of Rare Earth Elements from residual minerals generated during kaolin production. The subsequent utilization of cyanobacterial biomass for the Rare Earth-containing eluates obtained through the elution process is intended to complete the recycling procedure. An approach was to enhance this recycling procedure with a biosorption process. REE consist of 14+3 metal elements, which are categorized into two groups: Light Rare Earth Elements (LREE) (lanthanum, cerium, praseodymium, neodymium, samarium, and europium), and Heavy Rare Earth Elements (HREE) (gadolinium, terbium, dysprosium, holmium, erbium, lutetium, scandium, thulium, ytterbium, and yttrium).[1] The elements scandium, yttrium, and lanthanum are not conventional Rare Earth Metals because they do not possess filled f-orbitals, but they are included due to their chemical properties.[2] The nomenclature "Rare Earths" originated from historical perspectives on the scarcity of these elements. However, this statement is misleading, as some metals in this group are not rare at all. The Rare Earth Metals lanthanum, cerium, praseodymium, and neodymium are the most abundant; their elemental abundance in the upper continental crust is respectively $30\,\mu g\,g^{-1}$, $64\,\mu g\,g^{-1}$, $7\,\mu g\,g^{-1}$, and $26\,\mu g\,g^{-1}$.[3] For example, cerium occurs as frequently as copper and nickel.[4] The heavy lanthanides, such as terbium and lutetium, are indeed Rare Earth Elements with a proportion of $0.64\,\mu g\,g^{-1}$ and $0.32\,\mu g\,g^{-1}$.[3]

Chemical properties and applications

Rare Earth Elements exhibit almost identical chemical properties, with the exception that light and heavy lanthanides react notably differently to air.[1] The oxidation rate of light lanthanides is much faster than that of heavy lanthanides. This effect occurs due to the variation of the oxide product formed.[5] Most REE are strongly electropositive, reactive, and preferably in the oxidation state +3,[6, 7] though there are certain exceptions, like cerium or europium, which exist in oxidation states +4 or +2. In comparison to the 3d-transition metals, 4f-valence electrons are added to 14 lanthanide elements, which gradually fill up. In the shell model, the electrons of the 6s orbital constitute the outer orbit and thus shield the f-orbitals. The 4f-orbitals, which are shielded by the outer 6s- and 5d-orbitals, are not relevant for the chemical reactivity, but they have a decisive influence on the electromagnetic and optical properties.[8] These properties have enormous significance in the application of REE in modern high-tech applications,[9, 10] designating them as critical resources. Another effect of shielding is that the f-orbitals are predominantly protected from external interference fields, such as demagnetization by strongly ferromagnetic alloys.[8] According to the Hard and Soft Acids and Bases (HSAB) concept, the REE belong to the category of hard Lewis acids, characterized by a high charge and a small ionic radius, or a large charge/radius ratio. The consistent decrease in atomic radii across the lanthanide series, known as lanthanide contraction, is attributed to the increasing occupation of the 4f-valence orbitals from La to Lu.[11] As a result of the shielding of these orbitals, interactions with surrounding orbitals of other components are limited, leading to the absence of covalent bonds in the usually stable oxidation states of REE. Accordingly, the lanthanides typically exhibit an ionic chemical bonding behaviour.[12] Other specific features of REE are their spectroscopic and magnetic properties caused by the unique configuration of their 4f-valence electrons. These characteristics have many applications in the high-tech industry. For example, neodymium is the strongest permanent magnet and is utilized in wind turbines, electric motors, and medical magnetic resonance imaging scanners.[1, 13] Cerium compounds are used in catalytic converters of motor vehicles, for catalytic reactions and as fuel additives.[14] Europium and terbium are required as luminescent materials for the production of display screens.[15, 16] The oxides of lanthanum exhibit a high refractive index and low dispersion, which are well-suited for use in optical devices such as cameras, spectacles, and telescopes.[17] Lanthanum can also be used as a component of electrode materials for or solid oxide fuel or electrolysis cells.[18]

Rare Earth Element production

Lanthanide ore deposits are widespread around the world. However, only a minority of deposits have sufficiently high concentrations for economically profitable extraction of REE. A deposit is typically considered economically viable if it contains a REE concentration of 0.05 – 0.2 wt.% in the raw mineral.[19] Production of REE is inherently costly due to the energy-intensive and complex processing required, compounded by the low concentration in ore deposits. Therefore, REE are predominantly obtained as secondary products from the extraction of other raw materials. For nearly two decades, China held a monopoly on Rare Earths. After China reduced the export limit for REE in 2010,[20] a rapid price increase developed for the industry's essential Rare Earth Metals. Since then, extensive research has been carried out worldwide on REE production to achieve political and economic independence. The importance of REE was illustrated by the European Commission's decision in 2020 to list REE as critical resources.[21] The 2022 reports showed that annual REE-production reached about 300,000 t.[22] China, particularly Bayan Obo - the country's largest deposit,[19] was the world's top producer in 2022 with 210,000 t of Rare Earth Oxides (REOs), which currently accounts for 60-70% of total global REE-production.[22] After mining the ore deposits containing Rare Earths, the industrial purification of REE faces more complex, costly, and energy-intensive challenges due to their comparable physical and chemical properties. A common method for separating REE from the mineral concentrates is chemical leaching.[23] Industrially, Rare Earths are extracted from ores in a multi-stage and complex separation process, including fractional crystallization,[24] ion exchange,[25, 26] solvent extraction,[27, 28] and electro-refining.[29, 30] A solvent-based process, in particular solvent extraction, prevails as the dominant method for the extraction of lanthanide elements.[31]

Environmental issues and toxicity

Critical loads are defined as ecological effect tolerances that describe the sensitivity of the ecosystem to the eutrophying and acidifying deposition of precipitation.[32] These are harmful exposure limits of hazardous heavy metals, such as cadmium, mercury, or lead in air, water, soil, posing risks for the environment if the values are exceeded. Elevated concentrations of these pollutants can lead to adverse effects on human health and other living organisms.[33] Therefore, there is a necessity to remove the toxic heavy metals from industrial wastewater to mitigate negative impacts on ecosystems. This issue of toxic effects on the ecosystem has been extensively studied.[34, 35, 36] In contrast, there is limited scientific data on the potential ecological effect of Rare Earth Metals. Historically, there was no need to research this effect because Rare Earth Elements usually

only appeared in low concentrations. However, with the increasing demand for REE in high-tech products and processes over the last decade, the amount of REE released into the environment during the mining process has greatly increased.[37, 38] Considering that Rare Earths can be used in agriculture as feed additives and in medicine as radiocontrast agents, it further exacerbates the case.[39, 40, 41] The environment's accumulation of REE might have a detrimental effect on plant life, affecting plant growth, and can have adverse effects on human health.[42, 43, 44] The recovery of REE from industrial wastewater has environmental and economic incentives.[45] Unfortunately, existing industrial wastewater treatment systems are not designed to effectively remove REE from wastewater. Accordingly, the efficiency of the recovery process of REE from wastewater is considerably low.[46] Recent studies show that the selective separation of lanthanides from wastewater is viable with nanofiltration,[47, 48] but its application on an industrial scale is hindered by the high cost and maintenance of membranes and limitations in membrane pore size. Another way to optimize the recycling process for REE involves the use of cyanobacteria, which can selectively adsorb heavy metals from the aqueous medium.[49]

Minerals in earth's crust

The earth's crust, which forms the outermost shell of the earth, is predominantly comprised of oxygen, silicon, and aluminum. Other elements occur only in smaller quantities or even in trace amounts. The accessible layer of the earth's crust is composed of silicate-containing minerals, such as olivines, pyroxenes, amphiboles, mica, feldspars, quartz, and zeolites. These naturally occurring minerals take on different structural types due to their diversity of anionic compounds and the variability of the cationic compound part (see Table 1). This study investigated the mineral kaolinite, which belongs to the frequently occurring phyllosicates.

Table 1: Silicate classes and building units of occurring minerals.[2]

Class	**Building unit**
Nesosilicate	$[SiO_4]^{4-}$
Sorosilicate	$[Si_2O_7]^{6-}$
Cyclosilicate	$[SiO_3]_n^{2-}$ (n= 3, 4, 6, 8)
Single and double chain inosilicate	$[SiO_3]_x^{2-}/[Si_4O_{11}]_x^{6-}$
Phyllosilicate	$[Si_2O_5]^{2-}$
Tectosilicate	$[AlySi_{1-y}O_2]_x^{y-}$

The properties of the aluminosilicates are significantly influenced by the structure of the anionic framework.[2] Accordingly, the chain and band-type silicates exhibit good cleavage of the structure perpendicular to the propagation direction of the chains and bands. The layered silicates have easy cleavage across the layered structure, whereas the acyclic, cyclic, and framework silicates form compact units. The adsorption capacity of the phyllosilicates, such as the mineral kaolinite, is also based on the anisotropic structural features, which enables the storage of elements, such as REE, between the layers.[2]

1.2 Kaolinite

Kaolinite is a layered silicate belonging to the phyllosilicate group. This mineral consists of an octahedral alumina layer (A) and a tetrahedral silica layer (S) (ratio 1:1) by sharing a layer of oxygen atoms (Figure 1).[50, 51] This structure exposes the silica/oxygen and alumina/hydroxyl layers, which interact with various soil components.[52] The layer sequence of kaolinite follows the following pattern: ASAS.[53]

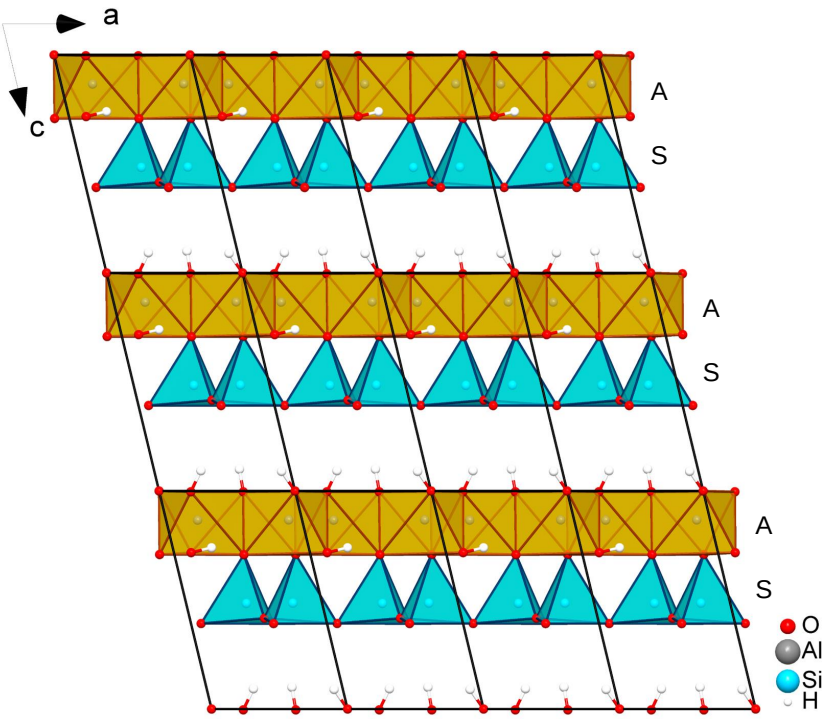

Figure 1: Crystal structure of kaolinite consists of an alumina octahedral sheet (A) and a silica tetrahedral sheet (S).[54]

Miranda et al. showed in their study that the hydroxyl groups of the alumina hydroxyl layer occur on the outside of the surface of the alumina sheet and on the inside between the layers.[52] More specifically, the outer hydroxyl groups are located along the

non-shared plane of the alumina hydroxyl layer, while the inner hydroxyl groups are found along the shared plane of the alumina hydroxyl and silicon oxide layers. Since both layers are connected via an oxygen atom, the libration of the inner hydroxyl group through the chemical bonding is limited.[52, 55]
Kaolinite is widely used around the world and serves as an important raw material in various applications. Due to its unique properties, such as particle size, chemical stability, white color, and crystal structure, kaolinite is extensively utilized in the production of ceramics, porcelain and paper.[56, 57] Beyond industrial applications, it is also used in pharmaceuticals, cosmetics, and even as an additive in the manufacturing of rubber.[58, 59, 60] Kaolinite's wide range of applications underscores its importance for daily goods and industrial processes.

Ion exchange in minerals

Ion exchange refers to a process where lower-valence cations are replaced by higher-valence cations, for example Al^{3+} displaces Ca^{2+}. The exchange of metal ions depends on the attraction of the clay minerals, specifically the selective adsorption.[61] Therefore, the larger alkali metals displace the smaller ions of the same group in the periodic table due to a higher attraction on the mineral. The following order of extraction efficiency can be defined for the exchangeability of cations:[62]

$$Ba^{2+} > Sr^{2+} > Ca^{2+} > Mg^{2+} > Cs^{+} > Rb^{+} > K^{+} > Na^{+} > Li^{+}$$

Ion exchange on clay minerals is dependent on both the crystal structure of the mineral and the chemical composition of the medium migrating into the intermediate layers of the mineral. In general, the ion exchange in minerals is in a reversible equilibrium, where lower-valence cations in excess also displace higher-valence cations.
In the crystal structure of kaolinite, the isomorphous substitution of cations, i.e. Al^{3+} for Si^{4+}, results in permanent negatively charged layers capable of adsorbing a cation from the interactive medium.[61] This dynamic process plays a fundamental role in the chemical behavior of clay minerals and contributes to their ion exchange capabilities.

1.3 Elution

Elution is a crucial process in various industrial and scientific fields, particularly referring to the process of extracting or leaching the adsorbed components from the stationary phase. The mobile phase is a solvent that passes through the stationary phase, carrying the sample component with it. In the elution process, adsorbed metal ions are extracted from a material, e.g., minerals, by using a solvent (eluent).[63] In this process, positively charged ions situated at negatively charged sites in the mineral are washed out through an ion exchange mechanism.

Elution process

In the elution process, the mineral containing various metals is treated with a mineral acid, which is used as an elution medium. This process can be conducted in a column, a beaker, or even an industrial microwave.[64, 65, 66, 67] Depending on the type or concentration of the medium, metals are eluted to varying extents. After the elution process, the metal-containing eluate is separated from the solid mineral waste. Suitable methods for separation include filtration, sedimentation, or centrifugation.[68] A change in pH induces the precipitation of dissolved metals at different pH values, which allows the separation of the eluted metals. The stability of a metal ion/solvent is described with a Pourbaix-diagram.[69] The recovery of eluted species, for example, REE, from metal-containing eluates holds significant economic value. This result might be achieved by a microalgae-based adsorption process as one prominent solution to the problem.[70]

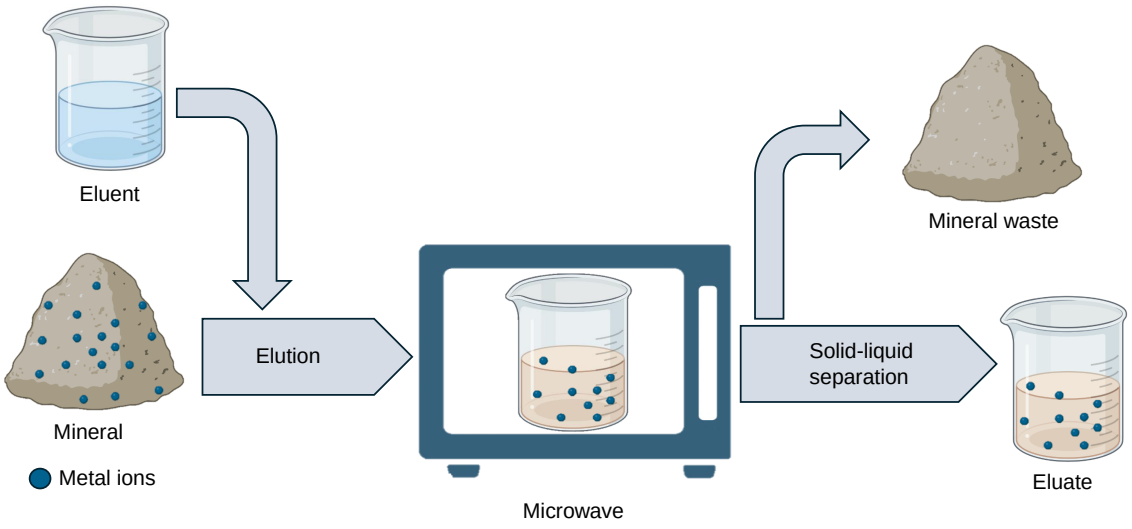

Figure 2: Schematic illustration of an elution process for extracting metal ions from the mineral; the icons were taken from BioRender.com.

REE are commonly extracted from ores in mineral processing using a variety of recovery processes including solvent extraction, ion exchange, and leaching. Elution particularly describes the process of desorbing or stripping metal ions from their solid matrix. In order to achieve this, an appropriate eluting agent — typically acids or complexing agents — is usually added., disrupting the electrostatic bonds between the REE ions and the mineral framework. There are numerous studies on related elution processes that enable the extraction of Rare Earth Metals from minerals.[71, 72, 73] In this work,

a microwave elution technique was employed to extract REE from a kaolin material (Figure 2). The efficiency and selectivity of REE recovery are significantly impacted by the utilized elution conditions. Following elution, additional separation techniques like precipitation may be employed to isolate individual REE, which contributes to the production of high-purity REE products used in advanced technologies, renewable energy and various high-tech industries. A crucial step in the entire production chain is the elution of REE from minerals, emphasizing the importance of effective and ecologically friendly methods for obtaining these essential components.

Factors influencing the elution process

An elution process in which the adsorbed ions are exchanged with the ions of the eluent can achieve the removal of metal ions from minerals. Various reaction parameters (e.g. pH value, temperature, acid concentration, kinetics, etc.) can influence the ion exchange in the elution process. The regulation of the ion exchange can be affected by these parameters and is fundamental for the configuration of an elution process in an industrial approach.

For the elution process, the pH value is one of the most decisive influencing factors. A lower pH correlates with a higher elution rate for REE.[74] This phenomenon occurs because the pH value is closely linked to the acid concentration, as there are significantly more H^+ ions in highly acidic conditions than under neutral conditions for ion exchange.

The concentration of the acid has a significant influence on the elution efficiency because with a higher acid concentration, the weight proportion of extracted metals also increases.[74] In addition, the elution efficiency also depends on the type of acid, because the elution rate for metals differs for each acid.[75, 76]

The temperature has a decisive effect on the elution rate. The elution rate for REE increases significantly by raising the temperature from RT to 90°C. Therefore, the elution efficiency increases with higher temperature. The elution process, in which the metals are extracted from the mineral, corresponds to an endothermic reaction.[74, 77, 78] As a result, an increase in temperature leads to an enhancement in the reaction equilibrium constant and the reaction activity.[79, 80]

A shrinkage-core model can be used to describe the process of removing metal ions from the mineral.[81] If diffusion through the mineral layer is a rate-determining step, the kinetics equation is expressed as:[73, 82]

$$1 - \frac{2}{3}x - (1-x)^{\frac{2}{3}} = \frac{2M_S D c_A}{\rho_S a r_0^2} t = k't \tag{1}$$

where x is the interacted fraction; M_S is the molecular mass of the solid; D is the diffusion coefficient of ions in the mineral layer; c_A is the concentration of the lixiviant; ρ_S is the density of the solid; a is the stoichiometric coefficient of the reagent; r_0 is the initial radius of the solid; t is the reaction time; k' is the rate constant.[73, 82]

If the reaction rate is determined by the surface reaction in the elution process, the kinetic equation can be expressed as:[82]

$$1 - (1-x)^{\frac{1}{3}} = \frac{2M_S D c_A}{\rho_S a r_0} t = k''t \tag{2}$$

where k" is a rate constant, D is a diffusion coefficient, c_A is concentration of the lixiviant, and r_0 is the initial radius of the solid. According to the equation 1 or 2, there must be a linear relationship between the left side of the equation and time if the elution rate is controlled by the surface reaction or by diffusion through the layer. Therefore, the slope of the straight-line results in the rate constant k' or k", which is proportional to the initial radius $1/(r_0^2)$ or $1/r_0$.[82]

These kinetic equations provide insights into the mechanisms driving the elution process and offer a basis for optimizing reaction conditions.

1.4 ICP-OES

Inductively coupled plasma (ICP) is an effective excitation source that can be combined with optical emission spectroscopy (OES). Specifically, ICP-OES is employed for the quantitative determination of various elements in very low concentrations from acidified aqueous solutions. This method has been a standard analytical technique since 1961, showcasing its enduring suitability for metal analysis.[83] ICP-OES offers advantages such as short measuring times, minimal sample preparation efforts, and the ability to detect multiple elements simultaneously. As a result, it is particularly valuable for determining heavy metal content in industrial wastewater or completely dissolved soil samples.

The plasma in the ICP-OES system reaches a relatively high temperature, ranging from about 6,000 to 10,000 K. The liquid sample is finely injected into the spray chamber using a nebulizer in combination with an autosampler and a peristaltic pump. This injection process generates small droplets (aerosol) that are directed into the torch. Within the torch, the droplets undergo vaporization, ionization, atomization, and excitation in the high-temperature plasma. The resulting emission from the energized analyte particles can be detected with OES.

The ignition process is coupled into the argon gas inside with the use of an induction coil that is water-cooled from the inside and has a low number of turns. For this purpose, a high-frequency alternating voltage is applied to the coil, which is generated by a high-frequency generator.[84]

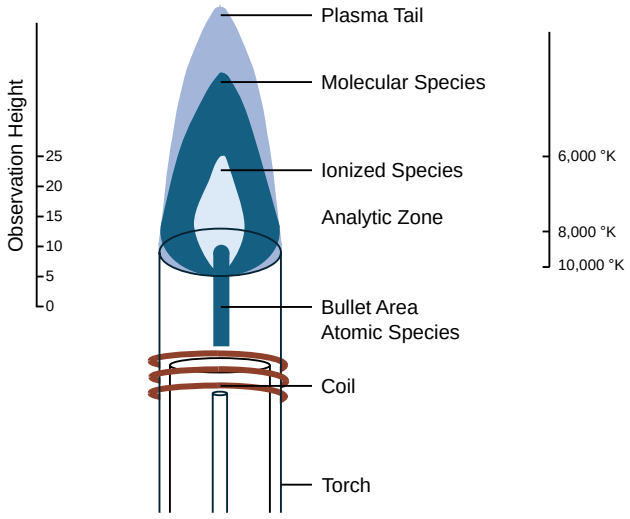

Figure 3: Schematic illustration of the plasma flare.[85]

The radio frequency (RF) generator provides 700 – 1,500 w of power output, which is necessary to sustain the plasma during ICP-OES analysis. This power is essential for maintaining the high-temperature plasma required for the excitation and detection of elements. The torch, a central component in this system, is constructed from several concentric cylinders of quartz glass with varying lengths and diameters (Figure 3).
The gas injected into the torch, typically argon due to its inert properties, plays a vital role in creating and maintaining the plasma. The required volume flow for ICP-OES comprises distinct components directed into the plasma. These components include the plasma gas flow, auxiliary gas flow, and nebulizer gas flow. The plasma gas flow, usually directed to the side of the torch, constitutes the highest volume supply and

is integral for sustaining the high-temperature plasma. Simultaneously, the nebulizer gas flow is supplied with the sample feed from below through the innermost tube, facilitating the fine injection of the liquid sample into the spray chamber.[84]

Excitation and ionization

During the ignition process in ICP-OES, energy is transferred by an ignition spark through the applied high-frequency field in the coil. As a result, free electrons within the plasma are accelerated by the electric field, heated, and ionized by collisions with the particles of the gas. The composition of the analyte (A) is calculated in a state of equilibrium – the local thermal equilibrium (LTE) – of the plasma. The electron impact ionization occurring in the plasma is generally described by the reaction:[86, 87]

$$A \rightarrow A^+ + e^- \tag{3}$$

The relationship as a function of temperature (T_{ion}) between the density of the ions (n_{A^+}), the density of the electrons (n_e), and the density of the atoms (n_A) is described by the ionization equilibrium constant $K(T_{ion})$:[86]

$$K(T_{ion}) = \frac{(n_{A^+})(n_e)}{n_A} \tag{4}$$

The temperature dependence of the ratio of the densities n (cm^{-3}) of particles in different ionization states ($A, A^+ + e$) is described by the Saha-Eggert equation (Eq. 5), which relates the ionization partition of an atom with T_{ion} and n_e:[84, 86]

$$\frac{(n_{A^+})(n_e)}{n_A} = 2\left(\frac{2\pi m_e k_B T_{ion}}{h^2}\right)^{\frac{3}{2}}\left(\frac{Z_{A^+}}{Z_A}\right)e^{-\frac{E_j}{k_B T_{ion}}} \tag{5}$$

In this equation, $m_e = 9.109 \cdot 10^{-31}$ kg is the mass of the electron, Z_A and Z_{A^+} are the partition functions, E_j is the ionization energy (eV) of the j-th partition, k_B is the Boltzmann constant, T_{ion} (K) is the ionisation temperature, and h $= 6.626 \cdot 10^{-34}$ Js is the Planck's constant.

1.5 Biosorption

Biosorption is a physicochemical process for the accumulation of substances on the surface of biological materials, such as algae, bacteria, and fungi, whereby the process can operate as both adsorption and absorption. In absorption, substances in the solid state can be absorbed into another substance in a different state of aggregation, such as the absorption of a solution into a solid material, whereas in adsorption the accumulation

of a substance occurs on the surface of a solid. For this purpose, the substance to be adsorbed is called "sorbate" and the solid is called "sorbent".
Functional groups such as -OH, -COOH, -$PO(OH)_2$, -SO_2OH, or -SH on the surface of the biomass have a decisive influence on the metal binding properties. The following mechanisms can occur when metals attach to the surface of the biosorbent: complexation, surface precipitation, ion exchange, and electrostatic attraction.[70, 88, 89, 90, 91] The biosorption process can involve living or dead cells as sorbents. In the case of living biomass, another mechanism, bioaccumulation – a metabolism-dependent process - is added. This mechanism transfers adsorbed metal ions from the surface of the biomass to its interior. The transport process into the cell membrane, which only occurs after the adsorption process of metal ions to the surface of the biological material, is a secondary mechanism step and this is slow.[92] The disadvantages of the process are the costs and the complexity. Therefore, the metabolism-independent process of biosorption is preferred for industrial applications.

Biosorption process

For a biosorption process (Figure 4), the biomass is first cultivated and then used as a biosorbent in the metal-containing water. The incubation of the biomass is carried out either in a stirring container or placed statically in a column. Based on the adsorption properties of the biosorbent and the process conditions, metal ions from the aqueous solution can be adsorbed onto the surface of the biomass. After the biomass has been enriched with metals, it is separated from the solution. The separation of metal-enriched biomass from the solution is achieved either by filtration,[93] sedimentation,[94] or centrifugation,[95] although the separation methods are not necessary for immobilized biomass. Subsequently, the enriched metals can be extracted by an elution process or by burning the algal biomass.[96] Incineration leads to the complete destruction of the biomass and the formation of metal-containing ashes, which cannot be used for repeated enrichment processes. The application of environmentally friendly elution processes for the recovery of metals is important from an economic point of view since the used biomass can be regenerated. By varying the biosorption conditions, such as adding complexing additives or changing the pH, the metals can be accessed. The latest research emphasizes addressing the limitations of adsorption with a biological material, as the adsorption capacity of such a material tends to decrease with each successive adsorption-desorption cycle.

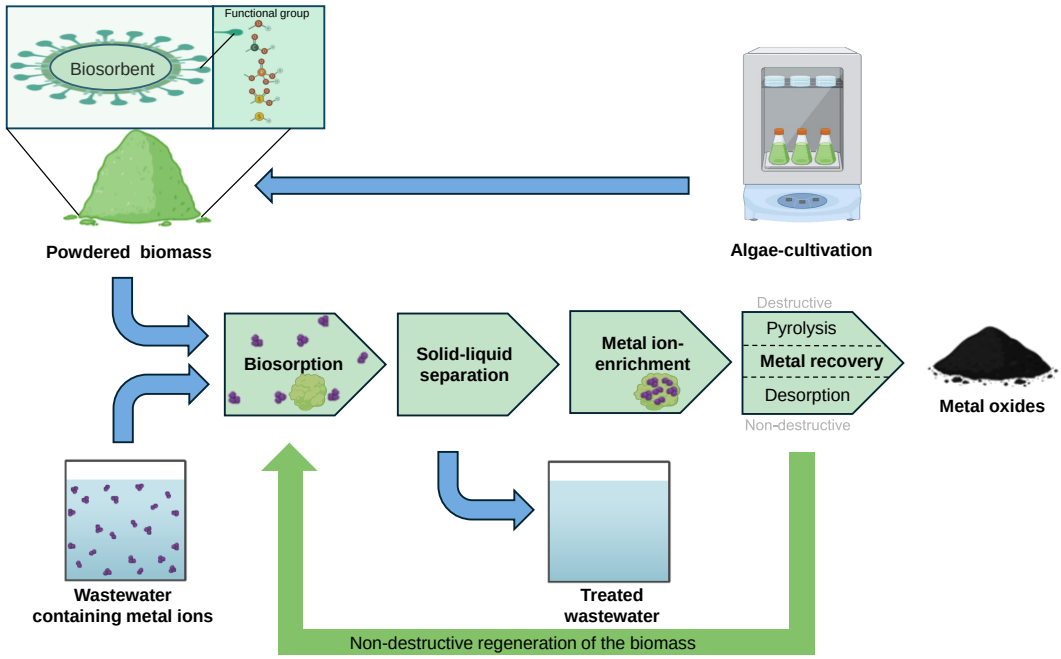

Figure 4: Schematic overview of a biosorption process by using powdered biomass to recover metals from wastewater containing metal ions; the icons were taken from BioRender.com.

Influencing factors for biosorption

The complex process of metal uptake by biomass is influenced by various factors. In addition to the viability of the cells and the composition of the biomass, physicochemical parameters (e.g. pH, temperature, time, etc.) can influence the biosorption process. For the technical application, they must be optimized and adapted for an industrial process.

With the pH value, the decisive parameters of the adsorption process can be easily varied, which influences the uptake of metal ions from the metal-containing solutions. The solubility of metals has an essential influence here because the pH change can cause metal hydroxides to be formed,[97] which can induce precipitation. This results in a decrease of adsorbed metals. Therefore, basic conditions are largely unsuitable for a biosorption-based process. In addition to solubility, pH also affects the functional groups on the surface of biomass. Under highly acidic conditions, the adsorption capacity is lowest due to the increased proportion of positively charged active spots on the surface of the biosorbent, because the positively charged metal ions are repelled at these spots in the acidic medium.[98] In order to grant optimal conditions for the adsorption of metals, the pH dependence of biosorbents and of the functional groups in the biosorption process must be taken into account. The ideal pH value differs de-

pending on the biomass and the functional groups. If the metal-containing solution is acidified from pH 6 to pH 2, the adsorbed amount of metals on the biomass decreases significantly.[99] Biosorption below pH 2 is commonly irrelevant because the biomolecules of the biosorbent are irreversibly denatured.[100] Therefore, an algae-based process in almost neutral conditions (pH 5-6) is most optimal.[101]

The reaction kinetics of biosorption vary depending on the composition of the biosorbent and the metal ions acted upon, but the free binding sites are rapidly occupied. Therefore, the contact time between the metal ions and the biomass does not directly affect the adsorption capacity. Saturation of the biosorbent is reached at equilibrium when all free binding sites are occupied. The description of the reaction kinetics for biosorption of metals is enabled with the utilization of two models, i.e., a pseudo-first order or pseudo-second order model.[102]

The temperature has no immediate effect on biosorption between room temperature (RT) and 35°C.[103] A higher reaction temperature leads to the decomposition of the biomaterial, which reduces the adsorption capacity. In addition, increasing the temperature is disadvantageous from an economic point of view.[104] Basically, the adsorption reaction is exothermic, but in some exceptions, depending on the biosorbent or metal ion, this reaction can also be endothermic.[105, 106]

In aqueous solutions, such as industrial wastewater, various metals are contained in high concentrations. There are numerous studies on biological materials that state that the metal ions in the solution compete for the same binding sites of the biosorbent.[107, 108] Therefore, the present ions competing for the free binding site and their concentration in solution influences the adsorption of certain metal elements. In this context, the chemical composition of the biomass and the type and abundance of the functional groups also determine the binding specificity of the biosorbent.[109] In order to develop a suitable algae-based biosorption process for the recovery of metal elements from industrial wastewater, many factors, such as the process parameters, the chemical composition of the biomass and that of the aqueous solution, need to be considered. These factors have a great influence on the adsorption capacity and the binding specificity. Furthermore, the biomass can have different binding affinities for certain metal ions under the same reaction conditions.[110, 111]

Metal concentration is a crucial factor influencing biosorption on biological materials in aqueous solutions. The relationship between uptake and metal concentration typically follows a normal saturation curve. Optimal metal uptake is usually achieved

at low metal concentrations. With sufficient biosorbent, metal uptake increases with increased metal concentration, and the different concentration curves can be determined by isothermal analysis. The isotherm illustrates the fraction of adsorbed metals in relation to the metal concentration in the aqueous solution.[112] Consequently, it can be used to determine a reference point for the evaluation of a biosorbent for the application of adsorption processes in wastewater. Isotherm curves are determined by varying the concentration of metal at a constant temperature. In general, the adsorption capacity increases with the adsorptive concentration until it reaches saturation.[113]

Influencing the cultivation conditions of the biomass

One strategy involves manipulating cultivation parameters during biomass production, where variations in environmental conditions, like nutrient supply and temperature, influence biomass composition.[114, 115] Various studies on cyanobacteria have shown that modifying cultivation conditions can enhance the adsorption capacity for specific metals.[116, 117] It is specifically suggested to investigate cultivation in nitrogen-limited conditions as this might boost the production of extracellular polymeric substances (EPS),[118] also known as extracellular polysaccharides.[119, 120] EPS are soluble in water and can be separated by filtration or centrifugation. These polysaccharides exhibit superior metal adsorption properties due to an accumulation of amide, carboxyl, and hydroxyl groups. Anionic characteristics are created by forming functional groups commonly present in cyanobacterial extracellular polymeric substances. These anionic properties increase the affinity to cations particularly. Further studies should inquire into the composition and role of EPS derived from the cyanobacterial strains concerning their potential for REE adsorption.

2 Materials and Methods

An overview of the main materials, methods, and procedures employed in this thesis is provided in the following section. Detailed information can be found in the corresponding material and method sections as well as in the supplementary data sections of the respective manuscripts included in this work.

Table 2: List of chemicals and reagents used in the elution process.

Chemical/reagent	**Purity [%] unit**	**Manufacturer**
67% Nitric acid (HNO_3)	ultra-pure	VWR-Chemicals
30% Hydrochloric acid (HCl)	ultra-pure	VWR-Chemicals
96% Sulfuric acid (H_2SO_4)	supra-pure	Merck
Ultra-pure water	demineralized water (DI-H2O) from the Direct-Q® 3 water treatment system with UV lamp, specific resistance 18.2 MΩ cm	
Raw soil samples		AKW

BG11 is a standard medium for the cultivation of cyanobacteria.[121] The calcium and trace element solutions were autoclaved or sterilized independently to avoid precipitation. Finally, they were added to the final medium. The composition of BG11 medium is listed below (see Table 3):

Table 3: List of chemicals and reagents used for calcium chloride solution, ethylenediaminetetraacetic acid (EDTA) solution, Fe-citrate solution, and trace elements solution in BG 11 medium.

Chemical/reagent for BG 11	**Quantity for 1L medium**
$K_2HPO_4 \cdot 3\,H_2O$	0.040 g
$MgSO_4 \cdot 7\,H_2O$	0.075 g
Na_2CO_3	0.020 g
$NaNO_3$	1.50 g
Ca solution	1 mL
EDTA solution	1 mL
Fe-citrate solution	1 mL
Trace elements solution	1 mL
Calcium chloride solution	**Quantity** [g L^{-1} DI-H_2O]
$CaCl_2 \cdot 2\,H_2O$	36.00
Ethylenediaminetetraacetic acid	**Quantity** [g L^{-1} DI-H_2O]
$Na_2EDTA \cdot 2\,H_2O$	1.00
Trace elements solution	**Quantity** [g L^{-1} DI-H_2O]
$Co(NO_3)_2 \cdot 6\,H_2O$	0.0494
$CuSO_2 \cdot 5\,H_2O$	0.079
H_3BO_3	2.86
$MnCl_2 \cdot 4\,H_2O$	1.81
$Na_2MoO_4 \cdot 2\,H_2O$	0.39
$ZnSO_4 \cdot 7\,H_2O$	0.222

The modified spirulina medium for cultivation of cyanobacteria was composed of two 500 mL solutions I and II, which were autoclaved separately and then mixed after cooling.[122]

Table 4: List of chemicals and reagents used for solution I, solution II, and trace element solutions of modified Spirulina medium.

Chemical/reagent for solution I	**Quantity for 500mL solution**
K_2HPO_4	0.50 g
Na_2CO_3	4.03 g
$NaHCO_3$	13.61 g
Chemical/reagent for solution I	**Quantity for 500 mL solution**
$CaCl_2{\cdot}2\,H_2O$	0.04 g
$FeSO_4{\cdot}7\,H_2O$	0.01 g
K_2SO_4	1.00 g
$MgSO_4{\cdot}7\,H_2O$	1.00 g
NaCl	1.00 g
$Na_2EDTA{\cdot}2\,H_2O$	1.00 g
Trace elements solution	1 mL

Chemical/reagent for trace element solution	**Stock solution [g L^{-1} DI-H_2O]**	**Quantity for 500 mL solution**
$Co(NO_3)_2{\cdot}6\,H_2O$	1.00	1 mL
$CuSO_4{\cdot}5\,H_2O$	0.005	1 mL
$FeSO_4{\cdot}7\,H_2O$	-	0.70 g
H_3BO_3	10.00	1 mL
$MnSO_4{\cdot}7\,H_2O$	2.00	1 mL
$Na_2EDTA{\cdot}2\,H_2O$	-	0.80 g
$Na_2MoO_4{\cdot}2\,H_2O$	1.00	1 mL
$ZnSO_4{\cdot}7\,H_2O$	1.00	1 mL

2.1 Chemical mobilization of Rare Earth Elements using a microwave

Microwave experiments on residual kaolinite minerals were conducted using an Ethos One (MLS GmbH, Leutkirch, Germany) to extract metal. 9 mm of mineral acid were added to 0.5 g of each analyzed sample, which was placed in a Teflon container. The concentrations employed in the experiments were concentrated nitric acid at 65%, hydrochloric acid at 30%, sulfuric acid at 96%, hydrofluoric acid at 47–51%, and diluted nitric acid at 15%, hydrochloric acid at 5%, and sulfuric acid at 19%. The Teflon container was heated to 65°C in the microwave for 25 min, then held there with stirring for an hour before cooling for 30 min. This complete method matched one elution process step in this investigation. By performing the operation many times, multiple elution periods helped to improve the elution process and raise the REE concentration from the same sample. To do this, the elution process was repeated several times

after the previous residue from one elution step was extracted from the elution solvent without additional drying or work-up. 9mL of fresh elution acid were subsequently added.

2.2 Analytics

XRD analysis

The atomic and molecular determination of crystalline minerals was carried out by powder XRD (X-ray diffraction). The STADI P powder diffractometer, equipped with a DECTRIS Mythen 1 K detector, provided the powder XRD data using Cu-Kα1 radiation ($\lambda = 1.54051$ Å, Ge-monochromator). For 14 hours, each sample was analyzed in an 80 mm long, 0.5 mm outer diameter, and 0.01 mm thick wall Hilgenberg glass capillary. The phase analysis was carried out in Jana2006,[123] and the powder data was examined using the STOE WinXPOW program. The literature data for kaolinite,[54] quartz,[124] orthoclase feldspar,[125] muscovite,[126] and gorceixite[127] were utilized to determine the most likely phases. The phases were chosen using the data that AKW provided. The published structural models were used for the Rietveld refinement without any further atomic coordinate or displacement parameter refinement. For all non-hydrogen atoms, the isotropic displacement parameters were universally adjusted to a default value of 0.02 Å^2, and for hydrogen atoms, to 0.04 Å^2. Refinement of the lattice parameters of each phase was permitted to deviate slightly from the stated lattice parameters for each phase considering substitutions and impurities in natural minerals.

XRF analysis

The elemental composition of minerals was obtained using a Bruker AXS S8 LION X-ray spectrometer (XRF, X-ray fluorescence). Following drying, the sample material was ground for 12 min in an analytical mill and reduced to the required quantity using a sample divider. The material was then homogenized for five minutes in a Turbula mixer. After that, a press and pressing tools were used to compress the blended powder into a tablet. The pressed material was further dried in a drying oven for two hours or in a microwave for two minutes. After adding the flux lithium tetraborate to the dried sample, it was melted for 15 min at 1150°C in a muffle furnace, then poured onto a platinum-gold mold, quickly chilled using compressed air, and measured. Each sample was measured for 60 s. The SpectraPlus software was utilized for the analysis of the measurement data.

SEM analysis

A scanning electron microscope (SEM) was used to capture images to investigate the morphology of the sample. An InTouchScopeTM (JEOL, Akishima, Japan) JEOL JSM-IT200 SEM was utilized to process the sample analysis. The samples were adhered to a steel holder with conductive glue. The acceleration voltage was set to 10 kV.

ICP-OES analysis

Metals in solutions were analyzed with an Agilent ICP-OES (inductively coupled plasma optical emission spectroscopy) 725 spectrometer (Agilent Technologies, Waldbronn, Germany) with radially-viewed plasma equipped with an autosampler and a polychromator which provides a complete wavelength range from 167 to 785 nm. For calibration, a TraceCERT® Rare earth element mix ICP-standard with 16 elements (Sigma-Aldrich, Taufkirchen, Germany) and a Certipur® multi-element ICP-standard solution IV (Merck, Darmstadt, Germany) were used. Five points (blank, 0.1, 1, 10, and 50 $mg\,L^{-1}$) were measured from each standard. Agilent ICP Expert II software was utilized to process the measurement data.

FT-IR analysis

Fourier-transform infrared spectroscopy (FT-IR) is a particularly suitable method for determining the functional groups of cyanobacterial biomass and identifying possible interactions of the isolated extracellular polymeric substances samples with metal samples, used in this study. Spectra were acquired using an FT-IR spectrometer (Nicolet iS50R, Thermo Fischer Scientific, Waltham, US) equipped with an iS50 ATR (attenuated total reflectance) multi-range diamond sampling station. All samples were measured in the wavelength range of 400 - 4000 cm^{-1}.

HPLC analysis

The sugar analysis was conducted utilizing an Infinity II LC 1260 HPLC (high-performance liquid chromatography) system (Agilent Technologies, Waldbronn, Germany), which was equipped with an autosampler, quaternary pump, column oven, DAD, and a Shodex RI detector (Showa Denko Europe GmbH, Munich, Germany). Before injection, each sample underwent filtration using Modified PES 500µL centrifugal filters with a cut-off of 10 kDa. Subsequently, the monomeric sugar mixture resulting from chemical hydrolysis underwent analysis using the HPLC system. The monomers were examined utilizing a Rezex ROA-Organic Acid H^+ (8%) ion-exclusion column (300 mm,

7.8 mm internal diameter; Phenomenex LTD, Aschaffenburg, Germany), employing an isocratic separation with 5 mM sulfuric acid at a flow rate of 0.5mL min^{-1} and a temperature of 70°C.

2.3 Cultivation of cyanobacteria

Strains of cyanobacteria and culture media used in this study are listed in Table 5. The algae strains were obtained from SAG Culture Collection of Algae (University of Göttingen, Germany); eight strains from environmental samples by the research group of Dr. Michael Lakatos (University of Applied Sciences Kaiserslautern, Germany); UTEX Culture Collection of Algae (University of Texas in Austin, USA).

Table 5: List of cultivated cyanobacteria; Key to media: B BG11 and S modified Spirulina. Key to cultivation vessel: SC submerse cultivation, SP 2.7 L stirred photobioreactor and SF 500 mL shaking flask.

Algae strain	**(strain number; Cultivation vessel)**	**Medium**
Calothrix brevissima	(SAG 34.79; SF and SP)	B
Desmonostoc muscorum	(90.03; SC)	B
Komarekiella sp.	(89.12; SC)	B
Komarekiella sp.	(90.01; SC)	B
Limnospira maxima	(SAG 49.88; SF)	S
Limnospira platensis	(SAG 85.79; SF)	S
Nostoc sp.	(20.02; SC)	B
Phormidium autumnale	(97.20; SC)	B
Reptodigitus sp.	(92.01; SC)	B
Scytonema hyalinum	(02.01; SC)	B
Symphyonema bifilamentata	(97.28; SC)	B
Synechococcus elongates	(UTEX 2973; SP)	B

For the adsorption experiments the cyanobacteria were produced in different cultivation systems. The algae biomass "SAG" was cultivated in an Infors Lab5 stirred photobioreactor (Infors HT, Bottmingen, Switzerland). The cyanobacteria (*Desmonostoc muscorum, Komarekiella sp., Komarekiella sp., Nostoc sp., Phormidium autumnale, Reptodigitus sp, Scytonema hyalinum, and Symphyonema bifilamentata*) from Lakatos's research group were grown in a cultivation flask as submerged cultures. *Calothrix brevissima* and *Synechococcus elongates* were cultivated in a 500 mL shaking flask.

Cultivation of cyanobacteria in nitrogen-depleted conditions

In this study, three cyanobacterial strains, *Desmonostoc muscorum*, *Komarekiella sp.*, and *Nostoc sp.*, were tested under nitrogen-limited conditions. 0.1 - 0.3 g of wet biomass were collected from the stock culture and added to a nitrogen-depleted BG 11 medium in a 5 L bubble column. All strains were cultivated for 4 weeks at 23°C and a light/dark interval of 16:8 hours at an illumination of 300 µmol photons $m^{-2}s^{-1}$ in a bubble column. After cultivation, the biomass was filtered through two sieves of 0.5 mm and 0.1 mm and paper filters with 40 µm pore sizes and then freeze-dried. The dried strains were visualized with a differential interference contrast (DIC) substance and the images were taken with an Olympus BX51 microscope (Evident Europe GmbH, Hamburg, Germany).

2.4 Biosorption

All adsorption experiments of various metal elements are based on the research work of Heilmann et al..[128, 129] The utilized biomass samples were washed three times with deionized water (DI-H_2O) to remove any impurities that could affect adsorption. This was followed by lyophilization and freezing of the biomass at -80°C. About 10-20 mg of the freeze-dried biomass in 2 mL of metal-containing solutions with known concentrations were used for the adsorption experiments. Quantification of the metal concentration was performed before and after incubation to determine the adsorption capacity. After incubation, the samples were centrifuged for 5 min at 10,000 rpm at RT. Afterwards, the supernatant was analyzed for metal concentration.

Adsorption capacities

The adsorption capacity (AC) for several metals was determined by incubating the dry biomass for 3 hours on a 10 mM metalliferous solution under slightly acidic conditions of pH 5 with constant shaking. In the following, the metal uptake was determined using the following equation by dividing the change in concentration by the mass of the incubated biomass:

$$AC = \frac{(c_i - c_f)V}{m_b} \tag{6}$$

where AC is the adsorption capacity; c_i and c_f are the initial and final concentrations; V is the solution volume; and m_b is the weight of the biomass.

Adsorption kinetics

To determine the adsorption kinetics, the biomass samples were tested in a 10 mM cerium(III) nitrate solution at pH 5 at different incubation times. All tested biomass samples were analyzed after an incubation time (2, 5, 15, 30, and 60 min).

Adsorption for multi-element system

Another series of experiments to investigate the adsorption capacity was carried out in a multi-metal system. Metal solutions contain aluminum, cerium, lead, nickel, and zinc. In addition, sample solutions with concentrations (0.5, 1, 2, and 4 mM) were used.

Influence of the pH value on biosorption

Biosorption is strongly dependent on the pH value. The experiments were carried out in the range of pH 1-6. Under basic conditions,[129] REE form insoluble hydroxides in aqueous solutions,[8, 130] which are unsuitable for the biosorption process. The pH value of the metal-containing solution added to the biomass was regulated with sodium hydroxide and hydrochloric acid.

Adsorption isotherms

For the evaluation of the sorption behavior of the biomass, the adsorption isotherm was examined at metal concentrations between 0.5 mM and 10 mM. The analysis of the one-hour incubation of the biomass at RT with constant shaking was carried out afterwards.

3 Research

Summaries of included publications

3.1 Rare earth element stripping from kaolin sands via mild acid treatment

Max Koch[a], Michael Paper[b], Thomas B. Brück[b], and Tom Nilges[a]

[a]Synthesis and Characterization of Innovative Materials, School of Natural Sciences, Department of Chemistry, Technical University of Munich, Garching, Germany

[b]Werner Siemens-Chair of Synthetic Biotechnology, School of Natural Sciences, Department of Chemistry, Technical University of Munich, Garching, Germany

Asia-Pacific Journal of Chemical Engineering, 19 (2), e3018
First published online: December 21st 2023
Link: `https://doi.org/10.1002/apj.3018`

In this study, the aim was to investigate a microwave-assisted elution process and clarify how various media affected the extraction of Rare Earth Elements (REE) from kaolinite samples. Residues from the kaolin refinement process from the kaolin production site in Amberg were used for this study. Furthermore, the refined residues were investigated instead of pure kaolinite because we expected an accumulation of REE in such residues after the industrial purification process. Based on the quantitative results, two residual samples RK1 and RK2 exhibited the most significant weight percentage accessible REE outcomes. The elution efficiency for REE accessibility over 80% for the concentrated acids, which increased in the following order $HNO_3 < H_2SO_4 < HCl$, with sulfuric acid being the preferred eluent despite being less efficient than hydrochloric acid because fewer secondary metal ions are mobilized with this eluent. An additional intent of this study was to permit the utilization of diluted acids to allow an ecologically friendly REE recovery process. When eluting REE from clays in a single step, the elution potential with diluted acid solutions did not surpass a REE weight proportion of $0.8\,g\,kg^{-1}$ – corresponds to 32% of efficiency. Hence, an enhancement of the one-step elution process was undertaken by a multiple-step process, which enabled an increase in efficiency of up to 69%. This research illustrated that using diluted acids in an elution process had benefits for further subsequent process steps, such as metal recovery by biosorption. Neutral conditions were applied in the biosorption, which are easier to manage when using diluted acids. Furthermore, an optimization of the

batch process to a semi-continuous process would be advantageous from an industrial perspective. The potential of this proposed elution procedure for the recovery of REE in large-scale operations ought to be the focus of future research.

Author contributions: All authors collaborated in developing the study's concept and method design. Max Koch was responsible for the planning and the execution of the quantitative analysis and data evaluation. Max Koch wrote the manuscript, which all authors completed and revised together.

Received: 20 June 2023 | Revised: 26 October 2023 | Accepted: 20 November 2023

DOI: 10.1002/apj.3018

RESEARCH ARTICLE

Asia-Pacific Journal of Chemical Engineering | Curtin University | WILEY

Rare earth element stripping from kaolin sands via mild acid treatment

Max Koch[1] | **Michael Paper**[2] | **Thomas B. Brück**[2] | **Tom Nilges**[1]

[1]Synthesis and Characterization of Innovative Materials, School of Natural Sciences (NAT), Department of Chemistry, Technical University of Munich, Garching, 85748, Germany

[2]Werner Siemens-Chair of Synthetic Biotechnology, School of Natural Sciences (NAT). Department of Chemistry, Technical University of Munich, Garching, 85748, Germany

Correspondence
Tom Nilges, Synthesis and Characterization of Innovative Materials, School of Natural Sciences (NAT), Department of Chemistry, Technical University of Munich, Lichtenbergstraße 4, 85748 Garching, Germany.
Email: tom.nilges@tum.de

Funding information
Graduate School, Technische Universität München; Bavarian State Ministry of the Environment and Consumer Protection, Grant/Award Number: Forcyle II project 8; TUM Graduate School

Abstract

Due to their chemical and physical properties, rare earth elements (REEs) are essential in modern applications such as energy conversion or IT technology. The increasing demand for these elements leads to strong incentives for REE recovery and induces the exploration of new, alternative sources for REEs. Accessing REEs from clay minerals, in our case kaolinite, by an elution process is a promising method. The present study investigates the potential application of REE recovery through elution with different mineral acids (HNO_3, H_2SO_4, and HCl) in a microwave process. The material used in this study—residues from an industrial kaolin production process—contained 2.47 g/kg REEs which is a significant amount for REE recovery. The ability of various mineral acids to solubilize metals was studied to assess the REE content of this residual resource. Around 1.87 g/kg of REEs was eluted from industrial kaolinite residues in hydrochloric acid, 1.71 g/kg in sulfuric acid, and 1.13 g/kg in nitric acid.

KEYWORDS

elution, extraction, process data, kaolinite, rare earth element recovery, rare earth elements

1 | INTRODUCTION

Rare earth elements (REEs) are essential materials in today's energy production and IT technology. Due to their wide range of applications, such as permanent magnets, lenses, catalysts, luminescent substances, light emitting diodes, and many others, the demand for REEs is forecast to keep growing in the near future.[1–4] REEs are usually accessed and extracted under harsh conditions.[5] China is the leading producer of rare earth oxides, with an annual production of 210.000 t out of 300.000 t worldwide (2022).[6] The technological importance of REEs leads to an economical supply dependency of industrialized nations on a few producers, which is also a geopolitical factor. New, more environmentally friendly and viable sources/processes to access or recover REEs are being intensely investigated.

The mineral kaolinite, $Al_2(OH)_4Si_2O_5$, belongs to the phyllosilicate group. In nature, this mineral is most abundant within kaolinite group. Kaolinite is a layered mineral that consists of an octahedral alumina layer and a silica layer of tetrahedrally coordinated Si atoms (1:1 ratio), which share a common plane of oxygen atoms.[7,8]

Kaolinite is extensively used in the ceramics production,[9] papermaking,[10] cosmetics,[11] and pigment

industry.[12] Furthermore, it appears to be an excellent ion-adsorbent for various cations. Bear et al. first discussed the cation exchange capacity (CEC) of kaolinite, describing the mineral's ability to exchange cations and retain nutrients in soil.[8,13,14] Due to the influence of abiotic factors (e.g., weathering), valuable metal ions readily accumulate between the layers, including REEs.

Recently, such ion-absorbing clays are becoming more and more important REE resources in the REE mining industry.[15,16] The REEs are not chemically bound to the clays but are rather physisorbed.[17] On the surface, most of the lanthanides are adsorbed in the acidic environment as simple or hydrated cations, such as "clay-REE" or "clay-REE$(H_2O)_n$" types.[17] According to Jun,[18] the ion adsorption in clays is divided into three categories due to the various weathering conditions: colloid phase, exchangeable phase, and mineral phase.[17,18] The REEs are deposited in the colloid phase as insoluble oxides and hydroxides in organometallic compounds. These occur only in small amounts in ores and can be recovered only by acid leaching. In the exchangeable phase, the REEs are present as free soluble cations on clays or in between the layers. These species form most of the total content of adsorbed REEs obtained by ion exchange leaching. The lanthanides are firmly attached in the mineral phase as fine solid particles in the crystal structure and can only be obtained by very elaborate and aggressive methods.[17] Unlike in ores, in the clay minerals, REEs can be easily obtained by ion exchange, described in detail by Hendricks et al.[16,19] REEs from kaolinite are accessible via acids or salts and can be classified in the first or second category, respectively.[1,15,20]

In the leaching process, concentrated salt solutions or weak acids are most often used as leachants to obtain REEs. Accordingly, the cation of the leachant can exchange the REE cations attached between the aforementioned layers.[15]

The aim of this paper is to investigate an energy-friendly process and elucidate the influence of different media on extracting REEs from kaolinite samples. For this study, we used residues from the kaolin refinement process at the production site Amberger Kaolinwerke (AKW, Hirschau, Germany). We investigated the refined residues instead of bare kaolinite because we expected an enrichment of REEs in such residues after the industrial purification process.

One example of REE recycling of dissolved REE ions in aqueous solution was recently reported, and the potential of cyanobacteria for the adsorption and enrichment of REEs was tested.[21] REEs were coordinated effectively to functional groups at the surface of these cyanobacteria at pH values between 5 and 6. With this study, we intend to illustrate an effective way to access REEs from mineral residues capable to be utilized in modern REE recycling processes.

2 | EXPERIMENTAL

2.1 | Materials and methods

The residual materials were obtained from different production steps of the kaolin refinement from AKW. This company provided various deposited samples (RK 1 to RK 15) from different steps in the kaolin production/refinement that could be considered a possible raw material for the subsequent extraction of REEs. These samples were characterized in detail, and their elemental composition was investigated with regard to REEs and other metals. In this study, the REE content of the residual material streams produced at AKW was quantified using inductively coupled plasma optical emission spectroscopy (ICP-OES). Various acids with different concentrations were used to extract REEs from these samples. Elution and digestion of REEs from residues of kaolin production were processed using microwave-assisted elution. All used chemicals are listed in Table 1. The phase analysis of all samples was performed by powder X-ray diffraction (XRD).

2.1.1 | Elution and digestion of REEs using microwave

The extraction experiments from kaolinite clay minerals residues were performed by *ETHOS One* Microwave Laboratory solutions of the company MLS GmbH. For this purpose, 0.5 g of each sample and 9 mL of a mineral acid (aqueous) were added to Teflon vessels. The acids were concentrated nitric acid (65%), hydrochloric acid (30%), sulfuric acid (96%), hydrofluoric acid (47–51%), diluted nitric acid (15%), hydrochloric acid (5%), and sulfuric acid (19%). The Teflon vessels were heated to 65°C for 1 h in a microwave oven at 400 W power during continuous stirring. The heating and cooling phases were set to 25 and 30 min, respectively. This entire protocol defines

TABLE 1 List of chemicals used in the elution process, manufacturer of the chemicals, and purity (analytical quality).

Substance	Manufacturer	Quality
Nitric acid (HNO_3)	VWR-Chemicals	67%, Ultrapure NORMATOM®
Hydrochloric acid (HCl)	VWR-Chemicals	30%, Ultrapure NORMATOM®
Sulfuric acid (H_2SO_4)	Merck	96%, Suprapur®
Ultrapure water	-	deionized, specific resistance according to Direct-Q® 3 UV: 18.2 MΩ.cm

one elution process step in the following study. Multiple elution steps, as stated later on in the manuscript, means that the protocol was performed several times. In this case, the previous residue from an elution step was filtered off of the elution solvent without further drying or workup, 9 mL of fresh elution acid was refilled, and the elution process was started again.

2.2 | Characterization methods

2.2.1 | Powder X-ray diffraction (XRD)

Powder XRD data were collected on a STOE STADI P powder diffractometer (Cu-$K_{\alpha1}$ radiation ($\lambda = 1.54051$ Å, Ge-monochromator) equipped with a *DECTRIS Mythen 1 K* detector. The powder XRD data were derived from a 14-h measurement in a *Hilgenberg* glass capillary with 80-mm length, 0.5-mm outside diameter, and 0.01-mm wall thickness. The program package *STOE WinXPOW* was used to process the raw data for phase analysis performed in *Jana2006*.[22,23] Literature data for kaolinite,[24] quartz,[25] orthoclase feldspar,[26] muscovite,[27] and gorceixite[28] were used to identify the most probable phases occurring in RK1 and RK2. This selection of phases is based on the knowledge provided by AKW. We used the published structure models without refining of atomic coordinates or displacement parameters. Isotropic displacement parameters were set uniformly to a standard value of 0.02 Å^2 for all non-hydrogen sites and 0.04 Å^2 for hydrogen sites. In order to allow a certain deviation from the published lattice parameters for each phase due to substitutions and impurities in natural minerals, we allowed the refinement of the lattice parameters of each component. We found a maximum deviation of 0.21% for the lattice parameters in our refinements compared with literature values. A detailed summary of the lattice parameters is given in Table S2. We refined the fractions of the five different phases neglecting the occurrence of additional phases which might be present in our samples. As a final outcome of such a rudimentary refinement, we estimated the overall composition of the samples based on these five components.

2.3 | Analytical methods

2.3.1 | Inductively coupled plasma optical emission spectrometry (ICP-OES)

The resulting samples were analyzed with an *Agilent 725* (ICP-OES) spectrometer with radially viewed plasma to determine the amount of REEs and other metals. The ICP-OES equipment includes a *VistaChip II CCD* detector that provides a complete wavelength range from 167 to 785 nm. Additionally, the ICP-OES system is equipped with an *Agilent SP3* auto-sampler, which allows automatic measurement. The operating conditions are shown in Table S1. Five points were measured for the calibration line (50, 10, 1, 0.1 mg/L, and blank). The resulting samples were diluted in the ratio 19:1 and then measured. The measurement data was processed using the software *Agilent ICP Expert II*. The ICP standards used are listed in Table 2.

2.3.2 | X-ray fluorescence (XRF)

XRF data were recorded on a *S8 LION* X-ray spectrometer from Bruker AXS. The dried sample was reduced to the required amount by a sample divider. Then the sample was ground in the analytical mill for 12 min. The sample material is homogenized in a Turbula mixer for 5 min after the addition of two *Widia* balls. After removal of the balls, the homogenized powder is pressed into a tablet using a press and pressing tools. In a drying cabinet (2 h) or microwave (2 min), the ground sample was dried. The dried sample was then mixed with the flux agent lithium tetraborate, melted in a muffle furnace at 1150°C for 15 min, poured onto a platinum-gold mold, and then rapidly cooled with compressed air. This was followed by the measurement. The measurement data were processed using the software *SpectraPlus*. Each sample was measured for 60 s.

2.3.3 | Scanning electron microscopy (SEM)

The samples were prepared on a steel holder with a double-sided conductive adhesive tape from Plano GmbH. Scanning electron microscope (SEM) images were collected by a Jeol JSM-IT200 InTouchScope™ electron microscope, and the acceleration voltage was set to 10 kV.

TABLE 2 ICP standards used for quantitative analyses.

Substance	Manufacturer	Quality
Rare earth element mix for ICP	Merck	50 mg/L: Sc, Y, La, Ce, Pr, Nd, Sm, Eu, Gd, Tb, Dy, Ho, Er, Tm, Yb, and Lu in 2% nitric acid
ICP multi-element standard solution IV	Merck	1000 mg/L: Ag, Al, B, Ba, Bi, Ca, Cd, Co, Cr, Cu, Fe, Ga, In, K, Li, Mg, Mn, Na, Ni, Pb, Sr, Tl, Zn

Note: ICP, inductively coupled plasma.

3 | RESULTS AND DISCUSSION

It has been shown that some natural sources of aluminosilicate minerals, such as kaolinite or feldspar, may contain up to 0.2 wt.% REEs.[29] REEs are often only physically adsorbed in the minerals or, in the case of kaolinite, intercalated between the mineral layers. These physisorbed ions are therefore rather easy to recover. The adsorption of cations in alumina-based minerals like kaolinite is enabled by the isomorphous substitution in the cation substructure of, that is, Si^{4+} against Al^{3+}, which induces a permanent negative charge in the aluminosilicates.[29] Unfortunately, the REE content in natural minerals is too low to be interesting for industrial REE recovery, and an enrichment of the REE content to significant levels > 2% is needed. Our intention with this study is to verify if accessible deposited industrial kaolinite residues are in principle suitable for REE recovery, and if a process can be developed to enable a more environmentally friendly REE recovery process than to entirely rely on the hazardous state-of-the-art production process.[30–32]

In the following paragraphs, we will illustrate that kaolinite residues, which are annually generated on a multi-ten-thousand-ton scale worldwide as a discarded side product, are suitable source for REE production. In our study, we concentrated our interest on residues from AKW, Germany. For this study, the kaolinite samples from AKW were eluted in various inorganic acids, and the amount of REEs was determined by ICP-OES in the obtained elution media.

3.1 | Phase analysis of kaolinite residues

The aim of this study is to evaluate the efficiency of elution processes for REE recovery from kaolinite residues that emerge after industrial kaolinite refinement. We used various forms of residues from AKW that were separated from the main products and deposited after the refinement process (RK1 and RK2) as well as samples (RK3 to RK15) taken at different steps in the separation and purification process. Natural kaolinite sources usually contain kaolinite as a major phase and also several other side phases. For raw material from AKW, the most likely ones are α-quartz, orthoclase feldspar, muscovite, and gorceixite.[25–28] Multiple separation steps are required to separate the different phases and to purify the single phases prior to the usage. The raw material at AKW is treated in a magnetic separation process, whereby the purer stream is separated from the magnetic impure side stream. Usually, kaolin and all other minerals that contain magnetic cations like Fe^{3+} are colored and are therefore separated from the white residues by a refinement process using strong magnets. This magnetic side fraction was concentrated in this process and formed the RK2 residue. RK1 resulted from another separation process step during the kaolin production that did not use magnetic separation. RK1 and RK2 are major residues that are produced on a multi-thousand-ton-scale annually at AKW and are deposited after the refinement process. On the other hand, RK3–RK15 are side residues in lower amounts, which occur during the refinement process at different stages within the industrial workup process of kaolin. Due to the overall low amount of REEs in RK3 to RK15 (see later on in the elution chapter of this study), we decided to perform a phase analysis for RK1 and RK2 only, because they are relevant for REE recovery due to their availability and the REE content. In addition, RK1 had a higher weight percentage of rare earth metals compared to samples RK3–RK15, which most likely resulted from abiotic environmental factors, for example, water (pH), light, atmosphere, temperature, and salinity.[33]

The powder diffraction pattern of the residue samples (RK1 and RK2) are shown in Figure 1. Beside $Al_2Si_2O_5[OH]_4$ (kaolinite)[24] itself, major expected side phases like SiO_2 (α-quartz),[25] $KAlSi_3O_8$ (orthoclase feldspar),[26] and $KAl_2(AlSi_3O_{10})(F,OH)_2$ (muscovite)[27] are denoted. Due to an XRF analysis provided by AKW (see Tables S3–S6) that contained Ba and phosphate as minor components we added $BaAl_3(PO_4)(PO_3OH)(OH)_6$ (gorceixite)[28] as an additional and most-probable phase in the XRD phase analysis. Calculated reflection intensities based on published structure data of those compounds are drawn with negative intensity for better visibility and comparison. The main reflections in the powder diffractograms belong to kaolinite, and they are denoted with stars in Figures 1 and 2. According to the Rietveld refinement of RK1 and RK2, in total, five phases were identified and used for phase analysis: kaolinite (k), quartz (q), feldspar (f), muscovite (m), and gorceixite (g). The refinement for RK1 ensued following phase ratios (k/q/f/m/g): 80.3/5.1/11.2/3.1/0.3 atomic ratio, and for RK2 the 80.1/5.0/11.2/3.4/0.3 atomic ratio.

3.2 | Utilization of various kaolinite residues for REE recovery

3.2.1 | General aspects

In the first step, 15 local kaolinite clay mineral residues (RK1–RK15) were collected from different deposition spots and process steps during the kaolinite refinement at AKW to identify the most valuable samples for REE

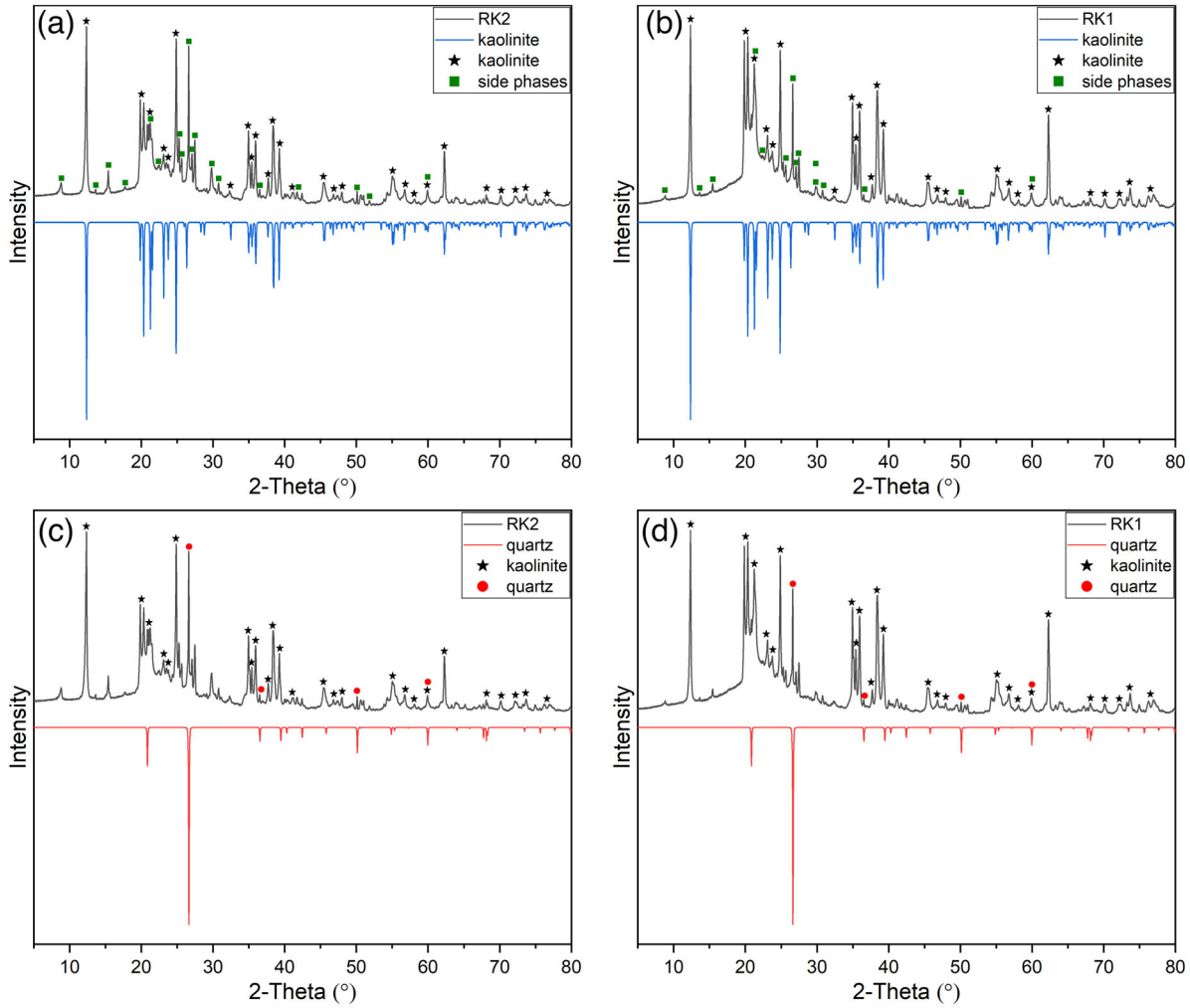

FIGURE 1 X-ray diffraction (XRD) data of RK1 (right) and RK2 (left) derived from a 14-h measurement in a capillary. Calculated diffractograms based on structure data of kaolinite[24] and quartz[25] are drawn with negative intensities. The main phase, kaolinite (star), and all side phase reflections (square) are denoted for the (a) RK2 and (b) RK1 samples; non-overlapping reflections of the minor phase, quartz (circle) are illustrated in the (c and d) diffractograms.

extraction. In a cation exchange elution process, we intend to extract as much REEs as possible rather than to perform a complete dissolution of the kaolinite matrix or to delaminate kaolinite into smaller fragments.

Grim et al. summarized the difference in the shape of adsorption isotherm for kaolinite and showed a variation depending on the cation-exchange capacity (CEC),[14] which describes the number of how many cations can be ingested between the negatively charged interlayer in the soil. The CEC depends on the size of the cation; the larger the ionic radius, the higher the relative adsorption.[14] The relation of hydration and interlayer expansion of dehydrated and contracted particles along the adsorption isotherms is described in five steps by adsorbing water molecules.[34] The ability to absorb water in the interlayer is proportional to the cation exchange capacity per unit area.[34]

Hendricks et al. discussed the cation exchange of crystalline silicates.[19] In general, silicate structures are determined by the ratios of negative ions (usually oxygen of the silicate units) to positive ions, the ratios of the ionic radii which determine the coordination number of cations, and a principle of microscopic neutrality.[19] The cations are located in the vicinity of the excess negative charge of the silicate framework to conform to the conditions of microscopic neutrality. Typically, the negative position in the lattice structure is caused by the replacement of low by higher charged cations, such as M^{2+} for M^{3+}, often showing a similar radius. The anion framework of kaolinite consists of octahedrally arranged oxide ions around aluminum (Al^{3+}) and tetrahedrally coordinated silicon cations (Si^{4+}), respectively. Due to this structure, the migration of ions through the layers is prevented. The compensation of the excess negative charge

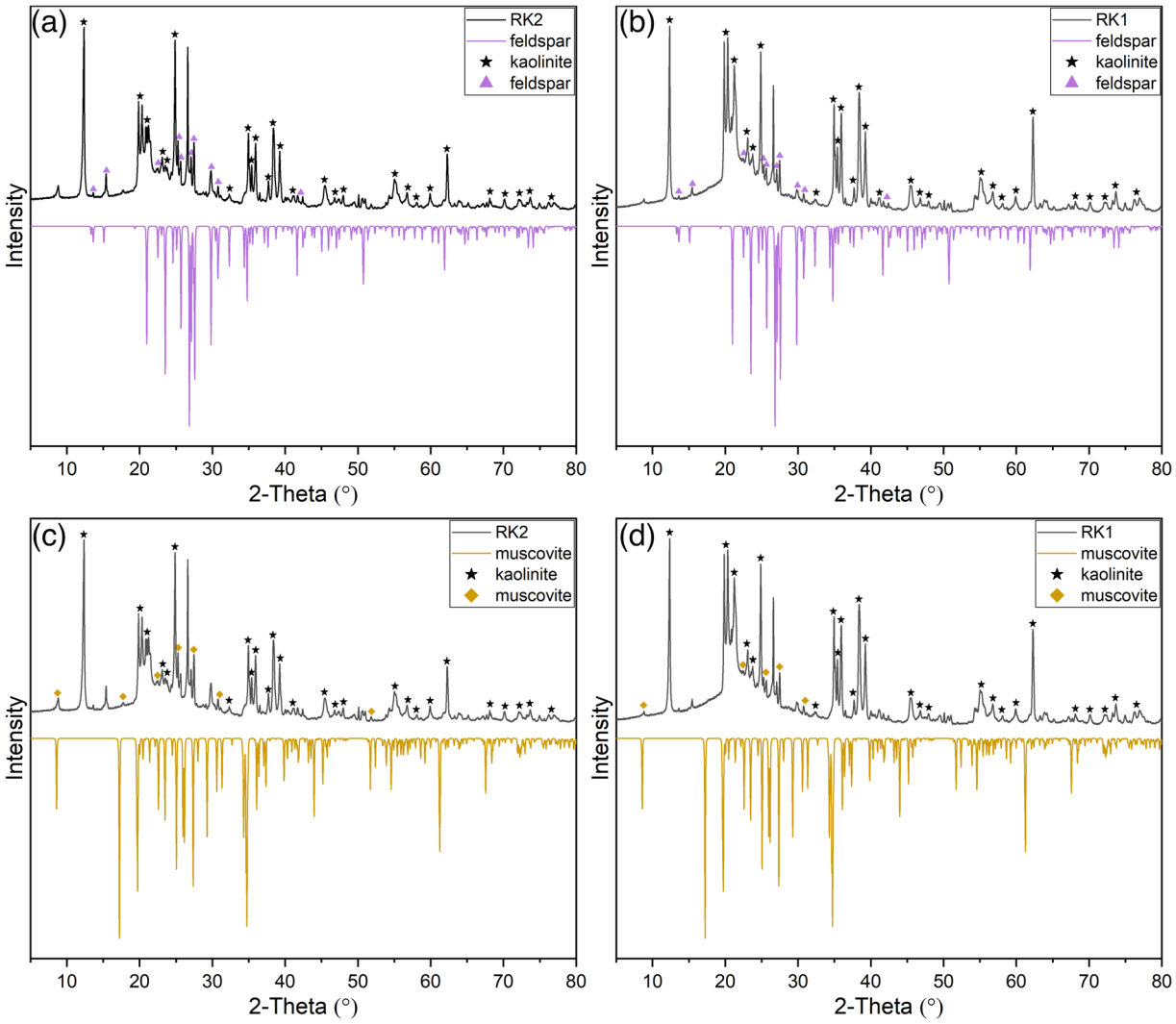

FIGURE 2 X-ray diffraction (XRD) data of RK1 (right) and RK2 (left) derived from a 14-h measurement in a capillary. Calculated diffractograms based on structure data of feldspar[26] and muscovite[27] are drawn with negative intensities. The main phase, kaolinite (star), and non-overlapping reflections of the minor phases, feldspar (triangle) and muscovite (diamond), are marked in the (a–d) diffractograms.

can only be achieved by external cation exchange in the interlayers to ensure the neutrality requirement.[19] The cation exchange by H^+ follows this principle, the positively charged cations in the interlayers are exchanged with H^+ in a stepwise manner migrating them out of the kaolinite framework. We took SEM images of selected samples before and after the elution process. Neither a significant change in morphology nor a tendency for degradation/delamination of the materials after the ion exchange could be observed. Selected SEM images are summarized in Figures S1 to S4.

Such an exchange procedure would allow an energy- and resource-effective elution process at low temperatures and with economic usage of elution solvents, most probable in a continuous, resource-efficient, and closed process cycle. Price and availability (even in existing industrial processes at kaolinite manufacturers) were the primary reasons for the examination of standard acids (HCl, HNO_3, and H_2SO_4) for the elution process. After the elution of REEs from the kaolin residues, the intention is to adsorb the REEs on cyanobacterial biomass from the diluted solutions that are generated by the process to make them accessible for further workup processes. Recently, this process was reported showing the efficiency of REE recovery.[21] Here, the influence of the concentration of REEs, the acidity of the solvent, and the type of REEs on the adsorption capacity of different cyanobacteria was evaluated. Five cyanobacteria (*Nostoc* sp. 20.02, *Synechococcus elongatus* UTEX 2973, *Calothrix brevissima* SAG34.79, *Desmonostoc muscorum* 90.03, and *Komarekiella* sp. 89.12) were identified that are capable to adsorb reasonable amounts of REEs. Dependent on the conditions, these cyanobacteria were able to absorb 84.2–91.5, 69.5–83.4, 68.6–83.5, 44.7–70.6, and 47.2–

67.1 mg g^{-1} (milligram REEs per gram dry biomass), respectively. After drying and burning the biomass, the accumulated REEs can be transferred to their respective oxides in a concentrated form, which are then ready for subsequent separation processes. This represents the first step towards an economic and environment-friendly process for biosorption-based REE recovery.

In the following discussion throughout the paper, the given results always refer to the sample mass and represent only the recovered amount of REEs in the investigated soil sample. Naturally, a certain fraction of REE cations remain physisorbed in the kaolinite residue.

3.2.2 | Elution of kaolinite residues for REE recovery with concentrated acids

A total number of 15 samples from AKW (RK1 to RK15) were analyzed as potential candidates for REE elution. Concentrated nitric acid (67%), sulfuric acid (96%), and concentrated hydrochloric acid (30%) were used as elution media.

A first series of elution experiments was conducted with concentrated (67%) nitric acid (Figure 3a). The results of this experiment series show that for samples RK3–RK15, only a certain low weight proportion of REEs (between 0.1 and 0.2 g/kg) can be extracted. In contrast, the aforementioned samples, RK1 and RK2, contain high amounts of accessible REEs. Those two samples are discussed in more detail as follows.

Elution in concentrated nitric acid yields a REE weight proportion of 1.13 g/kg for RK2 and 0.79 g/kg for RK1 (Figure 3a), respectively. To verify the elution efficiency, the overall REE content of these two samples by complete dissolution of the samples in HF/H_2SO_4 was determined. Obviously, RK1 adsorbed significantly less REEs than RK2. An overall REE content of 2.48 g/kg for RK2 was determined and 0.93 g/kg for RK1 (see also Figure 3, HF/H_2SO_4 column). Around 45.6% of REEs are recovered in RK2 in one extraction step, while this percentage increases to 84.9% for RK1. The elements Ce, La, Nd, Pr, and Y represent the majority of the retrieved REEs in the systems and belong to the LREEs (light rare earth elements, La-Sm) group in good accordance with the natural abundance.

For this purpose, the REEs were recovered by an ion exchange mechanism in which the adsorbed REEs in the mineral is exchanged by H^+ ions of the acid.[35–37] REE cations are transferred by this simple leaching process into solution with nitrate, chloride, or sulfate as counter ions. There are numerous studies on such a cation exchange reported in the literature.[38–40] Beside studies on minerals, they also include cation extraction in hyperaccumulator plants, seaweed, and algae.[38,41,42] Ion exchange is based on the chemical equilibrium in which the cations are exchanged and the state of equilibrium is influenced by the substance concentration. Accordingly, the adsorbed ions are displaced by the excess of other ions. Therefore, a higher concentration of acid leads in principle to a higher weight fraction of extracted REEs.

After the promising results for elution with concentrated nitric acid, the behavior of concentrated sulfuric acid (96%) and concentrated hydrochloric acid (30%) as elution media was investigated in order to optimize the elution process (Figure 3b and c). Using concentrated hydrochloric acid, a higher percentage of REEs can be obtained than with the previous method. Amounts of 1.89 g/kg (76% elution rate) for RK2 and 0.90 g/kg (97% elution rate) for RK1 were realized. A set of experiments using concentrated sulfuric acid indicates a slightly higher elution efficiency for RK1 but less efficiency for RK2. For RK2 and RK1, 1.73 g/kg (70%) and 0.95 g/kg (102%) could be recovered, respectively. Evidently, an efficiency of 102% is not possible, and one has to take the experimental errors during elution and elemental analysis into account. Additionally, the results can also be influenced by the inhomogeneity of the clays. It is obvious that the pH value plays a crucial role in the elution process and anions are not affecting the REE elution efficiency. Taking pKs values of the acids into account, the acid strength is $HCl > H_2SO_4 > HNO_3$ with values of -6, -3, and -1.32, respectively. This fits to the trend that HNO_3 shows the less-effective elution tendency followed by H_2SO_4 and HCl for RK2.

From our results, it can be concluded that there is no significant difference in the REE elution efficiency for RK 1 when different concentrated acids are used (see also Figure 4, right column). Concentrated sulfuric acid seems slightly more favorable than concentrated hydrochloric acid, but the elution appears to be almost quantitative for all cases. Nevertheless, all studied processes show a one-step elution efficiency greater than 85%.

Amounts of 0.87 g/kg in concentrated hydrochloric acid, 0.93 g/kg in concentrated sulfuric acid, and 0.79 g/kg in concentrated nitric acid were recovered for RK1 (Figure 4). The total REE content of 0.95 g/kg was determined by hydrofluoric acid dissolution of RK1. This total amount is only marginally higher than the amount of REEs found after a one-step elution process with all concentrated acids. As shown in Figure 4, the dissolving capability of RK1 for each concentrated acid is saturated at over 85%.

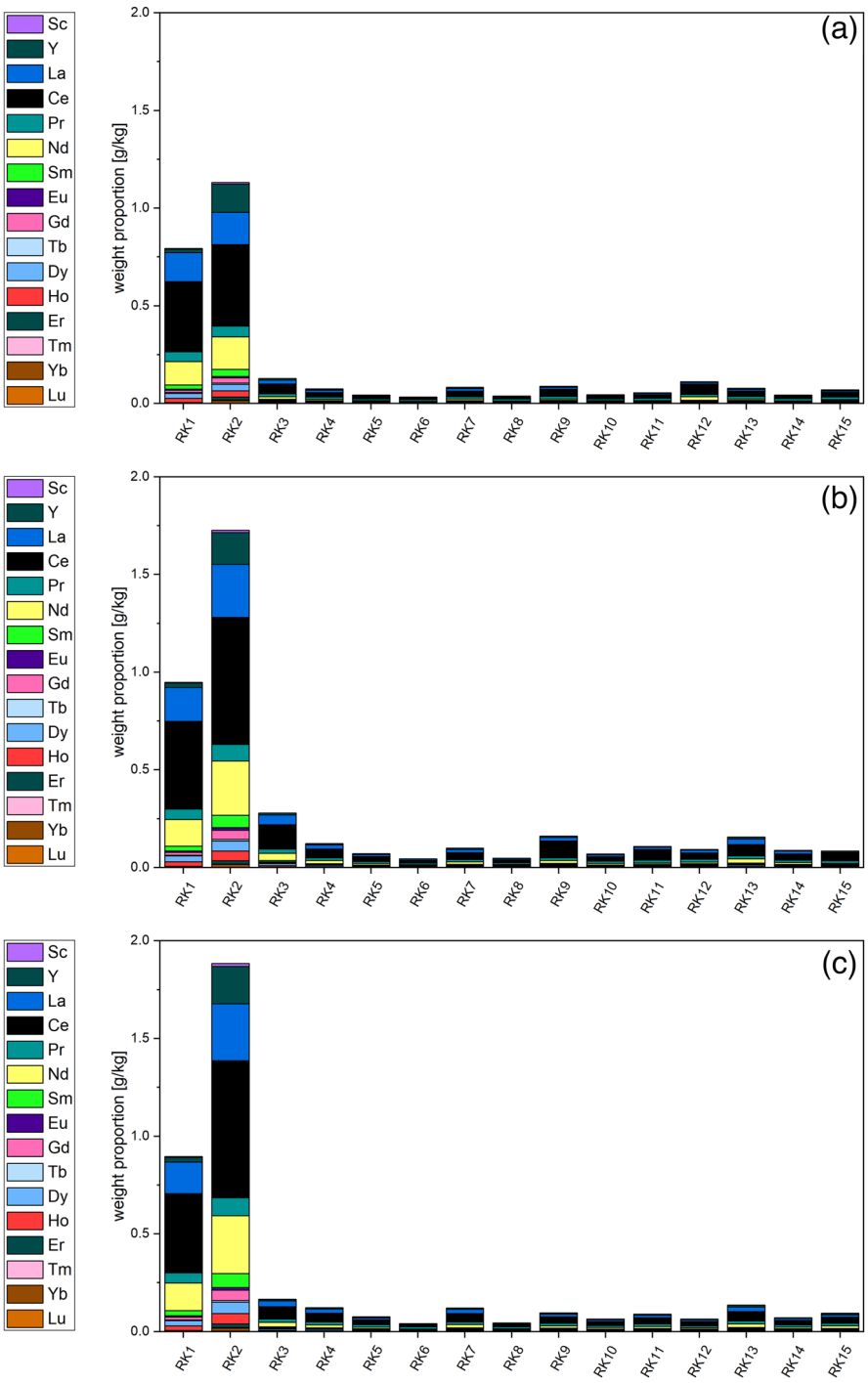

FIGURE 3 Weight proportion of REEs from different soil samples after concentrated acid treatment. (a) HNO_3, (b) H_2SO_4, and (c) HCl. Based on the results, the LREEs (light rare earth elements) were mainly recovered from the residual kaolinites. The investigation of all samples showed that only RK1 and RK2 are suitable for REE elution due to their elevated REE content.

3.2.3 | Elution of kaolinite residues for REE recovery with diluted acids

One focus of our study is the optimization, cost reduction, and development of a more environmentally friendly REE-elution process from kaolinite. Therefore, in order to pursue these objectives, we have replaced the concentrated mineral acids with diluted ones and verified the elution efficiency of these reagents.

In this regard, we have conducted a series of analogous elution experiments with diluted nitric acid (15%), hydrochloric acid (5%), and sulfuric acid (19%)—a dilution factor of approximately 4.5 compared to the concentrated acids. In Figure 4, it becomes evident that concentrated acids are beneficial for a one-step elution process for RK2. Between 46% and 76% of REEs can be accessed in a single elution step, resulting in weight fractions larger than 1 g/kg in all cases. This one-step

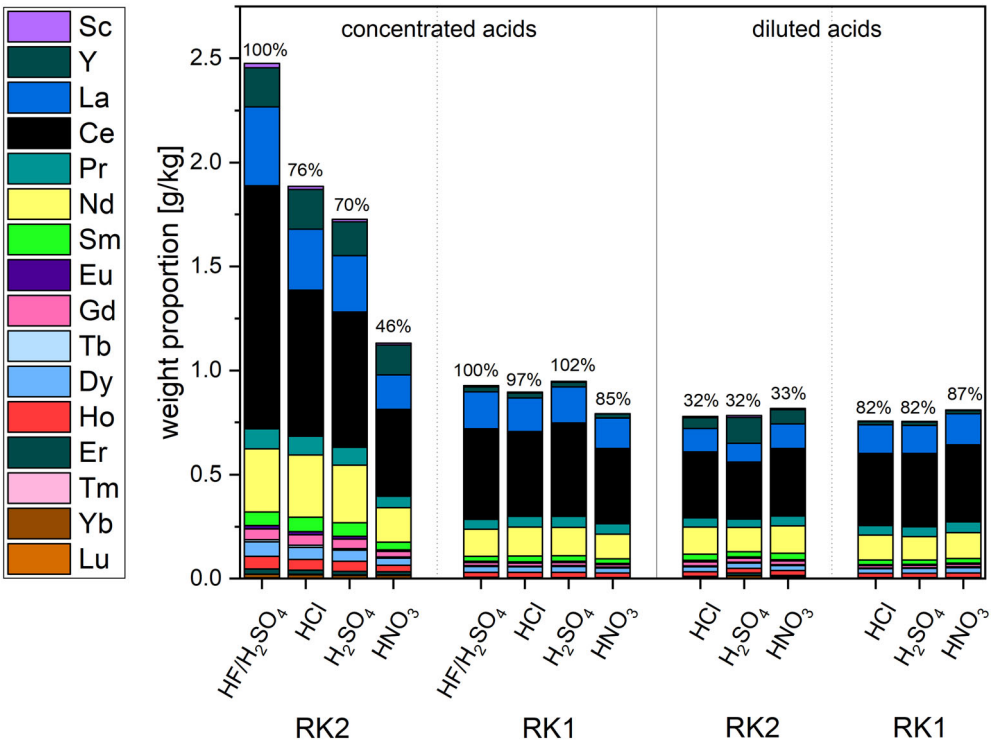

FIGURE 4 Summary of REE weight proportions after a single elution process from different soil samples RK2 and RK1. Concentrated (left set of columns) and diluted acids (right set of columns) are shown. RK2: Conc. hydrochloric acid 1.89 g/kg, conc. sulfuric acid 1.73 g/kg, and conc. nitric acid 1.13 g/kg of REEs were achieved after one single elution process from an overall REE content of 2.48 g/kg (HF/H_2SO_4 column). Using diluted acids for RK2, a single elution process resulted in values around 0.8 g/kg. RK1: almost the entire amount of REEs can be achieved in a single elution process using conc. acids. Amounts reaching 0.9 g/kg. Only conc. nitric acid is less effective with only 85% REEs. In the case of diluted acids, values of about 0.8 g/kg were observed.

efficiency drops to around 32% for diluted acids. In the case of RK1, the elution efficiency is significantly increased. Independent of the type and its concentration, this efficiency increases to values of 82 to >99%. Even the difference in efficiency for concentrated compared with diluted acids in the case of RK1 is marginal. Unfortunately, the accessed weight fraction of REEs is around 0.9 g/kg in all cases due to the overall lower REE content in RK1.

While the elution process for RK1 cannot be optimized further, there is potential for RK2. We therefore varied the elution acid amount and performed a multi-step elution to enhance the REE recovery outcome. Doubling the acid amount during one elution step did not significantly influence the elution efficiency for RK2, as illustrated in Figure 5. The elution capacity of the acids is therefore not the limiting factor in this process. However, the resulting weight proportion of REEs recovered remained approximately at 0.9 g/kg. Therefore, a multi-step elution process was tested to enhance the elution efficiency in the case of diluted acid treatment.

Here, an elution step was performed three times for RK2 using the same parameters as for the one-step case. With a total weight content REEs of 1.38 g/kg in a three-time elution process using diluted hydrochloric acid and 1.19 g/kg in diluted sulfuric acid, the weight proportions of REEs increased by 69% for hydrochloric acid, by 37% for sulfuric acid, and by 24% for nitric acid in comparison to a single step elution. After each elution step, the REE content in the elution medium was evaluated, and all results are summarized in Figure 5.

3.3 | Dissolution processes during REE recovery

Not only rare earth elements are accessed in the elution series. It is also necessary to determine the amount of non-REE ions that are accessed by the aforementioned processes. This knowledge is crucial for all upcoming processes like REE adsorption and enrichment using bacteria and REE separation in principle. All elements present in the elution solvents were quantified by ICP-OES analyses.

Out of all present elements in kaolinite (Figure 6, HF/H_2SO_4 column), mainly aluminum, iron, lead, alkali-

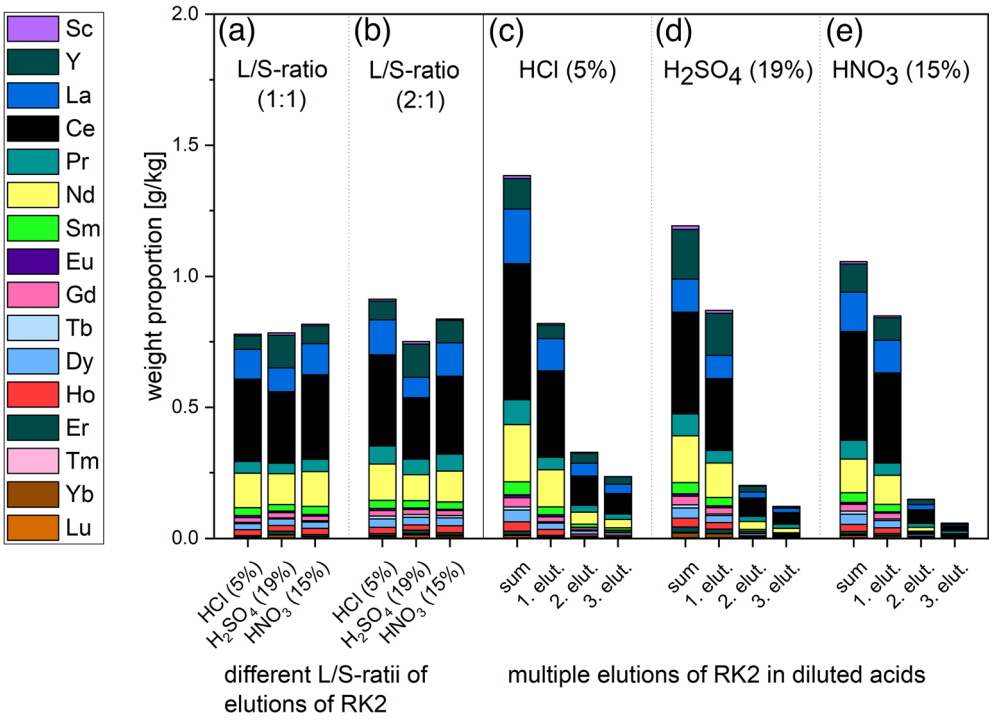

FIGURE 5 REE recovery from different soil samples after liquid/solid ratio variation and multiple diluted acid treatment. Results are denoted after varying the liquid–solid ratio (L/S ratio) from (a) 1:1 to (b) 2:1 in diluted HCl, dil. H_2SO_4, and dil. HNO_3. REE weight proportion of RK2 soil samples after diluted acid treatment in a multiple elution process (3 times) using (c) HCl, (d) H_2SO_4, and (e) HNO_3. After multiple elution of RK2 in dil. acids, an increase of REE recovery to 1.38 g/kg with HCl, 1.19 g kg with H_2SO_4, and 1.06 g/kg with HNO_3 were observed, which translates to 69% (dil. HCl), 37% (dil. H_2SO_4), and 24% (dil. HNO_3) increase compared with a one-step elution process (data see Figure 4).

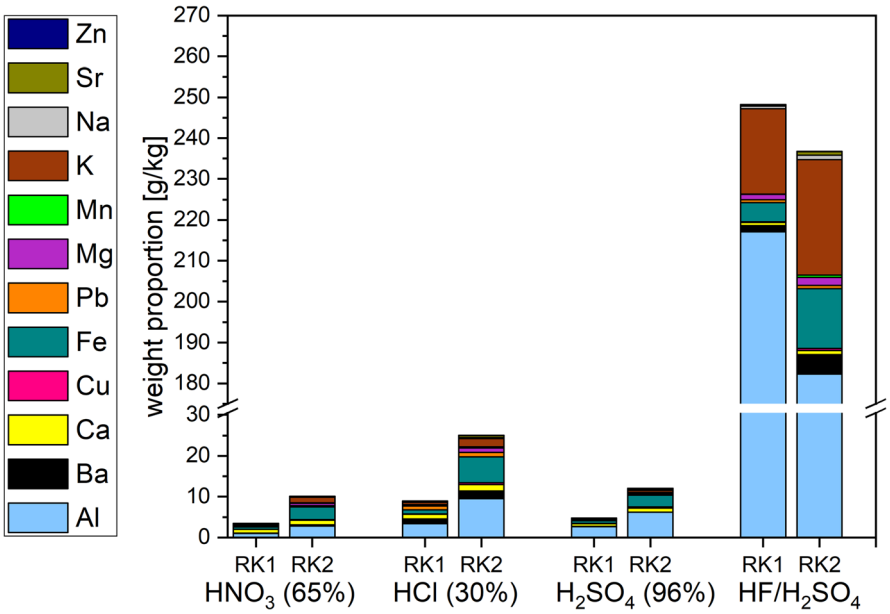

FIGURE 6 Weight proportion of non-REEs after elution of RK1 and RK2 samples in concentrated acids (HNO_3, HCl, and H_2SO_4). The HF/H_2SO_4 value represents the entire amount of all ions after dissolution. As expected for kaolinite, aluminum represents the main component.

and alkaline earth metals were found in solution. In Figure 6, the highest concentration of secondary metals (25.03 g/kg) was found after the elution of RK 2 in concentrated hydrochloric acid. In comparison, 8.94 g/kg is dissolved for RK1 in a similar process. The total metal ion contents after treatment of RK1 (4.18 g/kg) and RK2 (12.04 g/kg) with concentrated sulfuric acid are much lower than in concentrated hydrochloric acid and slightly

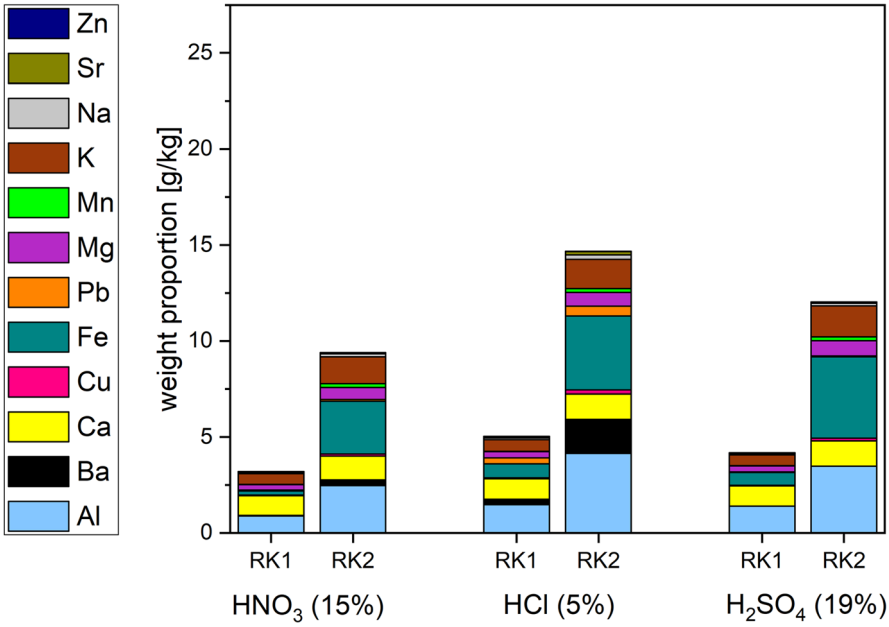

FIGURE 7 Weight proportion of non-REEs from RK1 and RK2 samples in diluted acids. (HNO_3, HCl, and H_2SO_4).

larger than in nitric acid (Figure 6). For the latter acid, we have achieved the lowest values of secondary metal extraction, 10.07 g/kg for RK2 and 3.44 g/kg for RK1.

High amounts of lead were observed after the hydrochloric acid process, and moderate amounts were retrieved with the nitric acid treatment. In contrast, no Pb^{2+} ions were found after sulfuric acid treatment due to the low solubility of $PbSO_4$ (Figures 6 and 7). K and Fe were dissolved in the expected large amounts. Still, the concentration of both elements is lower when using sulfuric acid compared to the other two acids. This phenomenon is most likely due to the solubility of the salts formed, which could be of interest for further processing of REEs.

The elution processes in concentrated sulfuric and nitric acid yielded similar amounts of non-REE metals. Again, the highest metal content was determined for the elution in concentrated hydrochloric acid (see Figure 6). Therefore, based on these data, the application of hydrochloric acid is rather unsuitable for REE recovery, particularly for the purification of the REE extracts.

The environmentally friendly elution in diluted nitric, hydrochloric, and sulfuric acid was investigated with regard to the secondary metals (Figure 7). For RK2, the proportion of metals is higher in hydrochloric acid (14.69 g/kg) than in the elution with nitric and sulfuric acid (9.38 and 12.03 g/kg, respectively). For RK1, the dissolution behavior is similar to RK2, except that the overall values are lower. The content of Fe ions is higher in RK2 than in RK1, which is a consequence of the fabrication process of RK2 where magnetic fractions were accumulated during the kaolinite purification process at AKW. Compared to elution with diluted sulfuric and nitric acid, the total non-REE metal contents after elution with concentrated acids are only slightly higher. The clear exception is hydrochloric acid. In this case, the differences in total proportions are minor, but the individual proportions differ to varying degrees, for example, the Al proportions (see Figures 6 and 7).

4 | CONCLUSIONS

In the present study, the elution of adsorbed REEs of 15 different kaolinite samples (RK1–RK15) was investigated using various acids in a microwave-assisted elution process. RK1 and RK2 samples showed the highest accessible REE outcome in weight percentages, while the other mineral samples (RK3-RK15) comprising only a minor proportion of REEs. After phase analysis, five different phases were identified in RK1 and RK2, although kaolinite is the major phase with contents >80%. The elution efficiency for REEs via ion exchange in concentrated acids for RK2 samples increases in the following order: $HNO_3 < H_2SO_4 <$ HCl. For RK1, similar efficiencies could be observed, as the REE accessibility for each concentrated acid lies well over 80%. During the applied elution process, secondary metal ions are eluted or dissolved from the samples. These metal ions are disadvantageous for the following REE separation and work up processes. According to our study, in the case where concentrated acids are applied, a sulfuric acid elution process seems to be the most preferable one.

Another intention of this study was to enable a more environmentally friendly REE recovery process by using diluted acids. With diluted acid solutions, the elution potential does not exceed a REE weight proportion of

0.8 g/kg when dissolving REEs from clays in an one-step elution process. Moreover, the elution efficiency can be enhanced through a multiple-step process. In the multiple-step process, the diluted hydrochloric acid provided the highest increase in REE content compared with a one-step elution process, with lower values for diluted sulfuric acid and for diluted nitric acid.

Furthermore, the application of diluted acids in an elution process is advantageous for subsequent process steps, such as the metal recovery by bio-sorption, which proceeds under pH 5–6 conditions. The optimization of the elution process, which is performed in a discontinuous batch process to a semi-continuous method, is a challenging task in the future. Future studies should address the potential of this developed elution process for the recovery of REE in large-scale industrial processes.

ACKNOWLEDGEMENTS

This work was funded by the Bavarian State Ministry of the Environment and Consumer Protection under the roof of the ForCycle II project group as subproject No. 8. (MiKa Project). M. Koch and M. Paper thank the TUM Graduate School for support. Open Access funding enabled and organized by Projekt DEAL.

CONFLICT OF INTEREST STATEMENT

All authors declare no conflict of interest. This manuscript has not been submitted or published elsewhere.

DATA AVAILABILITY STATEMENT

The data presented in this study are available upon request from the author.

ORCID

Tom Nilges https://orcid.org/0000-0003-1415-4265

REFERENCES

1. Ran X, Ren Z, Gao H, Zheng R, Jin J. Kinetics of rare earth and aluminum leaching from kaolin. *Minerals*. 2017;7(9):152. doi:10.3390/min7090152
2. Binnemans K, Jones PT, Blanpain B, et al. Recycling of rare earths: a critical review. *J Clean Prod*. 2013;51:1-22. doi:10.1016/j.jclepro.2012.12.037
3. Balaram V. Rare earth elements: a review of applications, occurrence, exploration, analysis, recycling, and environmental impact. *Geosci Front*. 2019;10(4):1285-1303. doi:10.1016/j.gsf.2018.12.005
4. Adler B, Müller R. *Seltene Erdmetalle: Gewinnung, Verwendung und Recycling*. Univ.-Verl; 2014. https://d-nb.info/1052037127/34
5. Huang XW, Long ZQ, Wang LS, Feng ZY. Technology development for rare earth cleaner hydrometallurgy in China. *Rare Met*. 2015;34(4):215-222. doi:10.1007/s12598-015-0473-x
6. U.S. Geological Survey. *Mineral commodity summaries 2023: US*; 2023, 21p. doi:10.3133/mcs2023
7. Yang M, Liang X, Ma L, Huang J, He H, Zhu J. Adsorption of REEs on kaolinite and halloysite: a link to the REE distribution on clays in the weathering crust of granite. *Chem Geol*. 2019;525:210-217. doi:10.1016/j.chemgeo.2019.07.024
8. Bear FE. *Chemistry of the soil*. Reinhold Pub. Corp.; 1965.
9. Aras A. The change of phase composition in kaolinite- and illite-rich clay-based ceramic bodies. *Appl Clay Sci*. 2004;24(3–4):257-269. doi:10.1016/j.clay.2003.08.012
10. Naijian F, Rudi H, Resalati H, Torshizi HJ. Application of bio-based modified kaolin clay engineered as papermaking additive for improving the properties of filled recycled papers. *Appl Clay Sci*. 2019;182:105258. doi:10.1016/j.clay.2019.105258
11. López-Galindo A, Viseras C, Cerezo P. Compositional, technical and safety specifications of clays to be used as pharmaceutical and cosmetic products. *Appl Clay Sci*. 2007;36(1–3):51-63. doi:10.1016/j.clay.2006.06.016
12. Morsy FA, El-Sherbiny S, Hassan MS, Mohammed HF. Modification and evaluation of Egyptian kaolinite as pigment for paper coating. *Powder Technol*. 2014;264:430-438. doi:10.1016/j.powtec.2014.05.040
13. Chapman HD. Cation-exchange capacity. Methods of Soil Analysis, Part 2: chemical and microbiological properties, 9.2. In: Norman AG, ed. *Agronomy monographs*; 1965:891-901. doi:10.2134/agronmonogr9.2.c6
14. Grim RE. *Clay mineralogy*. McGraw-Hill; 1968.
15. Peelman S, Sun ZH, Sietsma J, Yang Y. *Chapter 2—1 - Leaching of Rare Earth Elements: Review of Past and Present Technologies, Rare Earths Industry*. Elsevier; 2016:319-334. doi:10.1016/B978-0-12-802328-0.00021-8
16. Nie W, Zhang R, He Z, et al. Research progress on leaching technology and theory of weathered crust elution-deposited rare earth ore. *Hydrometallurgy*. 2020;193:105295. doi:10.1016/j.hydromet.2020.105295
17. Papangelakis VG, Moldoveanu GA. *Recovery of Rare Earth Elements from Clay Minerals*; 2014:191-202. https://www.eurare.org/docs/eres2014/fifthSession/VladimirosPapangelakis.pdf
18. Jun T, Jingqun Y, Kaihong C, Guohua R, Mintao J, Ruan C. Optimisation of mass transfer in column elution of rare earths from low grade weathered crust elution-deposited rare earth ore. *Hydrometallurgy*. 2010;103(1–4):211-214. doi:10.1016/j.hydromet.2010.04.003
19. Hendricks SB. Base exchange of crystalline silicates. *Ind Eng Chem*. 1945;37(7):625-630. doi:10.1021/ie50427a010
20. Sadri F, Rashchi F, Amini A. Hydrometallurgical digestion and leaching of Iranian monazite concentrate containing rare earth elements Th, Ce, La and Nd. *Int J Miner Process*. 2017;159:7-15. doi:10.1016/j.minpro.2016.12.003
21. Paper M, Koch M, Jung P, Lakatos M, Nilges T, Brück TB. Rare earths stick to rare cyanobacteria: future potential for bioremediation and recovery of rare earth elements. *Front Bioeng Biotechnol*. 2023;11:11. doi:10.3389/fbioe.2023.1130939
22. Stoe. *WinXPOW, version 3.05*. Stoe & Cie GmbH Darmstadt; 2011.
23. Petříček V, Dušek M, Palatinus L. Crystallographic computing system JANA2006: general features. *Z Kristallogr – Cryst Mater*. 2014;229(5):345-352. doi:10.1515/zkri-2014-1737
24. Neder RB. Refinement of the kaolinite structure from single-crystal synchrotron data. *Clays Clay Miner*. 1999;47(4):487-494. doi:10.1346/CCMN.1999.0470411

25. Antao SM. Quartz: structural and thermodynamic analyses across the [alpha] [left right arrow] [beta] transition with origin of negative thermal expansion (NTE) in [beta] quartz and calcite. *Acta Crystallogr*. 2016;72B(2):249-262. doi:10.1107/S205252061600233X
26. Tseng HY, Heaney P, Onstott TC. Characterization of lattice strain induced by neutron irradiation. *Phys Chem Miner*. 1995;22(6):399-405. doi:10.1007/BF00213338
27. Ishida K, Hawthorne FC. Far-infrared spectra of synthetic dioctahedral muscovite and muscovite–tobelite series micas: characterization and assignment of the interlayer I–O_{inner} and I–O_{outer} stretching bands. *Am Mineral*. 2013;98:1848. doi:10.2138/am.2013.4282
28. Dzikowski TJ, Groat LA, Jambor JL. The symmetry and crystal structure of gorceixite, $BaAl_3[PO_3(O,OH)]_2(OH)_6$, a member of the alunite supergroup. *Can Mineral*. 2006;44:951-958. doi:10.2113/gscanmin.44.4.951
29. Moldoveanu GA, Papangelakis VG. Recovery of rare earth elements adsorbed on clay minerals: I. Desorption mechanism. *Hydrometallurgy*. 2012;117-118:71-78. doi:10.1016/j.hydromet.2012.02.007
30. Xie F, An Zhang T, Dreisinger D, Doyle F. A critical review on solvent extraction of rare earths from aqueous solutions. *Miner Eng*. 2014;56:10-28. doi:10.1016/j.mineng.2013.10.021
31. Royen H, Fortkamp U. *Rare Earth Elements—Purification, Separation and Recycling IVL*. Vol. C211. Swedish Environmental Research Institute Ltd; 2016:7-17. ISBN 978-91-88319-12-8. https://www.ivl.se/download/18.694ca0617a1de98f47387e/1628417155010/FULLTEXT01.pdf
32. Tunsu C, Petranikova M, Gergorić M, Ekberg C, Retegan T. Reclaiming rare earth elements from end-of-life products: a review of the perspectives for urban mining using hydrometallurgical unit operations. *Hydrometallurgy*. 2015;156:239-258. doi:10.1016/j.hydromet.2015.06.007
33. Duman F. Uptake of mineral elements during abiotic stress. In: Ahmad P, Prasad M, eds. *Abiotic stress responses in plants*. Springer; 2015:267. doi:10.1007/978-1-4614-0634-1_15
34. Barshad I. Absorptive and swelling properties of clay-water system. *Clays Clay Miner*. 1952;1(1):70-77. doi:10.1346/CCMN.1952.0010108
35. Bian X, Yin S, Luo X, Wu W. Leaching kinetics of bastnaesite concentrate in HCl solution. *Trans Nonferrous Met Soc Chin*. 2011;21(10):2306-2310. doi:10.1016/S1003-6326(11)61012-1
36. Feng X, Long Z, Cui D, Wang L, Huang X, Zhang G. Kinetics of rare earth leaching from roasted ore of bastnaesite with sulfuric acid. *Trans Nonferrous Met Soc Chin*. 2013;23(3):849-854. doi:10.1016/S1003-6326(13)62538-8
37. Kim R, Cho H, Han KN, Kim K, Mun M. Optimization of acid leaching of rare-earth elements from Mongolian apatite-based ore. *Minerals*. 2016;6(3):63. doi:10.3390/min6030063
38. Moldoveanu GA, Papangelakis VG. An overview of rare-earth recovery by ion-exchange leaching from ion-adsorption clays of various origins. *Mineralogical Mag*. 2016;80(1):63-76. https://www.cambridge.org/core/journals/mineralogical-magazine/article/an-overview-of-rareearth-recovery-by-ionexchange-leaching-from-ionadsorption-clays-of-various-origins/A66B33EA2ACEC14361B71E7736C1D382. doi:10.1180/minmag.2016.080.051
39. Chour Z, Laubie B, Morel JL, et al. Recovery of rare earth elements from Dicranopteris dichotoma by an enhanced ion exchange leaching process. *Chem Eng Process - Process Intensification*. 2018;130:208-213. doi:10.1016/j.cep.2018.06.007
40. Motsi T, Rowson NA, Simmons MJH. Adsorption of heavy metals from acid mine drainage by natural zeolite. *Int J Miner Process*. 2009;92(1–2):42-48. doi:10.1016/j.minpro.2009.02.005
41. Figueira MM, Volesky B, Ciminelli VST, Roddick FA. Biosorption of metals in brown seaweed biomass. *Water Res*. 2000;34(1):196-204. doi:10.1016/S0043-1354(99)00120-7
42. Schiewer S, Volesky B. Modeling of the proton-metal ion exchange in biosorption. *Environ Sci Technol*. 1995;29(12):3049-3058. doi:10.1021/es00012a024

SUPPORTING INFORMATION

Additional supporting information can be found online in the Supporting Information section at the end of this article.

How to cite this article: Koch M, Paper M, Brück TB, Nilges T. Rare earth element stripping from kaolin sands via mild acid treatment. *Asia-Pac J Chem Eng*. 2024;19(2):e3018. doi:10.1002/apj.3018

Supporting Materials section

Table S1: ICP-OES operating conditions.

power (kW) 1.20	power (kW) 1.20
Plasma gas (L/min)	15.0
auxiliary gas (L/min)	1.50
nebulizer gas (L/min)	0.55
viewing	radial
observation height (mm)	10
measurement period (s)	10.00
sampling time (s)	30
pump speed (rpm)	12
flushing time (s)	10
Repetition	5
analyte wavelength (nm)	Sc 361.383, Y 377.433, La 408.671, Ce 418.659, Pr 410.072, Nd 430.357, Sm 359.259, Eu 397.197, Gd 342.246, Tb 350.914, Dy 364.540, Ho 389.094, Er 349.910, Tm 313.125, Yb 369.419, Lu 261.541; Na 589.592, Mg 279.553, Al 396.152, K 766.491, Ca 396.847, Mn 257.610, Fe 238.204, Cu 327.395, Zn 213.857, Sr 407.771, Ba 455.403, Pb 283.305
reference wavelength (nm)	Ar 420.067, 675.283, 703.025, 706.873, 737.212

Table S2: Refined and published lattice parameters of different phases used for Rietveld refinements of RK1 and RK2. Standard deviations of lattice parameters < 0.003 Å and cell volumes < 1 Å^3 unless otherwise stated.

Phase name	a [Å]	b [Å]	c [Å]	α [°]	β [°]	γ [°]	V [Å^3]	Literature
Kaolinite	5.1535(9)	5.154(4)	7.401(10)	84.23(9)	75.388(5)	60.177(4)	164.96(2)	[24]
Kaolinite	5.164	5.157	7.398	84.24	75.297	60.081	165.08	own refinement parameters used for RK1 and RK2
Feldspar	8.5912(9)	13.0009(14)	7.1919(7)	90	116.009(2)	90	721.9(2)	[26]
Feldspar	8.578	12.984	7.212	90	115.984	90	722.0	own refinement parameters used for RK1 and RK2
Quartz	4.9134(1)	4.9134(1)	5.405(1)	90	90	120	113	[25]
Quartz	4.917	4.917	5.410	90	90	120	113.3	own refinement parameters used for RK1 and RK2
Muscovite	5.236	9.08	20.677	90	95.751	90	978.1	[27]
Muscovite	5.251	9.06	20.154	90	96.207	90	953.4	own refinement parameters used for RK1 and RK2
Gorceixite	7.0538(3)	7.0538(3)	17.2746(6)	90	90	120	744.363(2)	[28]
Gorceixite	7.062	7.062	17.233	90	90	120	744.208	own refinement parameters used for RK1 and RK2

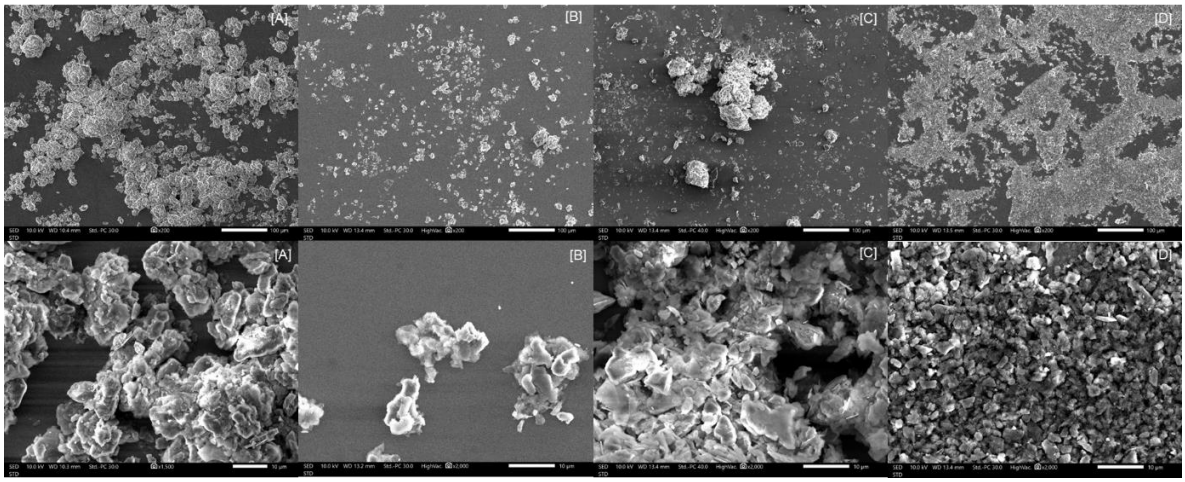

Figure S1: Scanning electron microscope image of residual kaolinite 1 (RK1) – top 200x and bottom 2000x magnification: [A] before treatment with concentrated acid. [B] after elution in concentrated nitric acid. [C] after elution in concentrated hydrochloric acid. [D] after elution in concentrated sulfuric acid.

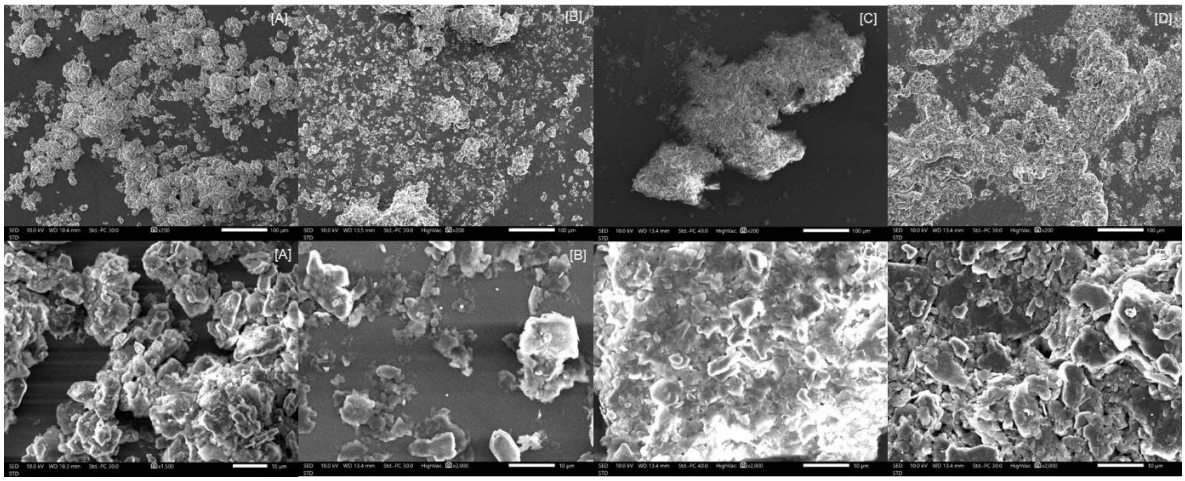

Figure S2: Scanning electron microscope image of residual kaolinite 1 (RK1) – top 200x and bottom 2000x magnification: [A] before treatment with diluted acid. [B] after elution in diluted nitric acid. [C] after elution in diluted hydrochloric acid. [D] after elution in diluted sulfuric acid.

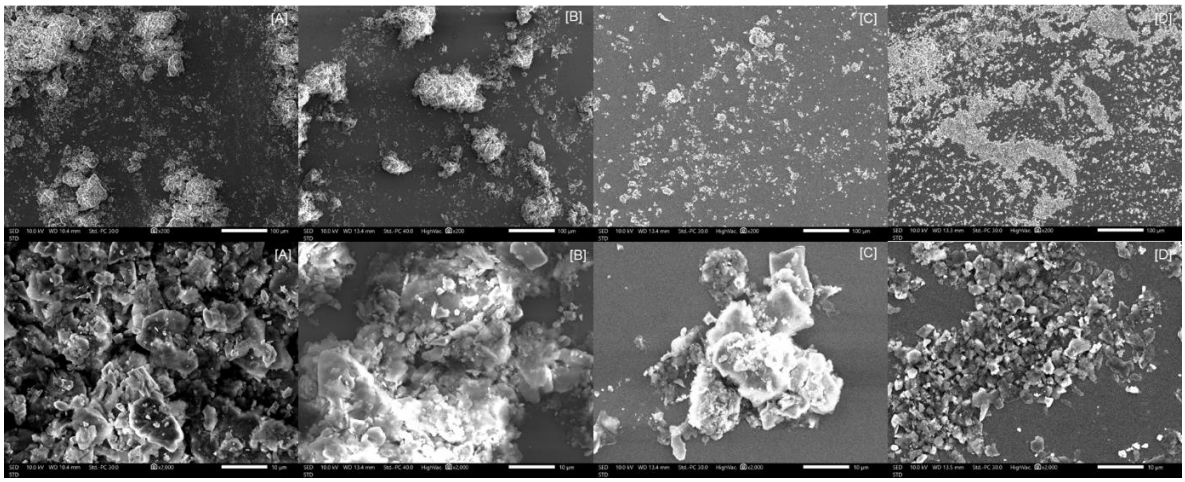

Figure S3: Scanning electron microscope image of residual kaolinite 2 (RK2) – top 200x and bottom 2000x magnification: [A] before treatment with concentrated acid. [B] after elution in concentrated nitric acid. [C] after elution in concentrated hydrochloric acid. [D] after elution in concentrated sulfuric acid.

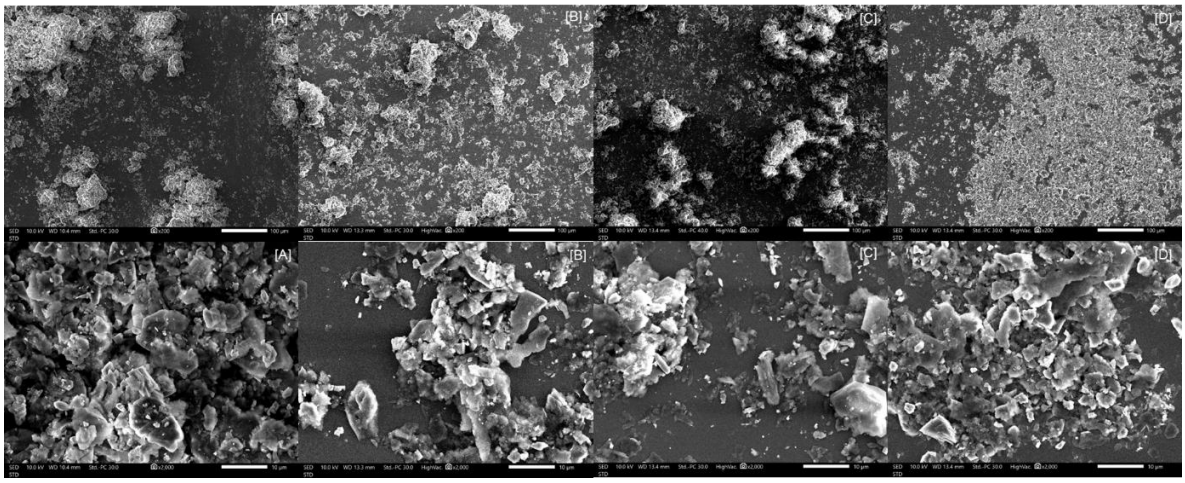

Figure S4: Scanning electron microscope image of residual kaolinite 2 (RK2) – top 200x and bottom 2000x magnification: [A] before treatment with diluted acid. [B] after elution in diluted nitric acid. [C] after elution in diluted hydrochloric acid. [D] after elution in diluted sulfuric acid

Table S3: X-ray fluorescence (XRF) of RK1. Standard deviations are < 0.2 at%.

	Values in [at. %]		Values in [at. %]
SiO_2	49.3	Si	23.0
Al_2O_3	34.6	Al	18.3
Fe_2O_3	0.7	Fe	0.5
TiO_2	0.5	Ti	0.3
CaO	0.1	Ca	0.08
MgO	0.3	Mg	0.2
Na_2O	0.02	Na	0.01
K_2O	2,0	K	1.7
P_2O_5	0.4	P	0.2
BaO	0.2	Ba	0.2
LOI (=loss on ignition)	11.6	-	-

Table S4: X-ray fluorescence (XRF) of RK2. Standard deviations are < 0.2 at%.

	Values in [at. %]		Values in [at. %]
SiO_2	46.6	Si	21.8
Al_2O_3	31.1	Al	16.5
Fe_2O_3	3,0	Fe	2.1
TiO_2	3.0	Ti	1.8
CaO	0.2	Ca	0.1
MgO	0.5	Mg	0.3
Na_2O	0.1	Na	0.08
K_2O	3.1	K	2.6
P_2O_5	1.1	P	0.5
BaO	0.6	Ba	0.6
LOI (=loss on ignition)	10.4		

Table S5: Atomic ratio of RK1 for XRD and XRF. Standard deviations are < 0.2 at%.

	XRD - Values in [at. %]	XRF - Values in [at. %]
Al	18.5	18.3
Si	23.4	23.0
K	1.8	1.7
P	0.04	0.2
Ba	0.08	0.2

Table S6: Atomic ratio of RK2 for XRD and XRF. Standard deviations are < 0.2 at%.

	XRD - Values in [at. %]	XRF - Values in [at. %]
Al	18.5	16.5
Si	23.4	21.8
K	1.9	2.6
P	0.04	0.5
Ba	0.07	0.6

3.2 Rare earths stick to rare cyanobacteria: Future potential for bioremediation and recovery of rare earth elements

Michael Paper[a], Max Koch[b], Patrick Jung[c], Michael Lakatos[c], Tom Nilges[b], and Thomas B. Brück[a]

[a]Synthesis and Characterization of Innovative Materials, School of Natural Sciences, Department of Chemistry, Technical University of Munich, Garching, Germany

[b]Werner Siemens-Chair of Synthetic Biotechnology, School of Natural Sciences, Department of Chemistry, Technical University of Munich, Garching, Germany

[c]Integrative Biotechnology, University of Applied Sciences Kaiserslautern, Pirmasens, Germany

Frontiers in Bioengineering and Biotechnology, 11, 1130939
First published online: February 28th 2023
Link: `https://doi.org/10.3389/fbioe.2023.1130939`

This study aimed to investigate novel species of cyanobacteria that may be used in biosorption-based enrichment procedures for REE. This study evaluated twelve cyanobacterial strains, seven terrestrial and five aquatic. A molecular analysis of cyanobacterial biomasses was performed to determine their 16S rRNA gene sequences, considering many of these strains are novel environmental species. A Maximum Likelihood phylogenetic tree was created using the obtained sequences, indicatingd that the investigated strains exhibited a wide range of genetic diversity. Six newly gene sequences were discovered from the analysis of twelve cyanobacteria and subsequently added to the gene database. Additionally, the maximum adsorption capacity of four REE (lanthanum, cerium, neodymium, and terbium) was evaluated for all cyanobacterial strains. Following the selection of five suitable strains, cerium was utilized to examine the influencing factors that affect the metal absorption of biomass, such as pH value, contact time, metal concentration, and binding specificity. The highest adsorption was achieved at pH 5. Based on the kinetic results, all investigated biomasses attained the adsorption equilibrium capacity in a matter of minutes, demonstrating a quick adsorption process. Low concentrations of cerium could be absorbed by the examined cyanobacterial biomasses, and this capacity was best explained by fitting the identified data points into the Langmuir model. Research on binding specificity revealed that the biomass showed a greater affinity for lead and aluminum than for

cerium. Nevertheless, the analyzed biomass demonstrated superior cerium adsorption at low metal concentrations. The Rare Earth and Alkali Metals adsorbed on the cell surface can be replaced by an ion exchange process. This resulted in a metal analysis of the investigated solution. Biosorption on the cyanobacteria was very likely to occur on carboxyl and hydroxyl groups, as determined by FT-IR analysis. This research delved into examining the metal-sorption characteristics of newly discovered cyanobacteria, which have not been extensively studied before. These cyanobacterial biomasses show potential for use in upcoming biosorption methods aimed at recovering REE from metal-containing wastewater. The study involved refining essential factors affecting metal absorption by these biomasses and identifying the primary chemical mechanisms responsible for metal binding.

Author contributions: All authors contributed to the conceptualization of the study and the methodological approach design. Max Koch shares first authorship of this manuscript with Michael Paper and Patrick Jung. Max Koch was responsible for the quantitative analysis and data evaluation. Michael Paper wrote the manuscript's initial draft and he carried out the planning, execution of the experiments, and data analysis. Patrick Jung performed the execution of the phylogenetic analysis.

frontiers | Frontiers in Bioengineering and Biotechnology

TYPE Original Research
PUBLISHED 28 February 2023
DOI 10.3389/fbioe.2023.1130939

OPEN ACCESS

EDITED BY
Eduardo Jacob-Lopes,
Federal University of Santa Maria, Brazil

REVIEWED BY
Alexey Vladimirovich Safonov,
Frumkin Institute of Physical Chemistry and Electrochemistry (RAS), Russia
Ludmila Rudi,
Institute of Microbiology and Biotechnology of Technical University of Moldova, Moldova
Negrea Petryu,
Politehnica University of Timişoara, Romania
Liliana Cepoi,
Institute of Microbiology and Biotechnology of Technical University of Moldova, Moldova

*CORRESPONDENCE
Thomas B. Brück,
brueck@tum.de

†These authors have contributed equally to this work

SPECIALTY SECTION
This article was submitted to Bioprocess Engineering, a section of the journal Frontiers in Bioengineering and Biotechnology

RECEIVED 23 December 2022
ACCEPTED 31 January 2023
PUBLISHED 28 February 2023

CITATION
Paper M, Koch M, Jung P, Lakatos M, Nilges T and Brück TB (2023), Rare earths stick to rare cyanobacteria: Future potential for bioremediation and recovery of rare earth elements. *Front. Bioeng. Biotechnol.* 11:1130939. doi: 10.3389/fbioe.2023.1130939

Rare earths stick to rare cyanobacteria: Future potential for bioremediation and recovery of rare earth elements

Michael Paper[1†], Max Koch[2†], Patrick Jung[3†], Michael Lakatos[3], Tom Nilges[2] and Thomas B. Brück[1,4*]

[1]Werner Siemens-Chair of Synthetic Biotechnology, School of Natural Sciences, Department of Chemistry, Technical University of Munich, Garching, Germany, [2]Synthesis and Characterization of Innovative Materials, School of Natural Sciences, Department of Chemistry, Technical University of Munich, Garching, Germany, [3]Integrative Biotechnology, University of Applied Sciences Kaiserslautern, Pirmasens, Germany, [4]TUM AlgaeTec Center, Ludwig Bölkow Campus, Department of Aerospace and Geodesy, Taufkirchen, Germany

Biosorption of metal ions by phototrophic microorganisms is regarded as a sustainable and alternative method for bioremediation and metal recovery. In this study, 12 cyanobacterial strains, including 7 terrestrial and 5 aquatic cyanobacteria, covering a broad phylogenetic diversity were investigated for their potential application in the enrichment of rare earth elements through biosorption. A screening for the maximum adsorption capacity of cerium, neodymium, terbium, and lanthanum was conducted in which *Nostoc* sp. 20.02 showed the highest adsorption capacity with 84.2–91.5 mg g^{-1}. Additionally, *Synechococcus elongatus* UTEX 2973, *Calothrix brevissima* SAG 34.79, *Desmonostoc muscorum* 90.03, and *Komarekiella* sp. 89.12 were promising candidate strains, with maximum adsorption capacities of 69.5–83.4 mg g^{-1}, 68.6–83.5 mg g^{-1}, 44.7–70.6 mg g^{-1}, and 47.2–67.1 mg g^{-1} respectively. Experiments with cerium on adsorption properties of the five highest metal adsorbing strains displayed fast adsorption kinetics and a strong influence of the pH value on metal uptake, with an optimum at pH 5 to 6. Studies on binding specificity with mixed-metal solutions strongly indicated an ion-exchange mechanism in which Na^+, K^+, Mg^{2+}, and Ca^{2+} ions are replaced by other metal cations during the biosorption process. Depending on the cyanobacterial strain, FT-IR analysis indicated the involvement different functional groups like hydroxyl and carboxyl groups during the adsorption process. Overall, the application of cyanobacteria as biosorbent in bioremediation and recovery of rare earth elements is a promising method for the development of an industrial process and has to be further optimized and adjusted regarding metal-containing wastewater and adsorption efficiency by cyanobacterial biomass.

KEYWORDS

cyanobacteria, biosorption, mechanism, rare earth elements, ion exchange

1 Introduction

Rare Earth Elements (REE) consist of scandium, yttrium, and 15 elements of the lanthanide series. These elements have exceptional electromagnetic, catalytic, and optical properties making them crucial for the production and development of modern high-technology products. Due to their similar chemical properties, separating REE demands sophisticated industrial processes that are energy-intensive and use environmentally toxic chemicals (Haque et al., 2014). Standard methods, for example, apply metal leaching with acids or bases and extraction methods to purify REE (Opare et al., 2021). Moreover, REE production is focused on a few countries, resulting in an oligopoly that can dictate supply and price regimes. REE are crucial for technology transition towards a renewable energy-driven society. For instance, cerium or lanthanum have applications in catalysts for air purification or chemical processing. Other metals like neodymium or terbium are crucial for producing permanent magnets or modern LEDs (Charalampides et al., 2015; Shan et al., 2020). Hence, industrialized countries increasingly focus on alternative supply routes and the development of cost and ecologically compatible recycling routes. In this context, REE recovered from dilute mining or industrial wastewater, as well as, electronic waste streams are opening new, regional supply routes. Establishing new biotechnologically based REE recovery methods therefore leads to enhanced market stability and supply chain independence for industrialized regions, such as the EU. Hence, there is a growing interest in the recovery and recycling of REE from industrial wastewater streams (Li et al., 2013; Barros et al., 2019). Over the past decades, biosorption has been regarded as a relatively simple and cost-efficient method for wastewater treatment (Volesky 2001). It is a physicochemical process that involves a solid phase (biosorbent) consisting of organic biomass and a liquid phase containing the dissolved or suspended chemical compounds to be sorbed (sorbate) (Fomina and Gadd 2014). Biosorption has a wide range of potential applications in wastewater remediation, including the removal of organic substances like dyes, pharmaceuticals, or pesticides (Bell and Tsezos 1987; Aksu 2005; Crini and Badot 2008; Menk et al., 2019). However, most research on biosorption in conjunction with the removal of pollutants has been conducted on metals, including heavy metals, actinides, and lanthanides (Dhankhar and Hooda 2011; Abbas et al., 2014; Giese 2020; Mattocks and Cotruvo 2020). Yet, developed processes based on biosorption have not achieved a commercial breakthrough. For example, it has been shown that environmental factors, such as changes in the pH value, can alter the affinity of biomass towards different elements (Zinicovscaia et al., 2019). A low technology readiness level, including a poor understanding of the underlying mechanisms, kinetics, and thermodynamics of the process are areas that require more research (Fomina and Gadd 2014; Elgarahy et al., 2021). It is widely accepted that the chemical structure, in particular the composition of functional groups on the cell surface, profoundly influences the adsorption properties of biomass (Eccles 1999; Volesky 2007). These active moieties may include hydroxyl-, carboxyl-, carbonyl-, phosphate-, sulfonate-, amine-, amide-, and imide-groups, among many others. Studies on biological, physical, or chemical modification of biomass by adding functional groups have shown that it is possible to improve binding specificity and capacity for target sorbates (Wang and Chen 2006; Park et al., 2010; Abdolali et al., 2015; Ciopec et al., 2020). Especially the recovery of REE with chemically modified organic polymers has been the focus of recent studies (Gabor et al., 2017; Negrea et al., 2018; Negrea et al., 2020). Nevertheless, these resulting biosorbents are still inferior in target selectivity to chemically synthesized ion-exchange resins with a defined structure and composition (Gadd 2009). Due to the heterogeneity of functional groups on the cell surface of microbial biomass, binding specificity for elements remains a challenging factor for industrial applicability. The adsorption of heavy metals by eukaryotic algae and cyanobacteria is well documented (Al-Amin et al., 2021; Ankit et al., 2022). At present, the screening of new species regarding biosorption and potential novel applications in metal recovery remains of great interest due to high variability in cell wall composition and structure, resulting in differences in adsorption properties [e.g. (Micheletti et al., 2008)]. Cyanobacteria have shown promising adsorption properties for heavy metals, which could be used in the sequestration of metals from water on a technical scale. If similar adsorption properties exist for the bioremediation of REE has not been studied extensively yet. Moreover, the adsorption properties of terrestrial cyanobacteria were seldom investigated. Therefore, we taxonomically and biotechnologically identified new and promising cyanobacterial strains and evaluated their properties for REE adsorption. In this context, we also aimed to correlate taxonomic identity and adsorption characteristics. In this study, 12 cyanobacterial strains with broad phylogenetic origin and inhabiting different ecological habitats such as terrestrial, freshwater, and saltwater habitats were investigated for their potential applicability in an adsorption process for the enrichment of REE. Their phylogenetic relationship was determined using 16S rRNA sequences. The screening for maximum adsorption capacity with four different REE (i.e. lanthanum, cerium neodymium, and terbium), as well as the effect of several parameters on biosorption, including initial pH value, incubation time, and metal concentration for cerium, were evaluated. Additionally, binding specificity for cerium in the presence of other metal cations was investigated.

2 Materials and methods

2.1 Cultivation of cyanobacteria

12 cyanobacterial strains with broad phylogenetic origins and from different habitats were used for the study (Table 1). The cultures were inoculated with approximately 0.1–0.3 g of wet biomass from a stock culture (stored at 17°C and light, dark rhythm 16:8 h at 30 µmol photons $m^{-2} s^{-1}$) in 1 L bubble columns containing BG11 cultivation medium (Stanier et al., 1971) (or Spirulina-medium for *Limnospira*) (Andersen 2005) and cultivated at 23°C and light, dark rhythm 16:8 h at 300 µmol photons $m^{-2} s^{-1}$ photosynthetic photon flux density). All cultivated cells were harvested using filters (two sieves of 0.5 mm and 0.1 mm and finally paper filters of 40 µm openings), and wet biomass was dried by lyophilization. *Synechococcus elongatus* UTEX 2973 was cultivated in a 3.7 L Labfors 5 Photobioreactor (Infors GmbH, Sulzemoos, DE) in BG11 medium at 37°C and constant

TABLE 1 Overview of all investigated cyanobacteria strains in this study.

Strain	Strain number	Origin	Isolator, year	Order
Nostoc. (sp.)	20.02	Epiphytic on lichen *Peltigera* sp.; Germany	B. Büdel, 2000	Nostocales
Synechococcus elongatus	UTEX 2973	Freshwater, United States	J.Yu, 2011	Synechococcales
Desmonostoc muscorum	90.03, PCC 7906	Soil, United States	F. E. Allison, before 1930	Nostocales
Calothrix brevissima	SAG 34.79	Freshwater, Asia	Watanabe, before 1969	Nostocales
Komarekiella sp	89.12	Hypolithic on quartz, Namibia, South Africa	B. Büdel 1989	Nostocales
Limnospira maxima	SAG 49.88	Marine, Italy, Europe	Unknown, before 1988	Oscillatoriales
Limnospira platensis	SAG 85.79	Natron lake, Chad, Africa	G. Laporte, 1963	Oscillatoriales
Phormidium autumnale	97.20	small brook, polluted with sewage, Versasca Valley, Swiss, Europe	A. Zehnder, 1964	Oscillatoriales
Komarekiella sp	90.01	Chasmolithic in stone, South Africa	B. Büdel, 1990	Nostocales
Reptodigitus sp	92.01	Endophilic, South Africa	B. Büdel, 1992	Nostocales
Symphyonema bifilamentata	97.28	Soil, Switzerland	A. Zehnder, 1965	Nostocales
Scytonema hyalinum	02.01	Ephedaphic on arid soil, Namibia, Africa	S. Dojani, 2002	Nostocales

illumination at 300 µmol photons m^{-2} s^{-1}. During cultivation, the pH was kept at eight by adding CO_2 gas. Biomass was harvested by centrifugation after reaching the stationary phase.

2.2 Phylogenetic characterization of strains

About 50 mg of biomass from all cultures were collected during stationary growth phase and used for gDNA extraction with the DNeasy PowerSoil Pro Kit (Quiagen, Hildesheim, Germany) following the manufacturer's instructions. The 16S–23S ITS gene region was amplified by PCR in a 50 µL reaction using the primers Wil1 and Wil18 (Wilmotte et al., 1993) and ready-to-go PCR mini beads (GE Healthcare, Chicago, United Sates) in a MiniAmp Plus Thermal Cycler (Thermo Fisher Scientific, Waltham, United Sates). PCR products were checked by gel electrophoresis using 1% (w, v) agarose and the E-Gel Power Snap Electrophoresis System (Invitrogen, Waltham, United Sates). Subsequently, PCR products of the expected length were purified with NucleSpin Gel and PCR Clean-up Kit (Macherey-Nagel GmbH & Co. KG, Düren, Germany) following the DNA and PCR cleanup protocol and sent for Sanger sequencing to Genewiz, Azenta (Germany GmbH, Leipzig, Germany) using the primers Wil1, Wil4, Wil5, Wil10, Wil11, Wil16, and Wil18 (Wilmotte et al., 1993). The generated sequences were assembled with Geneious Prime (v2021.0.1) software package (Biomatters Limited, New Zealand) and compared to already submitted sequences of those strains from public culture collections in terms of authenticity using the BLAST tool of the National Center for Biotechnology Information (NCBI) GenBank. Sequences of strains that are novel were submitted to GenBank, and their accession numbers are given in the phylogenetic tree. The assembled 16S rRNA gene sequences and related sequences of cyanobacterial strains cited from GenBank were used for phylogenetic analyses, including *Gloeobacter violacaeus* as outgroup for the 16S rRNA gene alignment, applying the Muscle algorithm in Mega X (Kumar et al., 2018). The evolutionary model that was best suited for the database used was selected based on the lowest Akaike information criterion value and calculated in Mega X which was the RGT G + I model of nucleotide substitutions. The maximum likelihood method (ML) with 1,000 bootstrap replications was calculated with Mega X and Bayesian inference (BI) phylogenetic analyses, with two runs of eight Markov chains executed for one million generations with default parameters with MrBayes 3.2.1 (Ronquist and Huelsenbeck 2003). Each analysis reached stationarity (average standard deviation of split frequencies between runs <0.01) before the end of the run.

2.3 Metal analysis

The metal concentration in the analyzed solutions was determined via ICP-OES (Inductively Coupled Plasma Optical Emission Spectrometry) (Agilent 725 Series ICP Optical Emission Spectrometer, Agilent Technologies Inc., United Sates). A TraceCERT® Rare earth element mix for ICP with 16 elements from Sigma-Aldrich (Sigma-Aldrich, Taufkirchen, Germany) and a Certipur® ICP multi-element standard solution IV from Merck (Merck KGaA, Darmstadt, Germany) with 23 elements, were used as standards for calibration. Data analysis was done with ICP Expert II Agilent 725-ES Instrument Software Version 2.0 (Agilent Technologies Inc., United Sates).

2.4 Biosorption

Before the experiments, all biomass samples were washed three times with demineralized water to remove residual media components that could falsify the measurement results. The washed biomass was frozen at −80°C and lyophilized. Sorption experiments were carried out by incubating lyophilized biomass in metal solutions with a defined concentration. Each experiment was performed in triplicates. Metal uptake was determined by

comparing the metal concentrations before and after incubation. Prior to measuring the metal concentration, each sample was centrifuged at 10,000 rcf for 5 min at room temperature. The supernatant was subsequently used for analysis. The adsorption experiments in this study predominantly focused on cerium, as it is the most prevalent REE.

2.5 Adsorption capacity

Adsorption experiments were performed based on a methodology described in previous studies (Heilmann et al., 2015; Heilmann et al., 2021). To determine the metal adsorption capacity (Q) of the different strains, 10–20 mg of dry biomass of individual species were weighed into centrifuge tubes and incubated in 2 mL metal solutions for 3 h under constant shaking at room temperature. Subsequently, the adsorption of the metals to the biomass was determined by dividing the changes in metal concentration by the amount of incubated biomass (see Eq. 1).

$$Q = \frac{n_i - n_f}{m} = \frac{\left(c_i - c_f\right) \times V}{m} \quad (1)$$

with Q = adsorption capacity, n_i = initial amount of substance, c_f = final amount of substance after incubation, c_i = initial metal concentration, c_f = final metal concentration after incubation, V = volume, and m = weight of biomass.

For the determination of the maximal adsorption capacity during the screening, metal solutions with a concentration of 10 mM and an initial pH value of 5 ± 0.2 were used.

2.6 Adsorption kinetics

Experiments on adsorption kinetic were carried out by varying the incubation time of the biomass in cerium (III) nitrate solutions with a concentration of 10 mM and a pH-value of 5 ± 0.2. Samples for analysis were taken after an incubation time of 2 min, 5 min, 15 min, 30 min, and 60 min.

2.7 Effect of initial pH value

The influence of the pH value in metal biosorption was investigated similarly to the method previously described. The pH value of the applied metal solution was adjusted using hydrochloric acid and sodium hydroxide. Due to the formation of insoluble REE hydroxides at pH values above 7 (Plancque et al., 2003; Heilmann et al., 2021) the experiments were carried out ranging from pH 1 to 6.

2.8 Adsorption isotherms

Adsorption isotherms were studied by varying the metal concentration of solutions applied to the biomass samples between 0.5 and 10 mM. Samples were incubated for 1 h at room temperature under constant shaking and analyzed as previously stated. The adsorption isotherms were described using the Langmuir and Freundlich model (see Eqs. 2, 3). The Langmuir model is often used for the description of metal adsorption as it assumes adsorption in the form of a monolayer onto a surface containing a finite number of identical binding sites (Dada et al., 2012). By contrast, the Freundlich model assumes metal adsorption on non-identical bindings sites over a heterogeneous surface (Koong et al., 2013).

$$\text{Langmuir model: } Q_{eq} = Q_{max}\frac{K \times C_{eq}}{1 + K \times C_{eq}} \quad (2)$$

$$\text{Freundlich model: } Q_{eq} = K_f {C_{eq}}^{bf} \quad (3)$$

with Q_{eq} = adsorption capacity at equilibrium, Q_{max} = maximum adsorption capacity, K = Langmuir adsorption coefficient, K_f = Freundlich adsorption capacity constant, C_{eq} = metal concentration at equilibrium, and b_f = Freundlich isotherm constant.

Calculations for data analysis and model fitting were done using OriginPro 2020.

2.9 Adsorption specificity

Wastewater usually contains a mixture of different metal cations. In addition to examining the capacity for a single element of interest, it is therefore important to investigate whether some metal cations are adsorbed preferentially over others by the cyanobacterial biomass. Experiments were carried out with equimolar mixed-metal solutions with concentrations of 0.5–4 mM to investigate the binding specificity of the biomass for different metals. Following previous experiments on green algae and cyanobacteria by Klimmek (Klimmek 2003), the adsorption of cerium in the presence of aluminum, lead, nickel, and zinc was investigated. The uptake of metals by the biomass was measured using ICP-OES measurements, analogous to determining the adsorption capacity with single metal solutions.

2.10 FT-IR analysis

IR spectroscopy is a useful tool for the qualitative measurement of organic functional groups. In this study, IR spectroscopy was used to identify functional groups in cyanobacteria biomass samples and to detect possible interactions with metal cations. Samples were incubated in a cerium (III) nitrate solution (1 µmol 1 mg^{-1} biomass) for 2 h and subsequently lyophilized. IR spectra were recorded using a Nicolet iS50R FT-IR spectrometer from Thermo Fisher Scientific (Thermo Fisher Scientific, Waltham, United Sates) equipped with an iS50 ATR (Attenuated total reflection) multi-range, diamond sampling station. For each sample, IR spectra were obtained in a range from 400–4,000 cm^{-1}.

3 Results

3.1 Phylogenetic analysis

Twelve different cyanobacteria, including four strains from public culture collections and eight environmental isolates were investigated. The identity of all strains from public culture collections was confirmed

10.3389/fbioe.2023.1130939

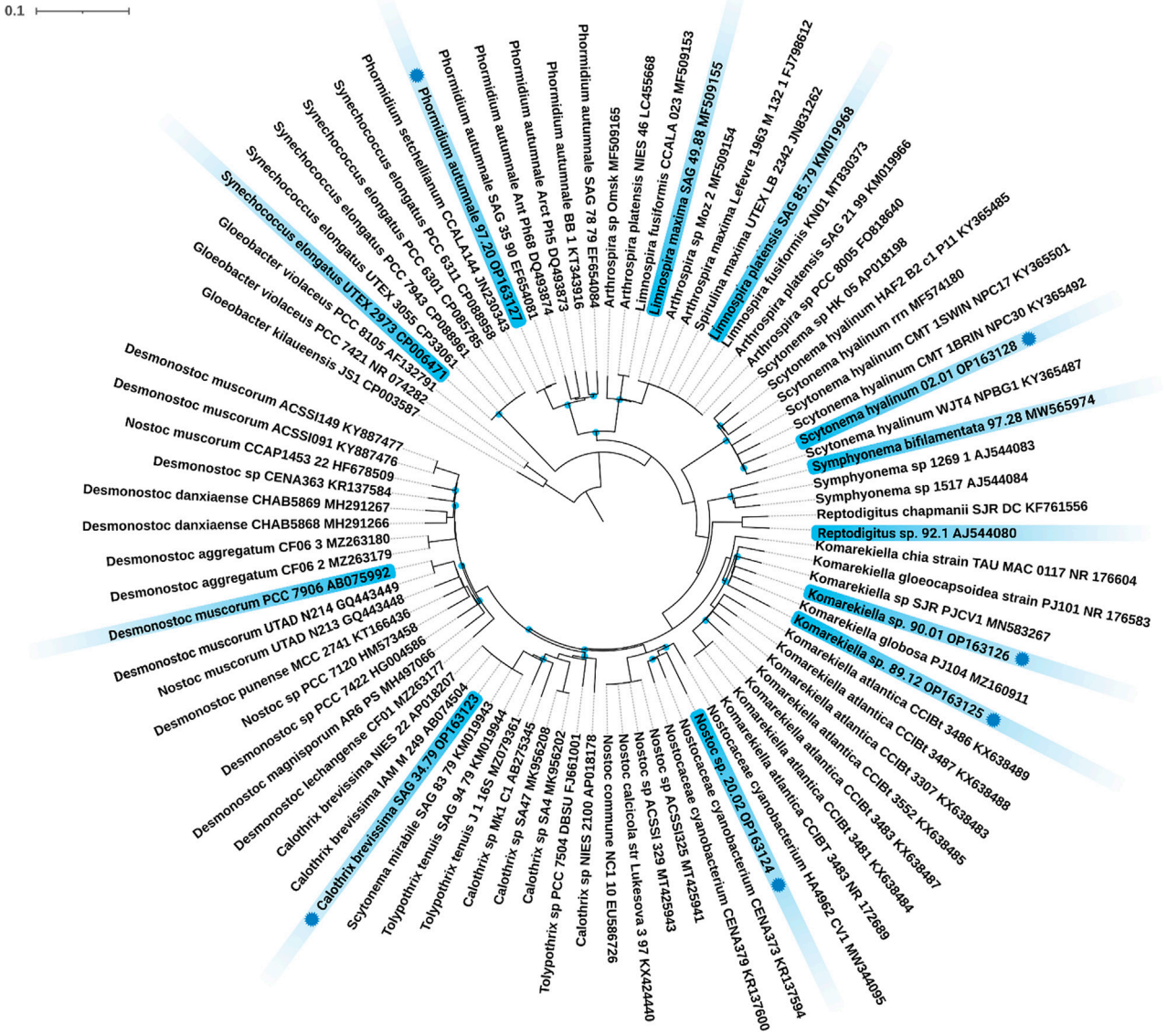

FIGURE 1
Maximum Likelihood (ML) phylogenetic tree based on the 16S rRNA gene region. Marked in blue are the twelve investigated strains including their strain number and NCBI accession number. Strains with a blue dot indicate novel 16S rRNA sequences generated during this study. Since the resulting Bayesian Inference (BI) and ML phylogenetic trees mostly showed the same topology, a single tree with both BI and ML bootstrap values is shown. Supports at the nodes greater than 90% statistical support from BI and ML represent posterior probabilities, and bootstrap values indicated as blue circles. The scale bar specifies 0.1 expected changes per site.

based on their 16S rRNA sequence using the BLAST tool of GenBank. The 16S rRNA sequences of the strains 97.20, 02.01, 90.01, 89.12, 20.02, and SAG 34.79 were originally recovered, and their phylogenetic position was analyzed (Figure 1). In detail, strains 90.01 and 89.12 clustered well supported within the filamentous, heterocyte-forming genus *Komarekiella* while strain 20.02 clustered within the genus *Nostoc sens. lat*. The strain *Calothrix brevissima* SAG 34.79 joined a cluster of other *C. brevissima* strains and strains assigned to the genera *Tolypothrix* and *Scytonema* with 100% identity. Strain 02.01 fell well supported in the large cluster of *Scytonema hyalinum,* whereas strain 97.20 could be assigned to *Phormidium autumnale* based on its high similarity with 16S rRNA sequences from other filamentous, non-heterocyte forming strains representing this species. Thus, the cyanobacterial strains represent a broad phylogenetic origin out of the three orders Synechococcales, Oscillatoriales and Nostocales, inhabiting different ecological habitats such as terrestrial, freshwater, and saltwater habitats and most are new for biotechnological applications, particularly for their adsorption process of REE.

3.2 Screening for maximum adsorption capacity

In this study, the maximum adsorption capacity for REE (cerium, neodymium, terbium, and lanthanum) of 12 different cyanobacteria was investigated. The results of this screening are shown in Figure 2,

10.3389/fbioe.2023.1130939

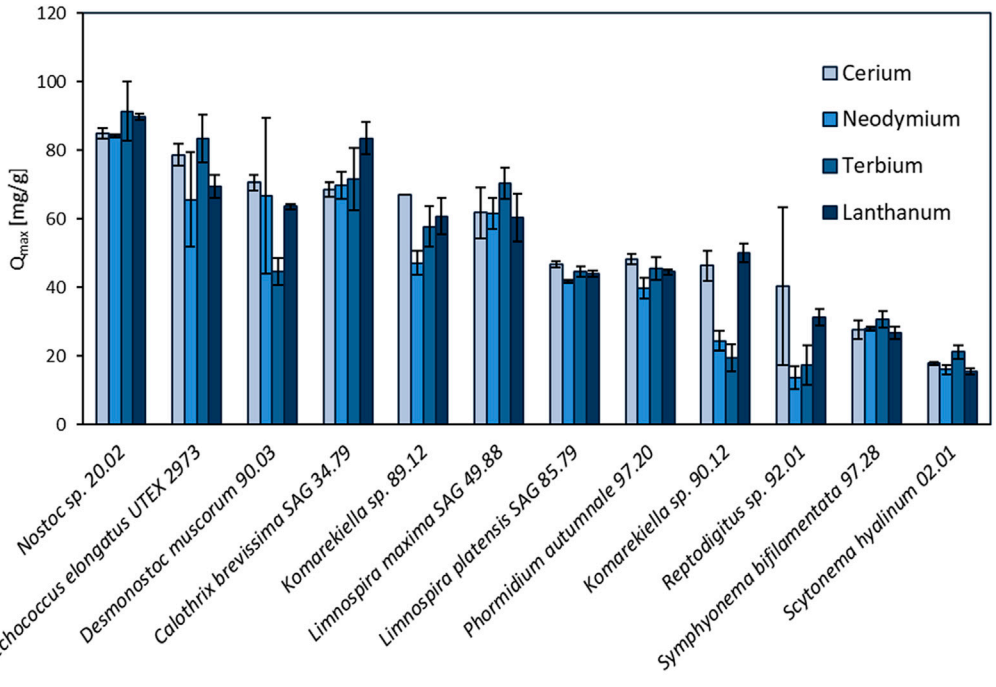

FIGURE 2
Screening of 12 different cyanobacteria for their maximum adsorption capacity (Q_{max}, mg REE g^{-1} dry mass) of cerium, neodymium, terbium, and lanthanum (pH: 5 ± 0.2, n = 3).

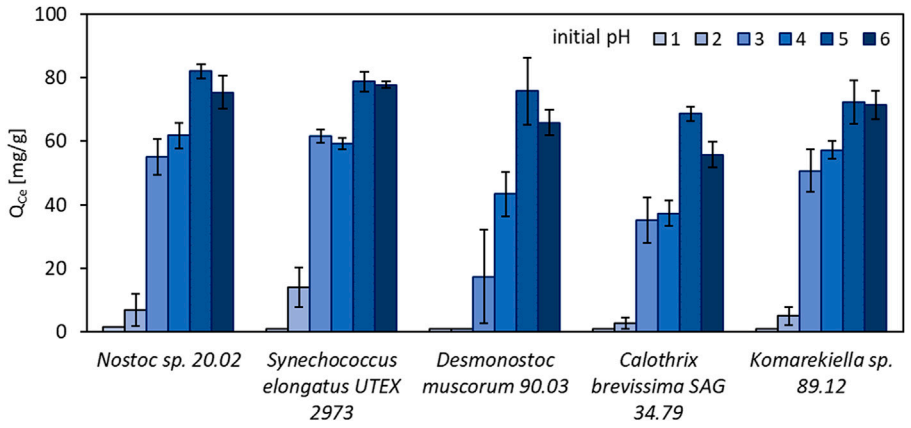

FIGURE 3
Adsorption capacity for Ce^{3+} (Q_{Ce}, mg Ce^{3+} g^{-1} dry mass) of different cyanobacteria in solutions with initial pH values between 1 and 6 (n = 3).

depicting distinct differences in total metal uptake depending on the species. There was no apparent correlation between the capacity for REE adsorption for the phylogenetic relationship and the ecological habitat. The highest overall metal uptake of the four tested REE was observed for *Nostoc* sp. 20.02 adsorption capacities between 84.2 and 91.5 mg g^{-1}, while *S. hyalinum* 02.01 exhibited the lowest maximum adsorption capacity with 15.5–21.2 mg g^{-1}. Based on these results, the biosorption properties of the five most efficient cyanobacteria (*Nostoc* sp. 20.02, *Synechococcus elongates* UTEX 2973, *Desmonostoc muscorum* 90.03, *C. brevissima* SAG 34.79, and *Komarekiella* sp. 89.12) were investigated in more detail.

3.3 Effect of different initial pH values on metal adsorption

The effect of the initial pH value of metal-solutions on biosorption of REE was examined in a pH range between 1 and 6. Experiments

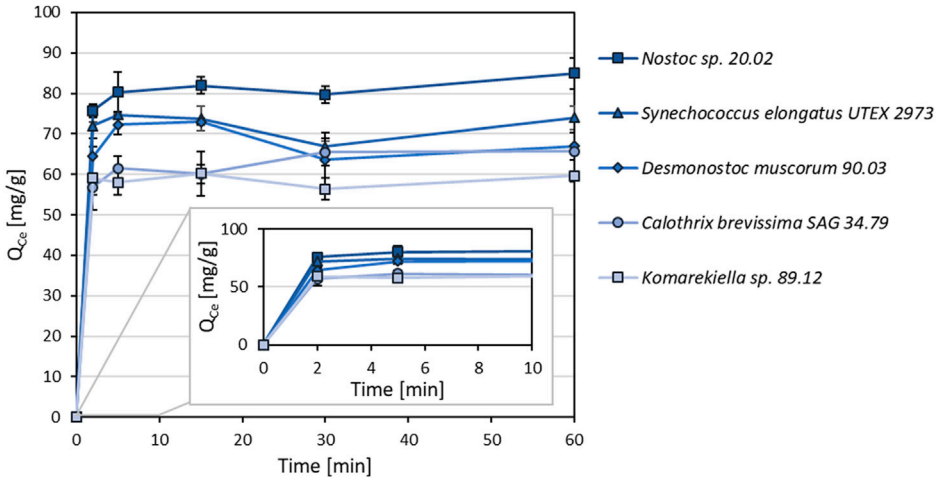

FIGURE 4
Adsorption kinetics of different cyanobacterial biomasses for Ce^{3+} (Q_{ce}, mg Ce^{3+} g^{-1} dry mass) with incubations times between 2–60 min (n = 3).

with 10 mM cerium (III) nitrate showed a strong influence of the pH value on metal adsorption (Figure 3). The highest metal uptake was observed at pH 5, with a minor decrease at pH 6. With increasing acidity, metal adsorption rapidly decreased. At pH 1, no notable metal adsorption was measured for all tested biomasses. These results are in accordance with previous studies on cyanobacteria, bacteria, and green algae regarding metal adsorption (Kuyucak and Volesky 1988; Gong et al., 2005; Lupea et al., 2012; Liang and Shen 2022).

3.4 Adsorption kinetics

As shown in Figure 4, metal adsorption for cerium (Ce^{3+}) to all tested cyanobacterial biomasses occurred rapidly. The adsorption capacity equilibrium was reached within an incubation time of 5 minutes. After this time, there was no significant change in adsorption capacity within 60 min.

3.5 Adsorption isotherms

For the intended application of cyanobacterial biomass for the removal of metals from wastewater, high sorption capacities at relatively low metal concentrations are beneficial. Sorption capacities for the biomass of five selected cyanobacteria species were investigated at concentrations between 0.5–10 mM. The resulting data points were fitted according to the Langmuir and Freundlich model. The best correlation was achieved using the Langmuir model (Figure 5). Although the overall correlation with the model was weak, maximum adsorption capacities predicted by the model are in accordance with the values determined during the screening experiments (Supplementary Tables S1, S2). Adsorption capacities for all tested cyanobacteria exhibited a steep increase at lower equilibrium metal concentrations, showing that sequestration of metals is possible even at low concentrations.

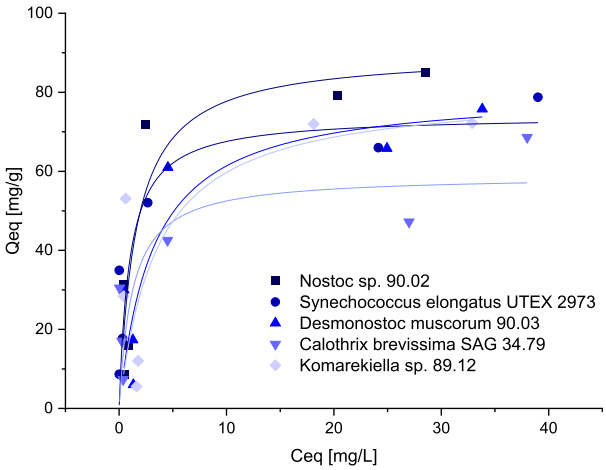

FIGURE 5
Isotherms for the adsorption of Ce^{3+} (adsorption capacity Q_{eq}, mg Ce^{3+} g^{-1} dry mass *versus* Ce^{3+}-concentration C_{eq}, mg L^{-1}) with biomass of five different Cyanobacteria, data points were fitted according to the Langmuir-model.

3.6 Binding specificity

The binding specificity of cyanobacterial biomass towards cerium was determined in adsorption experiments with other metals (Al, Pb, Ni, and Zn) in equimolar solutions. Starting with a concentration of 0.5 mM, the adsorption capacities were investigated for increasing metal concentrations up to 4 mM. The experiments showed that all elements could be adsorbed by the tested biomass. However, the metal uptake for some elements varied strongly amongst the tested metals (Figure 6). The adsorption capacity for zink and nickel was the lowest, whereas for cerium, the tested biomass showed the highest adsorption capacity in solution with a concentration of 0.5–2.0 mM. Nevertheless, the adsorption capacity for cerium in mixed metal solutions was

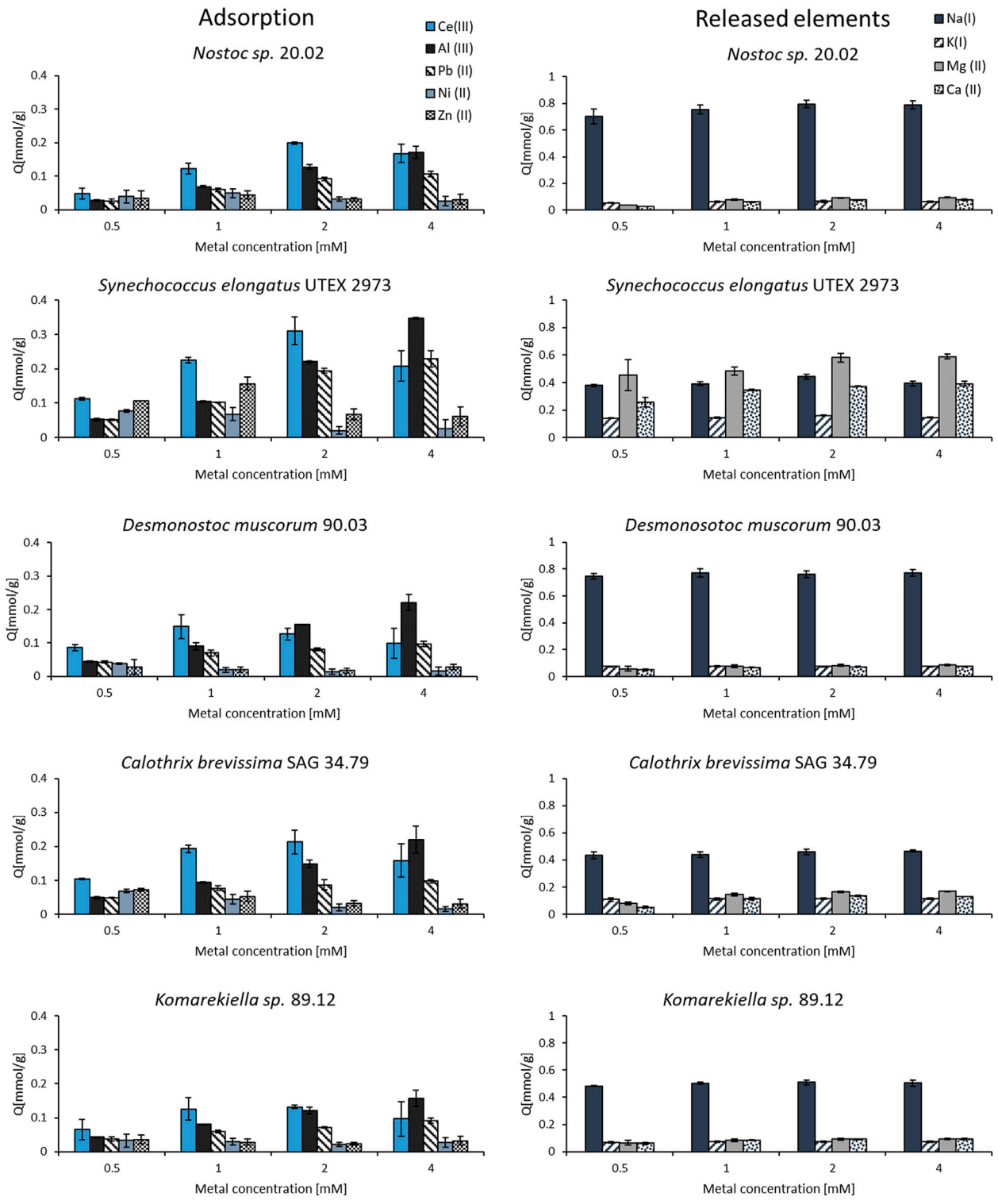

FIGURE 6
Adsorption and release of elements from biomass incubated in equimolar mixed-metal (Ce, Al, Pb, Ni, and Zn) solutions with concentrations between 0.5–4.0 mM (n = 3).

significantly lower compared to experiments with single-element solutions in previous experiments. This indicates a competition of different elements for the same, limited binding sites on the biomass. The metal uptake of aluminum and lead steadily increased with rising metal concentrations. At a metal concentration of 4 mM, these elements even seemed to replace cerium as the binding capacity for this element dropped for all tested cyanobacteria biomasses. The analysis of metal concentrations via ICP-OES revealed a release of

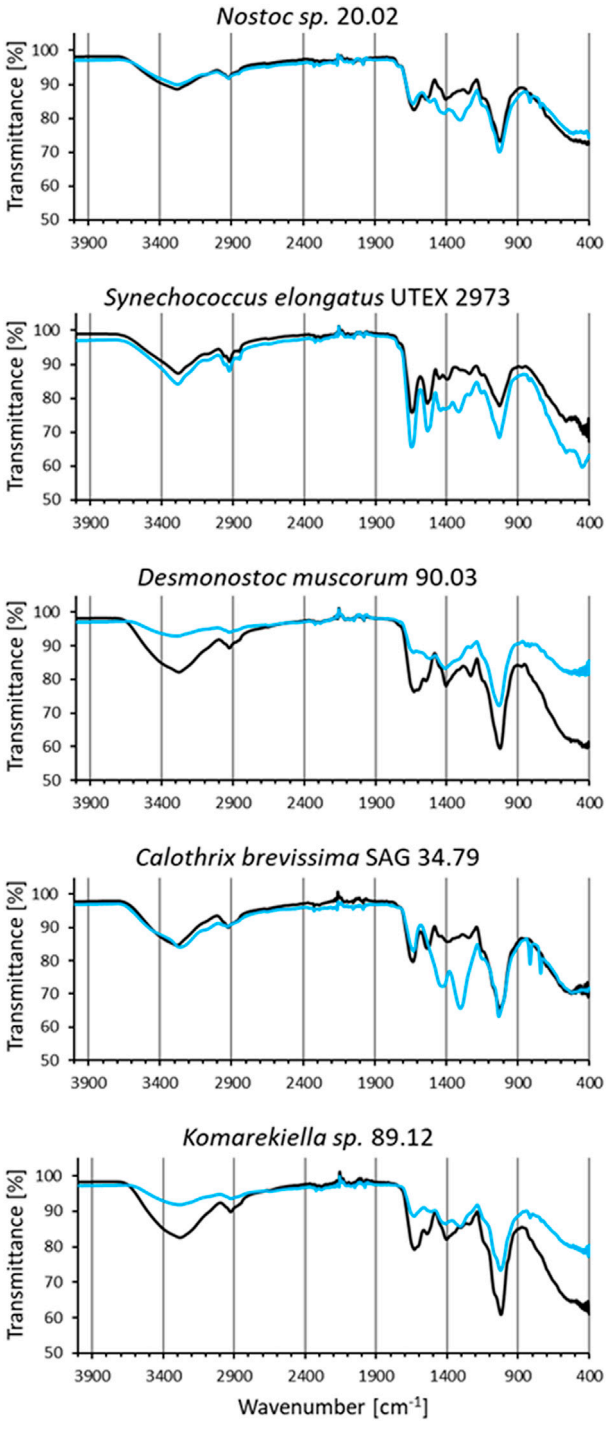

FIGURE 7
FT-IR spectra of biomass samples before (black) and after incubation in cerium (III) nitrate solution (1 µmol mg^{-1} dry mass) (blue).

alkaline and alkaline earth metals (Na, K, Mg, and Ca) during the adsorption process. The concentration of these elements increased after incubating the biomass in the equimolar metal solutions containing Ce, Al, Pb, Ni, and Zn. By contrast, mixing the biomass with pure demineralized water did not lead to a notable increase in the concentration of alkaline and alkaline earth metals. This indicates an ion-exchange mechanism in which positively charged metal ions bind to the biomass and replace other ions that exhibit a weaker interaction. For all tested cyanobacteria, Na^+ ions were the most prevalent ions being released. The biomass of *S. elongatus* was an exception, as Mg^{2+} and Ca^{2+} played a more important role in this case.

3.7 FT-IR analysis

IR spectra of all analyzed biomass samples displayed signals that can be assigned to different functional groups (Figure 7). The broad band in the region around 3,350 cm^{-1} in the spectra are linked to the stretching vibrations of hydroxyl groups (Qian et al., 2018), whereas the signal at 2,920 cm^{-1} can be related to the C-H stretching vibrations of CH_2 groups (Bhattacharya et al., 2014). Signals around 1,630 cm^{-1}, which can be assigned to C=O stretching vibrations, indicate the presence of carboxyl groups (Qian et al., 2009). The strong signals around 1,040 cm^{-1} can be assigned to C-O stretching vibration in polysaccharides (Nakamoto 2009). FT-IR spectra of biomasses after interaction with cerium (III) nitrate (Figure 7 blue lines) are characterized by changes in intensity and shifts in position of certain bands due to the interaction with the adsorbed metal ions. The first observed change was the attenuation of intensity in the region between 3,600–3,000 cm^{-1}, indicating a decrease of free hydroxyl groups in the biomass (Mitic-Stojanovic et al., 2011). This was most prominent in biomass samples from *D. muscorum* 90.03 and *Komarekiella sp*. 89.12. Likewise, changes in intensities around 1,630 cm^{-1} and 1,040 cm^{-1} indicate an interaction with carboxyl groups (Qian et al., 2009). These changes were more profound for *S. elongates* UTEX 2973, *D. muscorum* 90.03, and *Komarekiella sp*. 89.12. Distinct changes in signal intensities around 1,410 cm^{-1} and 1,290 cm^{-1}, which can be observed in samples of *Nostoc sp*. 20.02, *S. elongates* UTEX 2973, and *C. brevissima* SAG 34.79, might be linked to an interaction with aromatic C-C groups and C-O or C-N groups respectivly (Theivandran et al., 2015).

4 Discussion

4.1 Phylogenetic and taxonomical remarks

In the broad context of biotechnology, cyanobacterial strains are often used without respecting their ecological niche. This is a problem, because some taxa e.g. from aquatic habitats, often cannot be used during biotechnological processes that involve heat or desiccation, while others, such as terrestrial strains, are better candidates and *vice versa*. In addition, it happens quite often that results are not linked to strain identifiers or to wrongly identified taxa what can lead to an incorrect comparison and interpretation of data—a mistake that can remain uncorrected over decades (e.g., Jung et al., 2021b). For these reasons we respected the ecology of the strains used in this study and depicted the phylogenetic placement of the strains. This creates a transparent background for the cyanobacterial strains that we used and allows others to better compare their results. Besides publicly available cyanobacterial strains with a clarified identity, several new

isolates were phylogenetically analyzed during this work based on their 16S rRNA gene region (Figure 1). Among these were, for example, the heterocytous, false-branching strain *S. hyalinum* 02.01 that joined the large *S. hyalinum* cluster as outlined by Johansen et al., (Johansen et al., 2017). In addition, the two true-branching, heterocytous strains *Symphyonema bifilamentata* 97.28 and *Reptodigitus sp*. 92.1 were included in the study in order to complement the setup of heterocytous, branching cyanobacteria. The strain 97.28 was treated as *Fisherella ambigua* for the last 50 years of biotechnological research on secondary metabolites but was recently re-assigned as the type strain of the genus *Symphyonema* (Jung et al., 2021b). This strain has great biotechnological potential, because it grows fast and produces a diverse set of secondary metabolites, such as various ambigols (summarized in (Jung et al., 2021b)). The strain 92.1 was formerly treated as *Nostochopsis lobatus,* but doubts about this assignment arose because *N. lobatus* is only known from aquatic habitats. Recently, the new genus *Reptodigitus* was emerged, and the authors pointed out that strain 92.1 needs to be correctly described as a novel *Reptodigitus* species (Casamatta et al., 2020) which the authors of this study will carry out in a follow up study. In contrast to the above named strains, which are low producers of EPS (extracellular polymeric substances), the genus *Komarekiella* and related genera are well known to produce cells and filaments covered by thick EPS sheaths (Scotta Hentschke et al., 2017; Soares et al., 2021). EPS might play a role in metal adsorption (e.g. Al Amin et al., 2021). However, the two strains investigated here are the first strains of this genus described from a desert environment, while the other species of the genus have multiple origins, including lichen symbioses (Jung et al., 2021a; Soares et al., 2021; Panou and Gkelis 2022). All of them have a very complex life cycle in common that can hamper biotechnological applications due to different metabolic activity depending on the developmental stage of the culture. Also, the two strains 90.01 and 89.12 will be described as new species in the future. More challenging to interpret are the phylogenetic and taxonomical positions of *Nostoc* sp. 20.02 and *C. brevissima* SAG 34.79 (Figure 1). The strain 20.02 was isolated as an epiphyte on a cyanolichens and can be considered as a *Nostoc* strain not involved in the symbiosis because most true *Nostoc* lichen photobionts usually join distinct *Nostoc* 'photobiont clusters' based on their 16S rRNA (O'Brien et al., 2005). The overall taxonomic position of this strain remains unsure as it also does not cluster within the *Nostoc sensu stricto* clade. Similar uncertainties affect strain SAG 34.79 that could be assigned to *C. brevissima* based on its morphology and phylogenetic position, although there is no cohesive cluster formed and no type strain for the genus deposited. Closely related strains such as *Tolypothrix tenuis* SAG 94.79, *Scytonema mirabile* SAG 83.79, and *T. tenuis* J1 (Figure 1) need further investigation to clarify the state of the genus. *Calothrix* exhibits a notorious morphological heterogeneity and extreme polyphyly, which is evident from various independent clades in the phylogenetic trees of past research [reviewed in (Nowruzi and Shalygin 2021)]. However, even if no phylogenetic or habitat correlation with adsorption capacity could be found, biotechnological studies of cyanobacterial strains should be more often accompanied with phylogenetical studies applying the current standard for taxonomical classification by the so called polyphasic approach (Komárek et al., 2014) to identify taxonomic rearrangements and to avoid confusion regarding species names and strain names from culture collections for biotechnology.

4.2 Metal adsorption experiments

For microalgae, the bioremediation, bioaccumulation, or biosorption of common heavy metals such as Pb, Cd, Cr, As, Hg, Ni, etc. is often studied [e.g. (Ahuja et al., 1999; Ç etinkaya Dönmez et al., 1999; Mehta and Gaur 2005)]. The mechanisms behind these adsorption processes vary with species and environmental conditions (Kumar et al., 2015). However, different mechanisms are discussed, such as ion exchange, complexation, electrostatic attraction, and micro-precipitation (Kumar et al., 2015; Yadav et al., 2021). In contrast, the biosorption of REE is studied less. For the adsorption process of REE, the results in this study indicate an ion-exchange mechanism in which cations of alkaline and alkaline earth metals (Na, K, Mg, and Ca) are replaced by other metal cations during the biosorption process with cyanobacterial biomass (Figure 6). This is in agreement with previous experiments using biomass of different microorganisms (Crist et al., 1994; Matheickal et al., 1997; Sulaymon et al., 2013; Liang and Shen 2022). Ion exchange has been proposed as a dominant mechanism during biosorption (Chen et al., 2002; Iqbal et al., 2009). Apart from *Synechococcus elongates* UTEX 2973 biomass, sodium was the predominant element during the ion exchange process. This differs from previous reports in which cations of earth alkaline metals were released in higher percentages (Iqbal et al., 2009; Sulaymon et al., 2013). Additionally, studies reported the replacement of protons with metal cations leading to a decrease in pH during the sorption process (Mashitah et al., 1999; Vasudevan et al., 2002). However, this aspect was not focused on in the experimental setup of this study. The strong influence of pH value on metal uptake shown in this study further emphasizes the correlation between charges on the surface of the biosorbent and the adsorbed metal ions. In previous studies, the effect of pH value on biosorption has been confirmed (García-Rosales et al., 2012; Abdel-Aty et al., 2013). At low pH values, functional groups on the cell surface are either neutral or positively charged. Carboxyl groups for instance are protonated at pH values below 3, whereas amino groups are protonated at pH 4.1 (Eccles 1999). As similar charges create a repulsive force, positive charges on the biomass surface repel metal cations, leading to poor metal uptake at low pH values. Previous studies described a strong influence of hydroxyl and carboxyl groups on the adsorption process for different biomasses (Gupta and Rastogi 2008; Luo et al., 2010; Utomo et al., 2016). Experiments on adsorption kinetics showed a quick metal uptake for all tested biomasses, reaching equilibrium within only a few minutes. In general, the process of metal cations attaching to adsorbents with a mesoporous surface involves two stages (Zinicovscaia et al., 2021). Specifically, the steps involve the migration of ions from the main solution to the boundary layer surrounding the intermediate-pore matrices, and the attachment of the metal ions to the active sites of the adsorbent material *via* adsorption. Previous studies have reported fast kinetics for the adsorption of metals on biomass of other green algae and cyanobacteria (Klimmek et al., 2001). On the other hand, experiments in other studies resulted in incubation times of up to 60 min and more before reaching the maximum adsorption equilibrium (Ahuja et al., 1999; Zinicovscaia et al., 2017). Fast metal uptake is a beneficial factor for the process development beyond laboratory scale as long incubation periods can be avoided, and higher flow rates can be achieved. Adsorption

experiments with equimolar mixed-metal solutions were carried out, revealing a preference for certain elements influenced by the total metal concentration. The tested biomasses showed the highest overall adsorption capacity for Ce^{3+} at low metal concentrations. However, cations of these elements were replaced by Pb and Al at higher metal concentrations (2–4 mM) in this experimental setup. Zn and Ni showed to lowest affinity to the tested biomasses. Similar results have been reported for biomass of other microorganisms (Klimmek 2003; Wilke et al., 2006; Huang et al., 2018). At present, our ability to make predictions on binding specificity based on single-element adsorption experiments is limited (Wilke et al., 2006). Regarding a potential industrial application for the recovery of REE, these are promising results, as metal concentrations usually are lower than the highest concentrations in the experimental setup of this study. Furthermore, it should be considered that this study predominately focused on the adsorption of the element cerium. Due to high chemical similarities between REE, it is likely that the adsorption properties of the tested biomasses will be similar for other elements of this group. Nevertheless, additional experiments with other REE are advisable. Target elements could be extracted from the resulting metal-loaded biomass in follow-up processes. The destructive recovery by combustion, resulting in metal-enriched ash, is a simple method with the drawback of losing the initial biomass. An economically more desirable approach is the targeted desorption of elements from loaded biomass, enabling the recycling of the biosorbent. Previous studies have tested various approaches using different acids or complexing agents (Gong et al., 2005; Abdolali et al., 2015). Unfortunately, the adsorption properties of biosorbents are impaired over the curse of a few cycles (Hammaini et al., 2007). Future studies should address the binding specificity and durability of biosorbents to implement biosorption in industrial processes successfully. In competitive systems, the adsorption of different metal cations on biomass is influenced by functional groups on the cell surface. The interaction between metal cations and functional groups still requires more research. According to the current state of knowledge, various ionic properties of metal cations, such as electronegativity, redox potential, and ionic radius can influence the adsorption on biomass (Naja et al., 2010). Depending on the biomass and physico-chemical conditions, multiple mechanisms may be involved in metal sorption simultaneously (Gadd 2009). With respect to different cyanobacterial strains, FT-IR analysis indicated the involvement of various functional groups during like hydroxyl or carboxyl groups during metal adsorption. However, at present, there is no discrete chemical entity that has been identified as dominant cell wall feature that governs metal binding. In a previous study, for instance, it was shown that complex polymeric sugars are involved in the adsorption of terbium by *C. brevissima* (Jurkowski et al., 2022). Cell wall-derived binding entities most likely vary for every organism and metal presented.

5 Conclusion

In this study, a diverse group of 12 cyanobacteria was investigated for their potential in the enrichment of REE in a biosorption process. Metal uptake varied strongly among the tested strains, with *Nostoc* sp. 20.02 showing the highest maximum adsorption capacity of 84.2–91.5 mg g^{-1}. However, there was no apparent correlation between maximum adsorption capacity and phylogenetic relationship nor for the ecological habitat of the strains. This could be explained by variations in the composition of metal interacting functional groups located at the cell surface. Moreover, many cyanobacteria that showed high adsorption capacities for REE produce extracellular polymeric substances (EPS) that are known to facilitate metal adsorption (Pagliaccia et al., 2022). The composition of these EPS and their influence on the adsorption of REE should be further investigated in future studies. The determination of relevant parameters for improving the metal uptake revealed a pH optimum at 5 to 6 and fast adsorption kinetics reaching adsorption equilibrium within an incubation time of a few minutes. In addition, metal analysis strongly indicated an ion-exchange mechanism during the biosorption process in which Na^+, K^+, Mg^{2+}, and Ca^{2+} ions are replaced by metal cations that bind to the surface of the biomass. These observations are in accordance with previous studies that were conducted on algal, bacterial, and other biomasses (Acheampong et al., 2011; Sulaymon et al., 2013; Liang and Shen 2022). The isolation of single target elements in a technical biosorption process remains a challenging task due to the complex surface structure and the heterogeneity of functional groups. Nevertheless, based on the results of this study, the enrichment of metal elements from diluted solutions is possible. For the development of an industrial process, parameters need to be further optimized and adjusted depending on the metal composition in the wastewater and the biomass that is used as biosorbent.

Data availability statement

The original contributions presented in the study are included in the article/Supplementary Material, further inquiries can be directed to the corresponding author. The 16S rRNA gene sequences generated during this study were added to NCBI GenBank stated by their accession number in the phylogenetic tree (Figure 1).

Author contributions

MP, MK, and PJ contributed equally to this work. Conceptualization, MP, ML, and TB; Methodology, MP, MK, and PJ; Validation, all authors; Writing—original draft preparation, MP and PJ; Writing—review and editing, ML, TN, and TB; Visualization, MP and PJ; Supervision, ML, TN, and TB; Project administration, ML, TN, and TB; Funding acquisition, ML, TN, and TB All authors have read and agreed to the published version of the manuscript.

Funding

This project was funded by the Bavarian State Ministry of the Environment and Consumer Protection within the framework of the ForCycle II Project Group. ML was supported by the Ministry of Science and Health Rhineland-Palatinate (PhytoBioTech, 724–0116#2021, 004–1501 15405), by the Federal Ministry of Education and Research (W2V-Strategy2Value, 03WIR4502A & Technology2Value 03WIR4504B) as well as by EU-HORIZON (Waste2BioComp ID: 101058654). PJ was funded by the German Research Council (DFG; Grit Life; JU 3228, 1–1).

Conflict of interest

The authors declare that the research was conducted in the absence of any commercial or financial relationships that could be construed as a potential conflict of interest.

Publisher's note

All claims expressed in this article are solely those of the authors and do not necessarily represent those of their affiliated organizations, or those of the publisher, the editors and the reviewers. Any product that may be evaluated in this article, or claim that may be made by its manufacturer, is not guaranteed or endorsed by the publisher.

Supplementary material

The Supplementary Material for this article can be found online at: https://www.frontiersin.org/articles/10.3389/fbioe.2023.1130939/full#supplementary-material

References

Abbas, S. H., Ismail, I. M., Mostafa, T. M., and Sulaymon, A. H. (2014). Biosorption of heavy metals: A review. *J. Chem. Sci. Technol.* 3 (4), 74–102.

Abdel-Aty, A. M., Ammar, N. S., Abdel Ghafar, H. H., and Ali, R. K. (2013). Biosorption of cadmium and lead from aqueous solution by fresh water alga Anabaena sphaerica biomass. *J. Adv. Res.* 4 (4), 367–374. doi:10.1016/j.jare.2012.07.004

Abdolali, A., Ngo, H. H., Guo, W., Zhou, J. L., Du, B., Wei, Q., et al. (2015). Characterization of a multi-metal binding biosorbent: Chemical modification and desorption studies. *Bioresour. Technol.* 193, 477–487. doi:10.1016/j.biortech.2015.06.123

Acheampong, M. A., Pereira, J. P. C., Meulepas, R. J. W., and Lens, P. N. L. (2011). Biosorption of Cu(II) onto agricultural materials from tropical regions. *J. Chem. Technol. Biotechnol.* 86 (9), 1184–1194. doi:10.1002/jctb.2630/jctb.2630

Ahuja, P., Gupta, R., and Saxena, R. K. (1999). Zn2+ biosorption by Oscillatoria anguistissima. *Process Biochem.* 34 (1), 77–85. doi:10.1016/s0032-9592(98)00072-7

Aksu, Z. (2005). Application of biosorption for the removal of organic pollutants: A review. *Process Biochem.* 40 (3-4), 997–1026. doi:10.1016/j.procbio.2004.04.008

Al-Amin, A., Parvin, F., Chakraborty, J., and Kim, Y.-I. (2021). Cyanobacteria mediated heavy metal removal: A review on mechanism, biosynthesis, and removal capability. *Environ. Technol. Rev.* 10 (1), 44–57. doi:10.1080/21622515.2020.1869323

Andersen, R. A. (2005). *Algal culturing techniques*. Burlington, MA: Elsevier Academic Press.

Ankit, S., Bauddh, K., and Korstad, J. (2022). Phycoremediation: Use of algae to sequester heavy metals. *Hydrobiology*, 1, 288–303. doi:10.3390/hydrobiology1030021

Barros, Ó., Costa, L., Costa, F., Lago, A., Rocha, V., Vipotnik, Z., et al. (2019). Recovery of rare earth elements from wastewater towards a circular economy. *Mol. (Basel, Switz.* 24 (6). doi:10.3390/molecules24061005

Bell, J. P., and Tsezos, M. (1987). Removal of hazardous organic pollutants by adsorption on microbial biomass. *Water Sci. Technol.* 19 (3-4), 409–416. doi:10.2166/wst.1987.0221/wst.1987.0221

Bhattacharya, P., Mallick, K., Ghosh, S., Banerjee, P., Mukhopadhyay, A., and Bandyopadhyay, S. (2014). Algal biomass as potential biosorbent for reduction of organic load in gray water and subsequent reuse: Effect on seed germination and enzyme activity. *Bioremediation J.* 18 (1), 56–70. doi:10.1080/10889868.2013.847400

Casamatta, D. A., Villanueva, C. D., Garvey, A. D., Stocks, H. S., Vaccarino, M., Dvořák, P., et al. (2020). Reptodigitus chapmanii (Nostocales, hapalosiphonaceae) gen. Nov.: A unique nostocalean (cyanobacteria) genus based on a polyphasic Approach1. *J. Phycol.* 56 (2), 425–436. doi:10.1111/jpy.12954

Çetinkaya Dönmez, G., Aksu, Z., Öztürk, A., and Kutsal, T. (1999). A comparative study on heavy metal biosorption characteristics of some algae. *Process Biochem.* 34 (9), 885–892. doi:10.1016/s0032-9592(99)00005-9

Charalampides, G., Vatalis, K. I., Apostoplos, B., and Ploutarch-Nikolas, B. (2015). Rare earth elements: Industrial applications and economic dependency of europe. *Procedia Econ. Finance* 24, 126–135. doi:10.1016/S2212-5671(15)00630-9

Chen, J. P., Hong, L., Wu, S., and Wang, L. (2002). Elucidation of interactions between metal ions and Ca alginate-based ion-exchange resin by spectroscopic analysis and modeling simulation. *Langmuir* 18 (24), 9413–9421. doi:10.1021/la026060v/9413

Ciopec, M., Gabor, A., Davidescu, C. M., Negrea, A., Negrea, P., and Duteanu, N. (2020). Eu(III) removal by tetrabutylammonium di-hydrogen phosphate (TBAH2P) functionalized polymers. *Arabian J. Chem.* 13 (1), 3534–3545. doi:10.1016/j.arabjc.2018.12.005

Crini, G., and Badot, P.-M. (2008). Application of chitosan, a natural aminopolysaccharide, for dye removal from aqueous solutions by adsorption processes using batch studies: A review of recent literature. *Prog. Polym. Sci.* 33 (4), 399–447. doi:10.1016/j.progpolymsci.2007.11.001

Crist, R. H., Martin, J. R., Carr, D., Watson, J. R., and Clarke, H. J. (1994). Interaction of metals and protons with algae. 4. Ion exchange vs adsorption models and a reassessment of scatchard plots; ion-exchange rates and equilibria compared with calcium alginate. *Environ. Sci. Technol.* 28 (11), 1859–1866. doi:10.1021/es00060a016/1859

Dada, A. O., Olalekan, A. P., Olatunya, A. M., and Dada, O. (2012). Langmuir, Freundlich, temkin and dubinin–radushkevich isotherms studies of equilibrium sorption of Zn 2+ unto phosphoric acid modified rice husk. *IOSR J. Appl. Chem.* 3 (1), 38–45. doi:10.9790/5736-0313845

Dhankhar, R., and Hooda, A. (2011). Fungal biosorption--an alternative to meet the challenges of heavy metal pollution in aqueous solutions. *Environ. Technol.* 32 (5-6), 467–491. doi:10.1080/09593330.2011.572922

Eccles, H. (1999). Treatment of metal-contaminated wastes: Why select a biological process? *Trends Biotechnol.* 17 (12), 462–465. doi:10.1016/S0167-7799(99)01381-5

Elgarahy, A. M., Elwakeel, K. Z., Mohammad, S. H., and Elshoubaky, G. A. (2021). A critical review of biosorption of dyes, heavy metals and metalloids from wastewater as an efficient and green process. *Clean. Eng. Technol.* 4, 100209. doi:10.1016/j.clet.2021.100209

Fomina, M., and Gadd, G. M. (2014). Biosorption: Current perspectives on concept, definition and application. *Bioresour. Technol.* 160, 3–14. doi:10.1016/j.biortech.2013.12.102

Gabor, A., Davidescu, C. M., Negrea, A., Ciopec, M., Grozav, I., Negrea, P., et al. (2017). Optimizing the lanthanum adsorption process onto chemically modified biomaterials using factorial and response surface design. *J. Environ. Manag.* 204, 839–844. doi:10.1016/j.jenvman.2017.01.046

Gadd, G. M. (2009). Biosorption: Critical review of scientific rationale, environmental importance and significance for pollution treatment. *J. Chem. Technol. Biotechnol.* 84 (1), 13–28. doi:10.1002/jctb

García-Rosales, G., Olguin, M. T., Colín-Cruz, A., and Romero-Guzmán, E. T. (2012). Effect of the pH and temperature on the biosorption of lead(II) and cadmium(II) by sodium-modified stalk sponge of Zea mays. *Environ. Sci. Pollut. Res. Int.* 19 (1), 177–185. doi:10.1007/s11356-011-0537-x

Giese, E. C. (2020). Biosorption as green technology for the recovery and separation of rare Earth elements. *World J. Microbiol. Biotechnol.* 36 (4), 1–11. doi:10.1007/s11274-020-02821-6

Gong, R., Ding, Y., Liu, H., Chen, Q., and Liu, Z. (2005). Lead biosorption and desorption by intact and pretreated spirulina maxima biomass. *Chemosphere* 58 (1), 125–130. doi:10.1016/j.chemosphere.2004.08.055

Gupta, V. K., and Rastogi, A. (2008). Biosorption of lead from aqueous solutions by green algae spirogyra species: Kinetics and equilibrium studies. *J. Hazard. Mater.* 152 (1), 407–414. doi:10.1016/j.jhazmat.2007.07.028

Hammaini, A., González, F., Ballester, A., Blázquez, M. L., and Muñoz, J. A. (2007). Biosorption of heavy metals by activated sludge and their desorption characteristics. *J. Environ. Manag.* 84 (4), 419–426. doi:10.1016/j.jenvman.2006.06.015

Haque, N., Hughes, A., Lim, S., and Vernon, C. (2014r3040614). Rare earth elements: Overview of mining, mineralogy, uses, sustainability and environmental impact. *Resources* 3 (4), 614–635. doi:10.3390/resources3040614

Heilmann, M., Breiter, R., and Becker, A. M. (2021). Towards rare Earth element recovery from wastewaters: Biosorption using phototrophic organisms. *Appl. Microbiol. Biotechnol.* 105 (12), 5229–5239. doi:10.1007/s00253-021-11386-9

Heilmann, M., Jurkowski, W., Buchholz, R., Brueck, T., and Becker, A. M. (2015). Biosorption of neodymium by selected photoautotrophic and heterotrophic species. *J. Chem. Eng. Process Technol.* 06 (04), 1000241. doi:10.4172/2157-7048.1000241

Huang, Y., Hu, Y., Chen, L., Yang, T., Huang, H., Shi, R., et al. (2018). Selective biosorption of thorium (IV) from aqueous solutions by ginkgo leaf. *PloS one* 13 (3), e0193659. doi:10.1371/journal.pone.0193659

Iqbal, M., Saeed, A., and Zafar, S. I. (2009). FTIR spectrophotometry, kinetics and adsorption isotherms modeling, ion exchange, and EDX analysis for understanding the mechanism of Cd(2+) and Pb(2+) removal by mango peel waste. *J. Hazard. Mater.* 164 (1), 161–171. doi:10.1016/j.jhazmat.2008.07.141

Johansen, J. R., Mareš, J., Pietrasiak, N., Bohunická, M., Zima, J., Štenclová, L., et al. (2017). Highly divergent 16S rRNA sequences in ribosomal operons of Scytonema hyalinum (Cyanobacteria). *PloS one* 12 (10), e0186393. doi:10.1371/journal.pone.0186393

Jung, P., Brust, K., Schultz, M., Büdel, B., Donner, A., and Lakatos, M. (2021a). Opening the gap: Rare lichens with rare cyanobionts - unexpected cyanobiont diversity in cyanobacterial lichens of the order lichinales. *Front. Microbiol.* 12, 728378. doi:10.3389/fmicb.2021.728378

Jung, P., D'Agostino, P. M., Büdel, B., and Lakatos, M. (2021b). Symphyonema bifilamentata sp. nov., the right fischerella ambigua 108b: Half a decade of research on taxonomy and bioactive compounds in new light. *Microorganisms* 9 (4). doi:10.3390/microorganisms9040745

Jurkowski, W., Paper, M., and Brück, T. B. (2022). Isolation and investigation of natural rare earth metal chelating agents from Calothrix brevissima - a step towards unraveling the mechanisms of metal biosorption. *Front. Bioeng. Biotechnol.* 10, 833122. doi:10.3389/fbioe.2022.833122

Klimmek, S. (2003). *Characterisation of biosorption to algae of heavy metals, Charakterisierung der Biosorption von Schwermetallen an Algen*. Berlin, Germany: Springer.

Klimmek, S., Stan, H. J., Wilke, A., Bunke, G., and Buchholz, R. (2001). Comparative analysis of the biosorption of cadmium, lead, nickel, and zinc by algae. *Environ. Sci. Technol.* 35 (21), 4283–4288. doi:10.1021/es010063x/4283

Komárek, J., Kaštovský, J., Mareš, J., and Johansen, J. (2014). Taxonomic classification of cyanoprokaryotes (cyanobacterial genera) 2014, using a polyphasic approach. *Preslia* 86, 295–335.

Koong, L. F., Lam, K. F., Barford, J., and McKay, G. (2013). A comparative study on selective adsorption of metal ions using aminated adsorbents. *J. Colloid Interface Sci.* 395, 230–240. doi:10.1016/j.jcis.2012.12.047

Kumar, K. S., Dahms, H.-U., Won, E.-J., Lee, J.-S., and Shin, K.-H. (2015). Microalgae - a promising tool for heavy metal remediation. *Ecotoxicol. Environ. Saf.* 113, 329–352. doi:10.1016/j.ecoenv.2014.12.019

Kumar, S., Stecher, G., Li, M., Knyaz, C., and Tamura, K. (2018). Mega X: Molecular evolutionary genetics analysis across computing platforms. *Mol. Biol. Evol.* 35 (6), 1547–1549. doi:10.1093/molbev/msy096

Kuyucak, N., and Volesky, B. (1988). Biosorbents for recovery of metals from industrial solutions. *Biotechnol. Lett.* 10 (2), 137–142. doi:10.1007/BF01024641

Li, C., Zhuang, Z., Huang, F., Wu, Z., Hong, Y., and Lin, Z. (2013). Recycling rare Earth elements from industrial wastewater with flowerlike nano-Mg(OH)(2). *ACS Appl. Mater. interfaces* 5 (19), 9719–9725. doi:10.1021/am4027967

Liang, C.-l., and Shen, J.-l. (2022). Removal of yttrium from rare-Earth wastewater by *Serratia marcescens*: Biosorption optimization and mechanisms studies. *Sci. Rep.* 12 (1), 4861–4674. doi:10.1038/s41598-022-08542-0

Luo, J.-m., Xiao, X., and Luo, S.-l. (2010). Biosorption of cadmium(II) from aqueous solutions by industrial fungus Rhizopus cohnii. *Trans. Nonferrous Metals Soc. China* 20 (6), 1104–1111. doi:10.1016/s1003-6326(09)60264-8

Lupea, M., Bulgariu, L., and Macoveanu, M. (2012). Biosorption of Cd(ii) from aqueous solution on marine green algae biomass. *Environ. Eng. Manag. J.* 11 (3), 607–615. doi:10.30638/eemj.2012.076

Mashitah, M. D., Zulfadhly, Z., and Bhatta, S. (1999). Binding mechanism of heavy metals biosorption by pycnoporus sanguineus. *Artif. Cells, Blood Substitutes, Biotechnol.* 27, 441–445. doi:10.3109/10731199909117717

Matheickal, J. T., Yu, Q., and Feltham, J. (1997). Cu(II) binding by E. Radiata biomaterial. *Environ. Technol.* 18 (1), 25–34. doi:10.1080/09593331808616509

Mattocks, J. A., and Cotruvo, J. A. (2020). Biological, biomolecular, and bio-inspired strategies for detection, extraction, and separations of lanthanides and actinides. *Chem. Soc. Rev.* 49 (22), 8315–8334. doi:10.1039/d0cs00653j

Mehta, S. K., and Gaur, J. P. (2005). Use of algae for removing heavy metal ions from wastewater: Progress and prospects. *Crit. Rev. Biotechnol.* 25 (3), 113–152. doi:10.1080/07388550500248571

Menk, J., do Nascimento, A. I. S., Leite, F. G., Oliveira, R. A., Jozala, A. F., Oliveira Junior, J. M., et al. (2019). Biosorption of pharmaceutical products by mushroom stem waste. *Chemosphere* 237, 124515. doi:10.1016/j.chemosphere.2019.124515

Micheletti, E., Colica, G., Viti, C., Tamagnini, P., and Philippis, R. (2008). Selectivity in the heavy metal removal by exopolysaccharide-producing cyanobacteria. *J. Appl. Microbiol.* 105 (1), 88–94. doi:10.1111/j.1365-2672.2008.03728.x

Mitic-Stojanovic, D.-L., Zarubica, A., Purenovic, M., Bojic, D., Andjelkovic, T., and Bojic, À. L. (2011). Biosorptive removal of Pb^{2+}, Cd^{2+} and Zn^{2+} ions from water by agenaria vulgaris shell. *Water sa.* 37 (3), 68481. doi:10.4314/wsa.v37i3.68481

Naja, G. M., Murphy, V., and Volesky, B. (2010). *Biosorption, metals*. Berlin, Germany: Springer. doi:10.1002/9780470054581.eib166

Nakamoto, K. (2009). *Infrared and Raman spectra of inorganic and coordination compounds, Part B. Applications in coordination, organometallic, and bioinorganic Chemistry*. Netherlands: John Wiley & Sons.

Negrea, A., Gabor, A., Davidescu, C. M., Ciopec, M., Negrea, P., Duteanu, N., et al. (2018). Rare earth elements removal from water using natural polymers. *Sci. Rep.* 8 (1), 316–326. doi:10.1038/s41598-017-18623-0

Negrea, P., Gabor, A., Davidescu, C. M., Ciopec, M., Negrea, A., and Duteanu, N. (2020). Kinetics and thermodynamics modeling of Nd(III) removal from aqueous solution using modified Amberlite XAD7. *J. Rare Earths* 38 (3), 306–314. doi:10.1016/j.jre.2019.04.023

Nowruzi, B., and Shalygin, S. (2021). Multiple phylogenies reveal a true taxonomic position of Dulcicalothrix alborzica sp. nov. (Nostocales, Cyanobacteria). *Fottea* 21 (2), 235–246. doi:10.5507/fot.2021.008

O'Brien, H. E., Miadlikowska, J., and Lutzoni, F. (2005). Assessing host specialization in symbiotic cyanobacteria associated with four closely related species of the lichen fungus Peltigera. *Eur. J. Phycol.* 40 (4), 363–378. doi:10.1080/09670260500342647

Opare, E. O., Struhs, E., and Mirkouei, A. (2021). A comparative state-of-technology review and future directions for rare Earth element separation. *Renew. Sustain. Energy Rev.* 143, 110917. doi:10.1016/j.rser.2021.110917

Pagliaccia, B., Carretti, E., Severi, M., Berti, D., Lubello, C., and Lotti, T. (2022). Heavy metal biosorption by Extracellular Polymeric Substances (EPS) recovered from anammox granular sludge. *J. Hazard. Mater.* 424, 126661. doi:10.1016/j.jhazmat.2021.126661

Panou, M., and Gkelis, S. (2022). Unravelling unknown cyanobacteria diversity linked with HCN production. *Mol. phylogenetics Evol.* 166, 107322. doi:10.1016/j.ympev.2021.107322

Park, D., Yun, Y.-S., and Park, J. M. (2010). The past, present, and future trends of biosorption. *Biotechnol. Bioprocess Eng.* 15 (1), 86–102. doi:10.1007/s12257-009-0199-4

Plancque, G., Moulin, V., Toulhoat, P., and Moulin, C. (2003). Europium speciation by time-resolved laser-induced fluorescence. *Anal. Chim. Acta* 478 (1), 11–22. doi:10.1016/s0003-2670(02)01486-1

Qian, J.-Y., Chen, W., Zhang, W.-M., and Zhang, H. (2009). Adulteration identification of some fungal polysaccharides with sem, xrd, IR and optical rotation: A primary approach. *Carbohydr. Polym.* 78 (3), 620–625. doi:10.1016/j.carbpol.2009.05.025

Qian, S., Fang, X., Dan, D., Diao, E., and Lu, Z. (2018). Ultrasonic-assisted enzymatic extraction of a water soluble polysaccharide from dragon fruit peel and its antioxidant activity. *RSC Adv.* 8 (73), 42145–42152. doi:10.1039/C8RA06449K

Ronquist, F., and Huelsenbeck, J. P. (2003). MrBayes 3: Bayesian phylogenetic inference under mixed models. *Bioinformatics* 19 (12), 1572–1574. doi:10.1093/bioinformatics/btg180

Scotta Hentschke, G., Johansen, J. R., Pietrasiak, N., Rigonato, J., Fiore, M. F., and Leite Sant'Anna, C. (2017). Komarekiella atlantica (nostocaceae, cyanobacteria): A new subaerial taxon from the atlantic rainforest and kauai, Hawaii. *Fottea* 17 (2), 178–190. doi:10.5507/fot.2017.002

Shan, Y., Liu, Y., Li, Y., and Yang, W. (2020). A review on application of cerium-based oxides in gaseous pollutant purification. *Sep. Purif. Technol.* 250, 117181. doi:10.1016/j.seppur.2020.117181

Soares, F., Ramos, V., Trovão, J., Cardoso, S. M., Tiago, I., and Portugal, A. (2021). Parakomarekiella sesnandensis gen. et sp. nov. (Nostocales, Cyanobacteria) isolated from the Old Cathedral of Coimbra, Portugal (UNESCO World Heritage Site). *Eur. J. Phycol.* 56 (3), 301–315. doi:10.1080/09670262.2020.1817568

Stanier, R. Y., Kunisawa, R., Mandel, M., and Cohen-Bazire, G. (1971). Purification and properties of unicellular blue-green algae (order Chroococcales). *Bacteriol. Rev.* 35 (2), 171–205. doi:10.1128/br.35.2.171-205.1971

Sulaymon, A. H., Mohammed, A. A., and Al-Musawi, T. J. (2013). Competitive biosorption of lead, cadmium, copper, and arsenic ions using algae. *Environ. Sci. Pollut. Res. Int.* 20 (5), 3011–3023. doi:10.1007/s11356-012-1208-2

Theivandran, G., Mohamed, I. V., and Murugan, M. (2015). Fourier transform infrared (Ft-Ir) spectroscopic analysis of Spirulina fusiformis. *J. Med. Plants Stud.* 3 (4), 30–32.

Utomo, H. D., Tan, K. X. D., Choong, Z. Y. D., Yu, J. J., Ong, J. J., and Lim, Z. B. (2016). Biosorption of heavy metal by algae biomass in surface water. *J. Environ. Prot.* 7 (11), 1547–1560. doi:10.4236/jep.2016.711128

Vasudevan, P., Padmavathy, V., and Dhingra, S. C. (2002). Biosorption of monovalent and divalent ions on baker's yeast. *Bioresour. Technol.* 82 (3), 285–289. doi:10.1016/S0960-8524(01)00181-X

Volesky, B. (2007). Biosorption and me. *Water Res.* 41 (18), 4017–4029. doi:10.1016/j.watres.2007.05.062

Volesky, B. (2001). Detoxification of metal-bearing effluents: Biosorption for the next century. *Hydrometallurgy* 59 (2), 203–216. doi:10.1016/s0304-386x(00)00160-2

Wang, J., and Chen, C. (2006). Biosorption of heavy metals by *Saccharomyces cerevisiae*: A review. *Biotechnol. Adv.* 24 (5), 427–451. doi:10.1016/j.biotechadv.2006.03.001

Wilke, A., Buchholz, R., and Bunke, G. (2006). Selective biosorption of heavy metals by algae. *Environ. Biotechnol.* 2 (2), 47–56.

Wilmotte, A., van der Auwera, G., and Wachter, R. (1993). Structure of the 16 S ribosomal RNA of the thermophilic cyanobacterium chlorogloeopsis HTF (' mastigocladus laminosus HTF') strain PCC7518, and phylogenetic analysis. *FEBS Lett.* 317 (1-2), 96–100. doi:10.1016/0014-5793(93)81499-P

Yadav, A. P. S., Dwivedi, V., Kumar, S., Kushwaha, A., Goswami, L., and Reddy, B. S. (2021). Cyanobacterial extracellular polymeric substances for heavy metal removal: A mini review. *J. Compos. Sci.* 5 (1), 1. doi:10.3390/jcs5010001

Zinicovscaia, I., Safonov, A., Ostalkevich, S., Gundorina, S., Nekhoroshkov, P., and Grozdov, D. (2019). Metal ions removal from different type of industrial effluents using Spirulina platensis biomass. *Int. J. Phytoremediation* 1080, 1442–1448. doi:10.1080/15226514.2019.1633264

Zinicovscaia, I., Yushin, N., Humelnicu, D., Grozdov, D., Ignat, M., Demcak, S., et al. (2021). Sorption of Ce(III) by silica SBA-15 and titanosilicate ETS-10 from aqueous solution. *Water* 13 (22), 3263. doi:10.3390/w13223263

Zinicovscaia, I., Yushin, N., Rodlovskaya, E., and Kamanina, I. (2017). Biosorption of lead ions by cyanobacteria spirulina platensis: Kinetics, equilibrium and thermodynamic study. *Nova Biotechnol. Chimica* 16 (2), 105–112. doi:10.1515/nbec-2017-0015

frontiers

Supplementary Material

Rare Earths stick to rare Cyanobacteria: Future Potential for Bioremediation and Recovery of Rare Earth Elements

Michael Paper[1] †, Max Koch[2] †, Patrick Jung[3] †, Michael Lakatos[3], Tom Nilges[2], Thomas B. Brück[1,4*]

[1] Werner Siemens-Chair of Synthetic Biotechnology, School of Natural Sciences, Dept. of Chemistry, Technical University of Munich, Garching, Germany

[2] Synthesis and Characterization of Innovative Materials, School of Natural Sciences, Dept. of Chemistry, Technical University of Munich, Garching, Germany

[3] Integrative Biotechnology, University of Applied Sciences Kaiserslautern, Pirmasens, Germany

[4] TUM AlgaeTec Center, Ludwig Bölkow Campus, Department of Aerospace and Geodesy, Taufkirchen, Germany

***Correspondence:**
Thomas B. Brück − Werner Siemens-Chair of Synthetic Biotechnology, School of Natural Sciences, Dept. of Chemistry, Technical University of Munich, D- 85748 Garching, Germany; orcid.org/0000-0002-2113-6957; Phone: +49 89-28913253; Email: brueck@tum.de

† These authors contributed equally to this work.

Supplementary Table S1: Maximum adsorption capacity (Q_{max}, mg Ce^{3+} g^{-1} dry mass) and Langmuir adsorption coefficient (K) of the Langmuir model for the adsorption of Ce^{3+} by different cyanobacteria (n=3)

	Qmax	K	R^2
Nostoc sp. 20.02	90.0 ± 11.6	0.63	0.88
Synechococus elongatus UTEX 2973	74.1 ± 12.4	0.76	0.71
Desmonostoc muscorum 90.03	80.6 ± 13.5	0.32	0.83
Calothrix brevissima SAG 34.79	58.9 ± 11.6	0.82	0.68
Komarekiella sp. 89.12	80.8 ± 25.2	0.28	0.53

Supplementary Table S2: Adsorption capacity constant (K_f) and intensity constant (n) of the Freundlich model for the adsorption of Ce^{3+} by different cyanobacteria (n=3)

	K_f	n	R^2
Nostoc sp. 20.02	33.0± 9.8	3.4	0.74
Synechococus elongatus UTEX 2973	38.3± 6.3	5.3	0.84
Desmonostoc muscorum 90.03	24.2± 8.5	3.1	0.74
Calothrix brevissima SAG 34.79	27.2± 6.9	2.2	0.72
Komarekiella sp. 89.12	25.7± 11.4	3.3	0.52

3.3 Stripped: contribution of cyanobacterial extracellular polymeric substances to the adsorption of rare earth elements from aqueous solutions

Michael Paper[a], Patrick Jung[b], Max Koch[c], Tom Nilges[c], Michael Lakatos[b], and Thomas B. Brück[a]

[a]Werner Siemens-Chair of Synthetic Biotechnology, School of Natural Sciences, Department of Chemistry, Technical University of Munich, Garching, Germany

[b]Integrative Biotechnology, University of Applied Sciences Kaiserslautern, Pirmasens, Germany

[c]Synthesis and Characterization of Innovative Materials, School of Natural Sciences, Department of Chemistry, Technical University of Munich, Garching, Germany

Frontiers in Bioengineering and Biotechnology, 11, 1299349
First published online: December 20th 2023
Link: `https://doi.org/10.3389/fbioe.2023.1299349`

The aim of this study was to gain a deeper understanding of the metal adsorption properties of the EPS of cyanobacteria by investigating the structural components of the biomass involved in metal absorption. EPS that can be produced by cyanobacteria have the ability to bind to metal cations. The effects of EPS on Rare Earth biosorption were evaluated using three terrestrial cyanobacterial strains under nitrogen-limited and non-limited conditions. The investigation of metal uptake was performed by comparing the amount of adsorbed REE in a) the extracted EPS, b) the biomass with EPS removed, and c) the intact biomass with EPS. The maximum adsorption capacity of four Rare Earth Elements - cerium, lanthanum, neodymium, and terbium - was analyzed for the tested cyanobacterial strains. FT-IR analysis indicated that biosorption on the EPS of cyanobacteria of three tested cyanobacteria strains likely occurred on carboxyl and hydroxyl groups. This study revealed that glucose-rich EPS from nitrogen-limited cyanobacteria had higher biosorption rates for REE. The extracted EPS showed significantly higher maximum adsorption capacities than cells without EPS and untreated biomass, emphasizing the decisive role of EPS as binding sites for REE. This suggests that cyanobacterial EPS could find future applications in the recycling of Rare Earths, e.g., in wastewater treatment.

Author contributions: The conceptualization of the study and the design of the methodological approach involved contributions from all authors. Max Koch, Michael Paper, and Patrick Jung share the first authorship of this manuscript. Max Koch took charge of the quantitative analysis and data evaluation responsibilities. Michael Paper responsible of the experiments' planning, implementation, and data validation. Patrick Jung prepared the first draft of the manuscript and was responsible for the cultivation of cyanobacteria.

frontiers | Frontiers in Bioengineering and Biotechnology

TYPE Original Research
PUBLISHED 20 December 2023
DOI 10.3389/fbioe.2023.1299349

OPEN ACCESS

EDITED BY
Wenshan Guo,
University of Technology Sydney,
Australia

REVIEWED BY
Alberto Abrantes,
University of Galway, Ireland
Hamedreza Javadian,
Chemistry and Chemical Engineering
Research Center, Iran
Lijuan Deng,
University of Technology Sydney,
Australia

*CORRESPONDENCE
Thomas B. Brück,
brueck@tum.de

†These authors have contributed equally to this work and share first authorship

RECEIVED 22 September 2023
ACCEPTED 01 December 2023
PUBLISHED 20 December 2023

CITATION
Paper M, Jung P, Koch M, Lakatos M, Nilges T and Brück TB (2023), Stripped: contribution of cyanobacterial extracellular polymeric substances to the adsorption of rare earth elements from aqueous solutions.
Front. Bioeng. Biotechnol. 11:1299349.
doi: 10.3389/fbioe.2023.1299349

Stripped: contribution of cyanobacterial extracellular polymeric substances to the adsorption of rare earth elements from aqueous solutions

Michael Paper[1†], Patrick Jung[2†], Max Koch[3†], Michael Lakatos[2], Tom Nilges[3] and Thomas B. Brück[1,4*]

[1]Werner Siemens-Chair of Synthetic Biotechnology, Department of Chemistry, School of Natural Sciences, Technical University of Munich, Garching, Germany, [2]Integrative Biotechnology, University of Applied Sciences Kaiserslautern, Pirmasens, Germany, [3]Synthesis and Characterization of Innovative Materials, Department of Chemistry, School of Natural Sciences, Technical University of Munich, Garching, Germany, [4]Department of Aerospace and Geodesy, TUM AlgaeTec Center, Ludwig Bölkow Campus, Taufkirchen, Germany

The transformation of modern industries towards enhanced sustainability is facilitated by green technologies that rely extensively on rare earth elements (REEs) such as cerium (Ce), neodymium (Nd), terbium (Tb), and lanthanum (La). The occurrence of productive mining sites, e.g., is limited, and production is often costly and environmentally harmful. As a consequence of increased utilization, REEs enter our ecosystem as industrial process water or wastewater and become highly diluted. Once diluted, they can hardly be recovered by conventional techniques, but using cyanobacterial biomass in a biosorption-based process is a promising eco-friendly approach. Cyanobacteria can produce extracellular polymeric substances (EPS) that show high affinity to metal cations. However, the adsorption of REEs by EPS has not been part of extensive research. Thus, we evaluated the role of EPS in the biosorption of Ce, Nd, Tb, and La for three terrestrial, heterocystous cyanobacterial strains. We cultivated them under N-limited and non-limited conditions and extracted their EPS for compositional analyses. Subsequently, we investigated the metal uptake of a) the extracted EPS, b) the biomass extracted from EPS, and c) the intact biomass with EPS by comparing the amount of sorbed REEs. Maximum adsorption capacities for the tested REEs of extracted EPS were 123.9–138.2 mg g^{-1} for *Komarekiella* sp. 89.12, 133.1–137.4 mg g^{-1} for *Desmonostoc muscorum* 90.03, and 103.5–129.3 mg g^{-1} for Nostoc sp. 20.02. A comparison of extracted biomass with intact biomass showed that 16% (*Komarekiella* sp. 89.12), 28% (*Desmonostoc muscorum* 90.03), and 41% (*Nostoc* sp. 20.02) of REE adsorption was due to the biosorption of the extracellular EPS. The glucose- rich EPS (15%–43% relative concentration) of all three strains grown under nitrogen-limited conditions showed significantly higher biosorption rates for all REEs. We also found a significantly higher maximum adsorption capacity of all REEs for the extracted EPS compared to cells without EPS and untreated biomass, highlighting the important role of the EPS as a binding

site for REEs in the biosorption process. EPS from cyanobacteria could thus be used as efficient biosorbents in future applications for REE recycling, e.g., industrial process water and wastewater streams.

KEYWORDS

extracellular polymeric substances, polysaccharides, *Komarekiella*, *Nostoc*, *Desmonostoc*, biosorption

1 Introduction

Rare earth elements (REEs), such as cerium (Ce), neodymium (Nd), terbium (Tb), and lanthanum (La), are expensive metals used in various modern electronic devices, like mobile phones, computers, and LCDs, and in emerging green technologies, e.g., in wind turbines or electric cars. Beyond their incorporation into these electronic devices and their pivotal role in manufacturing processes (Klingelhöfer et al., 2022), REEs also find extensive applications as medical products or as fertilizers for crops in agriculture. In addition, they are of new interest to veterinary practice since antibiotics as feed additives that promote growth have been banned due to global health concerns. Furthermore, REEs have been shown to have various beneficial impacts on animal growth and performance, leading to a discussion because this comes with adverse ecotoxicological effects (Abdelnour et al., 2019).

As such, there is a rising global demand for REEs that has become eminent, especially in recent years, resulting in a pronounced increase in production. This surge in REE output has led to the release of substantial quantities of anthropogenic REEs into rivers and streams through wastewater discharges. During a 15-year monitoring approach, e.g., it could be estimated that the Gironde Estuary in the Bordeaux Metropole of France transports more than 27 kg per year of the REE gadolinium (Gd), which is used as a contrast agent for magnetic resonance imaging (MRI) (Lerat-Hardy et al., 2019). Unfortunately, this and other studies also showed that wastewater treatment plants (WWTPs) often exhibit limited efficiency in removing REEs. Consequently, these valuable components are highly diluted in wastewater streams and rivers, where efficient and environmentally friendly recovery methods are hard to apply (Pereao et al., 2018). Several procedures, like precipitation, ion exchange, electrochemical methods, reverse osmosis, and adsorber resins, are utilized, but they come with high process costs and environmental impact due to toxic resins or inefficient recovery of highly diluted REEs (Chen et al., 2018; Jyothi et al., 2020; Pramanik et al., 2020). According to a study published in 2023, the recovery of some metals from highly diluted sources, e.g., from industrial wastewater, will become an economically viable option in the years to come, especially as the demand for such metals keeps rising (DuChanois et al., 2023). The elements regarded as high-priority metals are energy-intensive to obtain, geologically rare, and essential for high-tech sectors. In this context, REEs were listed alongside other metals like gallium, vanadium, or lithium.

In contrast to traditional recycling processes, microbiological and biotechnological approaches have gained increasing attention recently as they are considered sustainable and associated with low costs (da Costa et al., 2020; Dev et al., 2020). Among these processes, biosorption has been studied, a process describing the passive uptake of substances, such as metal ions, by biological materials, including biomass derived from diverse microorganisms (Giese, 2020; Brown et al., 2023). In the context of bioremediation, biosorption has been successfully applied to effectively sequester heavy metals from diluted solutions (Cho and Kim, 2003; Gupta et al., 2000). Along with heterotrophic microorganisms like *Escherichia coli* (e.g., Park et al., 2020) or *Saccharomyces cerevisiae* (Ojima et al., 2019), algae and cyanobacteria have emerged as particularly promising candidates for such purposes (e.g., Romera et al., 2006; Fischer et al., 2019; Al-Amin et al., 2021; Paper et al., 2023).

Cyanobacteria are assumed to have evolved approximately 3.5 billion years ago (Sánchez-Baracaldo and Cardona, 2020) and are adapted to nearly every habitat on Earth, from the aquatic systems of oceans and freshwater rivers to hot and cold deserts of extreme environments (e.g., Makhalanyane et al., 2015). Moreover, cyanobacteria have established stable symbiotic relationships between fungi, bryophytes, ferns, and plants (e.g., Rai et al., 2002). Fischer et al. (2019) showed that two heterocystous (nitrogen-fixing) cyanobacterial strains of the genus *Anabaena* were able to promote the enrichment of REE europium, samarium, and neodymium, while other species, such as *Arthrospira platensis*—which is already used in industrial food-additive production worldwide—can act as a safe and efficient bioremediator of erbium (Er)-contaminated wastewater (Yushin et al., 2022).

However, several mechanisms, such as ion exchange, complexation, or electrostatic attraction, can be simultaneously involved in the process of metal adsorption (Bilal et al., 2018). The contribution of EPS to the overall adsorption of REEs in cyanobacterial biomass has not been part of extensive research yet. In this context, the following major factors have been discussed for cyanobacteria: 1) the chemical composition of extracellular polymeric substances (EPS), also known as sheaths, capsules, and mucilage built by cyanobacteria (De Philippis et al., 2011), 2) the characteristics of their outer cell wall (Singh et al., 1998), 3) the viability state of their biomass (Singh, 2020), and 4) intracellular active uptake (bioaccumulation) vs. extracellular passive binding (biosorption, Olguín and Sánchez-Galván, 2012).

Following a contradicting discussion, biosorption is likely influenced by all of these factors, including the type of the metal ion itself, and thus metal adsorption is specific for each cyanobacterial biomass and each metal being taken up (Wilke et al., 2006; Dixit and Singh, 2013; Rzymski et al., 2014). Some studies, e.g., have presented evidence that REEs are adsorbed by living biomass and subsequently transported into the cell lumen and, at the same time, excluded the role of extracellular polymeric substances (EPS) (Fischer et al., 2019). It has also been reported that the viability of the biomass appears to be the most important factor in the process (Acharya et al., 2012). In contrast, others

demonstrated that solely specific compounds of EPS, e.g., the large molecular weight and sulfated polysaccharide sacran from *Aphanothece sacrum*, are responsible for the biosorption of the REE Nd (Okajima et al., 2010).

Hence, EPS must play a major role in biosorption when considering that most cyanobacteria produce these substances in copious amounts as they alleviate environmental stress conditions, prevent desiccation, store UV-protecting pigments such as scytonemin, and act as temporary storage to balance the intracellular C:N ratio (Tamaru et al., 2005; Pannard et al., 2016). As such, two forms of EPS can be distinguished: the free fraction composed of soluble extracellular polymeric substances (S-EPS; Underwood et al., 1995) and the particulate fraction corresponding to the transparent exopolymer particles known from, e.g., cyanobacterial blooms in water bodies (TEP; Passow and Alldredge, 1995). An overproduction of both types of EPS is triggered under nutrient-limited (N or P) conditions (Myklestad, 1995; Reynolds, 2007; Qian et al., 2022), during which photosynthetic carbon can still be accumulated, while protein production and growth are inhibited (De Philippis and Vincenzini, 1998). Consequently, carbon overflow can either be stored as reserve compound or excreted as EPS, which becomes especially apparent in terrestrial cyanobacterial species, such as *Nostoc commune*, that forms macroscopic thalli, which considerably improves the water holding capacity (Tamura et al., 2005). S-EPS have been reported to exhibit higher metal adsorption capacities due to their particularly high number of carboxyl and hydroxyl groups (Pereira et al., 2011; Mota et al., 2016).

Compared to EPS produced by other microorganisms, cyanobacterial EPS exhibit several unique compositional features, such as the presence of uronic acids or a high content of sulfate groups (Klock et al., 2007; Pereira et al., 2009). The accumulation of functional groups that are typically found in cyanobacterial EPS leads to particular anionic properties, which are beneficial for the attraction of positively charged metal ions.

Furthermore, during the biosorption process, functional units present in EPS, such as certain proteins, which can form complexes with metal cations, have frequently been discussed as the binding site (De Philippis et al., 2011). If the EPS should not be involved in the biosorption process, the REE must penetrate the EPS, which can be difficult because, in many species, these substances create a multi-layered sheath, and its thickness can reach up to double the diameter of the actual cell size (Mota et al., 2022).

In order to step into this ongoing discussion, we evaluated the role of EPS in biosorption of cerium (Ce), neodymium (Nd), terbium (Tb), and lanthanum (La) from three terrestrial, heterocystous cyanobacterial strains: *Nostoc* sp. 20.02 (epiphyte on lichen *Peltigera* sp.), *Desmonostoc muscorum* 90.03/PCC7903 (isolated from soil), and *Komarekiella* sp. 89.12 (hypoliths on quartz), which have been reported to be efficient REE adsorbers in our previous studies (Paper et al., 2023). We cultivated all three strains under N-limited and non-limited conditions, forcing EPS production, and harvested the EPS for structural and compositional analyses. Subsequently, we incubated 1) the separated EPS, 2) the EPS-free biomass, and 3) the intact biomass with EPS with Ce, Nd, Tb, and La, respectively. Afterward, we evaluated and compared the amount of each sorbed REE.

2 Materials and methods

2.1 Cultivation of cyanobacterial strains

Three terrestrial and nitrogen-fixing cyanobacterial strains, *Nostoc* sp. 20.02 (epiphyte on lichen *Peltigera* sp.; Germany), *Desmonostoc muscorum* 90.03/PCC7903 (soil, United States), and *Komarekiella* sp. 89.12 (hypolithic on quartz, Namibia, South Africa) were used for the study. Their phylogenetic placement based on their complete 16S rRNA sequence was recently elucidated, from which it can be deduced that *Komarekiella* sp. 89.12 represents a novel species (Paper et al., 2023).

All strains were inoculated with approximately 0.1–0.3 g of wet biomass from a stock culture (17°C; light/dark rhythm 16:8 h; 30 µmol photons m^{-2} s^{-1}) in 1-L bubble columns containing BG11 cultivation medium and additionally in nitrogen-depleted BG 11_0 medium (Lama et al., 1996). In the bubble columns, they were cultivated at 23°C under a light/dark rhythm of 16:8 h at 300 µmol photons m^{-2} s^{-1} photosynthetic photon flux density for 4 weeks. All cultivated cells were first harvested using two sieves of 0.5 mm and 0.1 mm and then using paper filters of 40 µm openings. Afterward, wet biomass was dried by lyophilization.

In addition, all strains were cultivated on 0.9% solidified BG11 medium for 4 weeks in order to visualize their EPS structures by light microscopy under the conditions described above.

2.2 Microscopy

All three strains were visualized through differential interference contrast (DIC) microscopy using an Olympus BX51 microscope (Evident Europe GmbH, Hamburg, Germany) equipped with ×10, ×20, ×40, and ×100 magnifications, oil immersion equipped with a MicroLive multi-format camera (Lifesolution, Bremen, Germany), and software MicroLive (v5.0). To visualize the sheath material of the cells, ACN staining was performed (20:1: 1 mix; 0.1 g Astra blue in 79.5 mL H_2O and 2.5 mL acetic acid; 0.1 g chrysoidine in 100 mL H_2O; and 0.1 g new fuchsine in 100 mL H_2O; Carl Roth, Karlsruhe, Germany), which allows differentiation of structures according to colors due to the binding characteristics of the substances. Acid mucopolysaccharides are stained blue by Astra blue, cellulose and lignin are stained red by new fuchsine, and hydrophobic substances, such as cutin, are stained yellow.

2.3 Separation of EPS

Wet biomass was harvested as described above and used for EPS extraction (modified after Strieth et al., 2020). The wet biomass was collected in 50-mL tubes, and five times the amount (v/w) of ddH_2O preheated to 55°C was added. The tubes were then mixed for 60 min in an overhead shaker at 55°C in an incubator, followed by ultrasonic treatment for 5 min (at 240 W and 40 kHz, Emmi-H60, EMAG, Mörfelden, Germany) and centrifugation at 14,000 rcf. The supernatant was transferred into 50-mL centrifuge tubes for lyophilization (at 0.1 mbar and 21°C, Epsilon 2-4 LSCplus, Christ, Osterode, Germany).

2.4 Metal adsorption experiments

Metal adsorption was tested for EPS, untreated biomass, and biomass after EPS separation. The experiments were carried out following an experimental setup described by Heilmann et al. (2015) and Heilmann et al. (2021). Single-metal REE solutions with a concentration of 10 mM and a starting pH value of 5 ± 0.2 were used to determine the maximal adsorption capacity of the tested biomasses. The influence of the pH value on metal biosorption and experiments on adsorption kinetic carried out by varying the incubation time of the biomass in cerium(III) nitrate solutions were determined in previous studies on the untreated biomass (see Paper et al., 2023). Therefore, to compare the untreated and treated conditions investigated here, an optimal pH value of 5 was assumed to be efficient for a preliminary standard protocol. To determine the maximum adsorption capacity (*Q*), 10–20 mg of dry biomass was weighed into centrifuge tubes and incubated in 2 mL of metal solutions for 3 h under constant shaking at room temperature. Afterward, the metal adsorption to the tested biomass was calculated by dividing the changes in metal concentration by the amount of incubated biomass (see Eq. 1).

$$Q = \frac{n_i - n_f}{m} = \frac{\left(c_i - c_f\right) \times V}{m}, \quad (1)$$

where Q = adsorption capacity, n_i = initial amount of substance, n_f = final amount of substance after incubation, c_i = initial metal concentration, c_f = final metal concentration after incubation, V = volume, and m = weight of biomass.

2.5 FT-IR analysis of cyanobacterial biomass and EPS

Infrared (IR) spectroscopy is a valuable method for determining the qualitative composition of organic functional groups. In this study, it was used to detect and identify interactions of metal cations with functional groups in isolated EPS samples. Following incubation in cerium(III) nitrate solution (1 µmol 1 mg^{-1} biomass) for 2 h, the samples were lyophilized. A FT-IR spectrometer (Nicolet iS50R, Thermo Fisher Scientific, Waltham, US) equipped with an attenuated total reflection multi-range diamond sampling station (iS50 ATR) was used to obtain the IR spectra. The IR spectra were recorded in a range from 400 to 4,000 cm^{-1} for each sample.

2.6 HPLC analysis of EPS

Polysaccharides are known to play an important role in biosorption processes due to their ability to form complexes with metal cations (Joly et al., 2020). As EPS comprise chemically complex polymeric carbohydrates, the monomeric sugar composition of the extracted EPS samples was analyzed using an HPLC-based method. The monomeric sugar composition of the cyanobacterial biomass was determined for all three selected strains following a reported protocol (Jurkowski et al., 2022). Each sample was hydrolyzed with 2% H_2SO_4 in an autoclave for 1 h at 121°C at 1 bar in order to release monomeric carbohydrate building blocks from the samples constituting polymeric carbohydrates. Afterward, each sample was centrifuged at 10,000 rcf for 10 min. Following hydrolysis, the solutions were neutralized with calcium carbonate (pH 7). Precipitated calcium salt was removed by centrifugation at 10,000 rcf for 10 min after neutralization. The supernatant was frozen at −20°C overnight. Subsequently, the samples were heated to 5°C and centrifuged at 10,000 rcf for 10 min to remove any residual precipitate. Sugar analysis was carried out using an HPLC system (Agilent Infinity II LC 1260, Agilent Technologies, Waldbronn, Germany) equipped with an autosampler, quaternary pump, column oven, DAD, and a Shodex RI detector (Showa Denko Europe GmbH, Munich, Germany). Prior to injection, each sample was filtered using modified PES 500-µL centrifugal filters (VWR, Ismaning, Germany) with a cut-off of 10 kDa. In a subsequent step, the monomeric sugar mixture resulting from chemical hydrolysis was analyzed using the HPLC system previously described. A Rezex ROA-Organic Acid H+ (8%) ion-exclusion column (300 mm, 7.8 mm internal diameter; Phenomenex Ltd., Aschaffenburg, Germany) was used for the isocratic separation with 5 mM sulfuric acid at a flow rate of 0.5 mL min^{-1} and a temperature of 70°C.

2.7 Statistical analyses

Analyses were performed using the software package PAST (Hammer et al., 2001). Multivariate normality is assumed by a number of multivariate tests. PAST computes Mardia's multivariate skewness and kurtosis with tests based on chi-squared (skewness) and normal (kurtosis) distributions. Differences in the adsorption capacity of the tested biomass samples were statistically evaluated with a two-sided *t*-test and one-way ANOVA followed by a *post hoc* analysis according to the Scheffé test (N-limited condition) or by one-way and two-way ANOVA tests (multivariate treatment conditions) depending on the selected dependent and independent variables and verified assuming equal variances by Tukey's *post hoc* test regarding different factors and interactions (comparison of adsorption capacities).

3 Results

3.1 Composition of extracellular polymeric substances

EPS staining with ACN solution (Figure 1) showed that the structure of the three investigated strains differed. *Desmonostoc muscorum* 90.03 formed thin and firm EPS sheaths around hormogonia (Figures 1A–C arrows), while adult cells loosely grouped in micro-colonies surrounded by a common, limited, and firm sheath. The strain *Nostoc* sp. 20.02 showed the greatest amplitude of cell differentiation and life stages ranging from adult micro-colonies (Figure 1D) to akinetes (Figure 1E) and multiseriate filaments (Figure 1F). During most stages, cells were brownish and surrounded by excess EPS material. Adult micro-colonies were surrounded by a very wide, diffluent, hardly limited, soft, and multi-layered EPS sheath (Figure 1D, arrows). At the same time, akinetes and filaments were encapsulated in firm and limited sheaths

10.3389/fbioe.2023.1299349

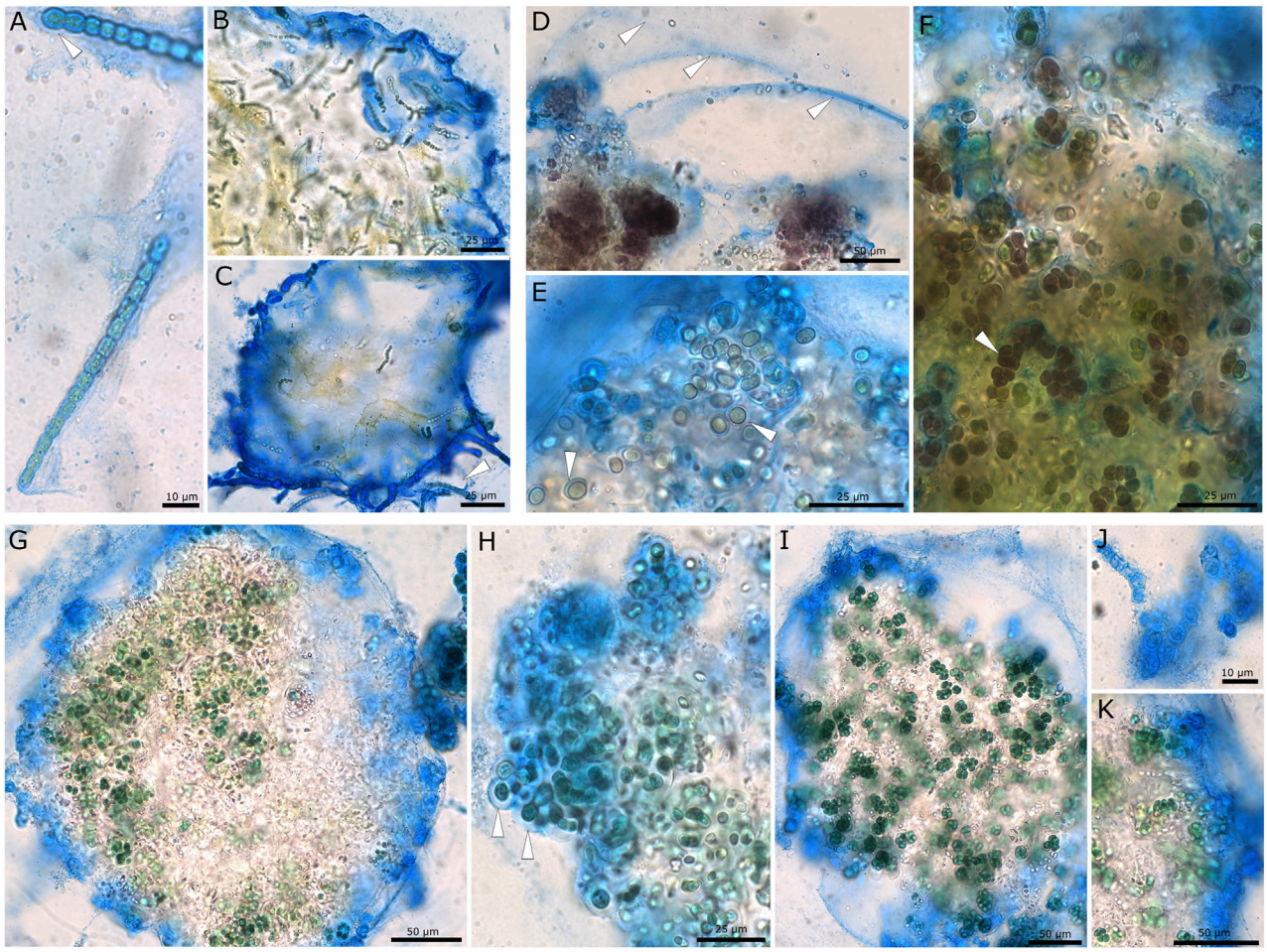

FIGURE 1
Microscopic images showing EPS of cyanobacterial strains stained with ACN solution. **(A–C)** *Desmonostoc muscorum* 90.03 with thin EPS on hormogonia **(A,C)** and a limited, firm, and wide common sheath surrounding micro-colonies **(B,C)**. **(D–F)** Brownish pigmented cells of *Nostoc* sp. 20.02. **(D)** Wide, diffluent, and hardly limited EPS (arrows), **(E)** akinetes with firm sheaths, and **(F)** small cell packages and multiseriate filaments (arrow) encapsulated by wide, limited sheaths. **(G–K)** *Komarekiella* sp. 89.12 with a limited common sheath encapsulating micro-colonies **(G)**, wide, non-lamellated sheaths surrounding single cells (arrows) **(H)**, small cell packages surrounded by a common sheath **(I)**, firm and narrow capsules of dead cells **(J)** and layers of outer EPS membranes **(K)**.

(Figures 1E, F). *Komarekiella* sp. 89.12 mainly formed small, densely packed cell packages that were grouped within shared EPS material (Figures 1G, I). The micro-colonies were surrounded by a common, limited, and more or less narrow sheath, while the single cells and small cell packages were coated by wide, limited, and non-layered EPS (Figure 1H, arrows) or firm, narrow, and hard capsules (Figures 1J, K).

Following chemical hydrolysis with 2% H_2SO_4, the monomeric sugar composition of isolated EPS samples from *Nostoc* sp. 20.02, *Desmonostoc muscorum* 90.03, and *Komarekiella* sp. 89.12 was determined using HPLC analysis (Figure 2; Supplementary Table S1). All strains differed in their relative content of detected organic acids and sugar monomers of EPS. The main components of EPS from *Nostoc* sp. 20.02 were 42.7% glucose, 20.0% rhamnose, and 21.0% xylose, mannose, galactose, or fructose (differentiation was not possible because of peak-overlapping). EPS of *Desmonostoc muscorum* 90.03 comprised 36% xylose, mannose, galactose, or fructose, 26.0% rhamnose, and 15.0% glucose. With 10.3%, the portion of glucuronic acid was relatively high. The EPS isolated from *Komarekiella* sp. 89.12 also had high portions of glucose at 29.8% and those of xylose, mannose, galactose, or fructose at 33.7%. Compared to the other samples, the EPS of *Komarekiella* sp. 89.12 included relatively high amounts of fucose monomers at 16.9%.

3.2 Maximum adsorption capacity of EPS for REEs under nitrogen-limited vs. non-limited conditions

Nostoc sp. 20.02, *Desmonostoc muscorum* 90.03, and *Komarekiella* sp. 89.12 produce enhanced amounts of EPS under nitrogen-limited cultivation conditions. Adsorption experiments with biomass produced under these conditions displayed a higher maximum adsorption capacity for REEs compared to biomass produced under standard conditions (Figure 3). A two-sided

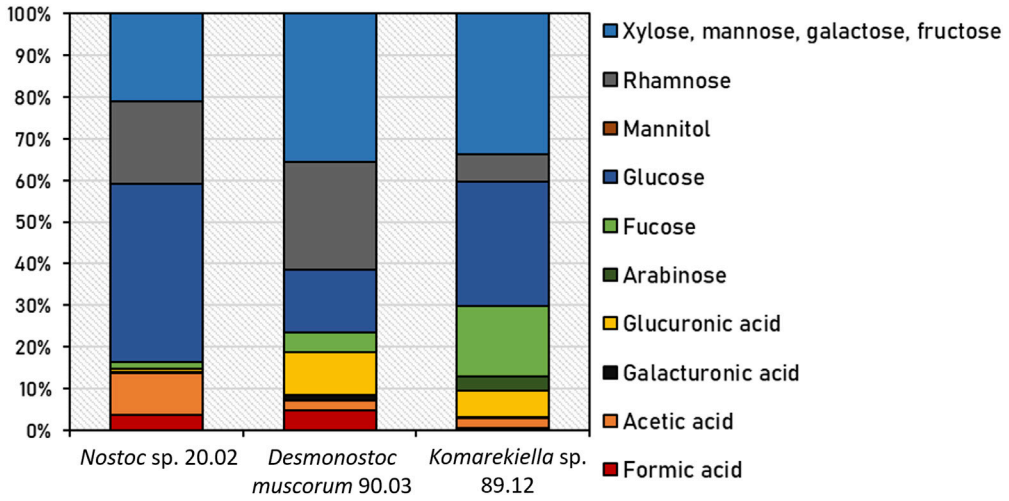

FIGURE 2
Relative content of detected organic acids and sugar monomers of EPS from *Nostoc* sp. 20.02, *Desmonostoc muscorum* 90.03, and *Komarekiella* sp. 89.12 after chemical hydrolysis with 2% H_2SO_4. Underlying data are listed in Supplementary Table S1.

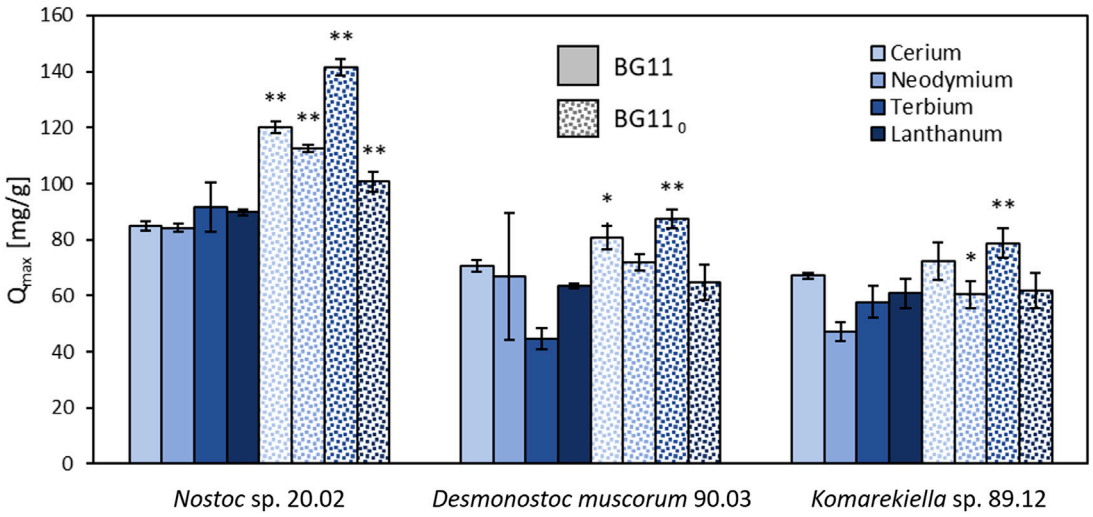

FIGURE 3
Maximum adsorption capacity for cerium, neodymium, terbium, and lanthanum of the lyophilized biomass (including EPS) of *Nostoc* sp. 20.02, *Desmonostoc muscorum* 90.03, and *Komarekiella* sp. 89.12. Biomass cultivation on BG11 compared to cultivation on nitrogen-depleted BG 11_0, (two-sided *t*-test: $*p < 0.05$; $**p < 0.01$; n = 3).

t-test revealed significant ($p < 0.05$) and highly significant ($p < 0.01$) differences in maximum adsorption capacity for REEs, especially for *Nostoc* sp. 20.02.

3.3 Maximum adsorption capacity of EPS, biomass after EPS extraction, and untreated biomass for REEs

Extracted EPS of all three tested cyanobacteria displayed high adsorption capacities for REEs (Figure 4). The separation of EPS from cyanobacterial biomasses significantly reduced the capacity for metal adsorption of the remaining biomass for all tested strains. Consequently, the maximum adsorption capacity of EPS for all tested metals was significantly higher than the maximum adsorption capacity of EPS-extracted biomass for all three tested cyanobacteria (see Supplementary Material). Although the differences were not as pronounced as for EPS samples, the metal adsorption capacities of EPS-extracted and untreated biomass varied significantly for *Desmonostoc muscorum* 90.03 and *Komarekiella* sp. 89.12. Regarding Ce, Nd, and La, *Nostoc* sp. 20.02 had the significantly highest adsorption capacity for all treatments except for extracted EPS. The extracted EPS of *Desmonostoc muscorum* 90.03 showed the most significantly highest adsorption capacity within the tested

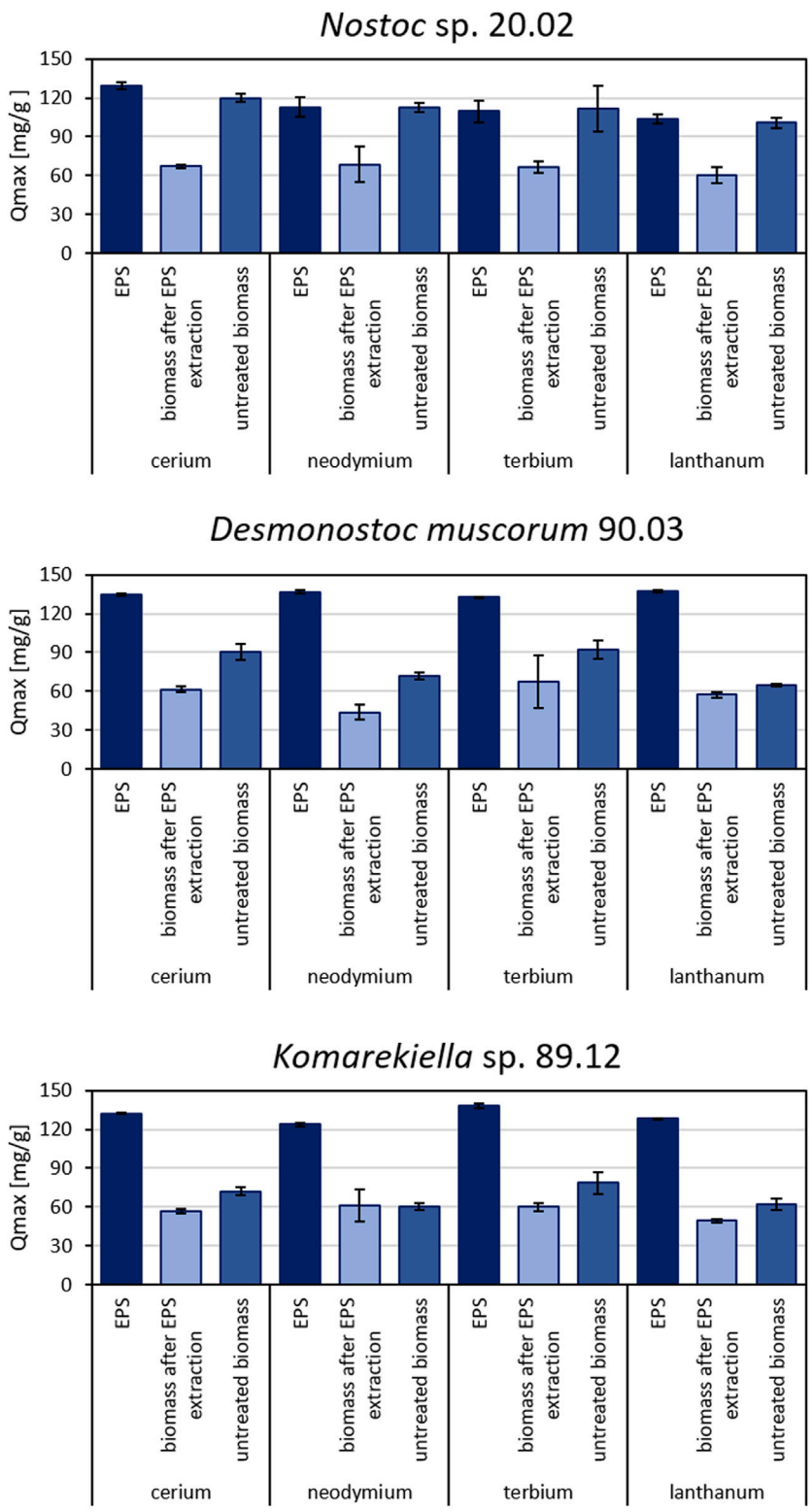

FIGURE 4
Maximum adsorption capacity for cerium, neodymium, terbium, and lanthanum for different biomass samples of *Nostoc* sp. 20.02, *Desmonostoc muscorum* 90.03, and *Komarekiella* sp. 89.12. Statistically significant differences in metal adsorption capacity were determined in a two-way ANOVA ($p < 0.05$; n = 3), followed by Tukey's *post hoc* test. (For detailed significant differences see Supplementary Tables S2–S5).

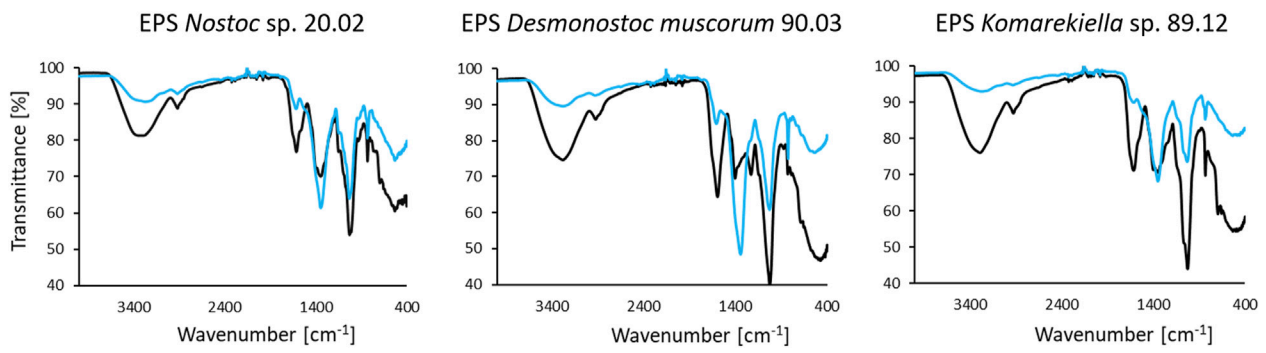

FIGURE 5
FT-IR spectra of EPS samples separated from indicated species' biomass before (black) and after incubation in cerium(III) nitrate solution (1 µmol mg^{-1} biomass) (blue).

species. While differences between treatments exist, no significant differences in adsorption capacities between species exist for Tb. The adsorption of Nd by *Komarekiella* sp. 89.12 and Tb by *Desmonostoc muscorum* 90.03 were an exception in that context. Interestingly, untreated biomass and EPS from *Nostoc* sp. 20.02 displayed similar adsorption capacities for the tested REEs (see Supplementary Material).

3.4 FT-IR analysis of EPS before and after incubation in cerium(III) nitrate solution

The IR spectra of all three analyzed EPS samples displayed signals that are characteristic of substances comprising polysaccharides (Figure 5). The broad band in the region between 3,500 and 3,200 cm^{-1} in the spectra can be assigned to the stretching vibrations of hydroxyl groups, whereas the signal at approximately 2,900 cm^{-1} is attributed to C-H stretching vibrations of CH_2 groups (Liang and Marchessault, 1959). The presence of carboxyl groups is indicated by signals at 1,630 cm^{-1}, which are linked to C=O stretching vibrations (Qian et al., 2009). Distinct signals at approximately 1,040 cm^{-1} can be assigned to C-O stretching vibration in polysaccharides (Nakamoto, 2009). Furthermore, the signals at approximately 1,340 cm^{-1} and in the area of 830 cm^{-1} could be attributed to asymmetric and symmetric stretching vibrations of NO_3 (Trivedi et al., 2015). The interaction of biomass with the adsorbed metal ions induced changes in intensity and shifts in position for some signals in the FT-IR spectra following contact with cerium(III) nitrate.

Most notably, an attenuation of intensity is observed in the region between 3,500 and 3,200 cm^{-1} for all samples, indicating a decrease in free hydroxyl groups in the biomass (Mitic-Stojanovic et al., 2011). Likewise, direct interactions with carboxyl groups are indicated by differences in signal intensities at approximately 1,630 cm^{-1} and 1,040 cm^{-1} (Qian et al., 2009).

4 Discussion

Although it is accepted that EPS production is triggered under unfavorable metabolic conditions, such as N and/or P limitations (Flaibani et al., 1989; Vincenzini et al., 1990), this does not generally hold true. Nicolaus et al. (1999) reported a dramatic decrease in EPS production for two *Anabaena* species, which was also reported earlier for another *Anabaena* species byLama et al. (1996). This is in line with results by De Philippis et al. (1998) and Khattar et al. (2010) who found the same effect for five strains of *Cyanothece* and *Limnothrix redekei*, respectively. One reason might be that all of these strains are aquatic cyanobacteria, which rely less on the protecting properties of EPS during nutrient-limiting periods. The water body, e.g., alleviates temperature shifts and enhances the equal distribution of nutrients, and desiccation is rarely occurring—some of the primary protecting purposes of EPS. Alternatively, cyanobacteria can invest their photosynthetic carbon overflow during nutrient-limited conditions in the synthesis of intracellular energy storage compounds, such as glycogen, rather than releasing excess amounts of mucilage. For terrestrial cyanobacteria like the three strains examined in our study, an opposing situation is often reported: most of the cyanobacteria grow somehow attached to a substrate like soil or the surface of stones, where the contact between the substrate and the organisms is the site of nutrient uptake. These nutrients can only be taken up or distributed during humid periods when they are dissolved in the water layer. During these times, EPS play a crucial role as this is the contact interface between the cells and the substrate, e.g., the EPS of thalli formed by *Nostoc commune* can drastically increase their volume (Shaw et al., 2003; Tamaru et al., 2005), effectively absorbing water and nutrients. During subsequent desiccation periods, the EPS matrix can retain water and nutrients, which can be delivered to the cells, resulting in an extended phase of photosynthetic activity and, therewith, growth. In terrestrial cyanobacteria, the EPS consist of at least 10%–20% of dry matter (Huang et al., 1998), and under biotechnological control, the production can be induced to 50% of DM by drought stress at air-exposed cultivation (emersed) in biofilm-photobioreactors (Strieth et al., 2017; Lakatos and Strieth, 2018). In addition, a lot of terrestrial genera—and especially those of the Nostocales, such as *Nostoc*, *Desmonostoc*, and *Komarekiella*, that were part of this study—have complex life cycles (Figure 1) during which they undergo cell differentiation (Mollenhauer et al., 1994; Hrouzek et al., 2013; Johansen et al., 2017). These cyanobacteria not only have the ability to produce different types of cells, such as akinetes,

which serve as resting stages that come along with a thick cell wall and EPS capsule (Figure 1E) but can also create cell stages, such as mobile hormogonia with a weakly pronounced EPS sheath (Figure 1A). Additionally, primordia and adult stages can be formed, which display extraordinarily thick EPS capsules surrounded by S-EPS (Mollenhauer et al., 1994; Hrouzek et al., 2013; Johansen et al., 2017). These differences are especially pronounced in terrestrial cyanobacteria compared to aquatic species and might indicate that terrestrial cyanobacterial strains have multiple triggers to metabolically invest in EPS during adverse environmental conditions. This opens new prospects for biosorption and other biotechnological approaches linked to cyanobacterial EPS because their formation and the properties of a strain, such as the produced EPS amounts, can be artificially triggered and directed (e.g., Moore et al., 2005; Sukenik et al., 2013). This is especially interesting for the strains tested here because they can grow under N-limitation due to the presence of heterocytes that bind N from the atmosphere. Our results demonstrate that the maximum adsorption capacity for Ce, Nd, Tb, and La was significantly increased for all strains cultivated under N-limited conditions compared to those grown under non-limiting growth conditions (Figure 3). This effect can be explained by i) a change in the composition of the EPS caused by the N-limitation, which consequently increases the adsorption capacity, or ii) an overproduction of EPS in response to N-limitation, resulting in a greater number of binding sites for REE biosorption. Although both effects can hardly be differentiated in this study, one can make the following conclusions: cultivation under N-limitation of the three tested strains significantly increased the maximum adsorption capacity for REE. This is in accordance with previous studies on metal adsorption by cyanobacterial EPS, where a direct positive correlation between metal uptake and EPS presence has been reported (Singh et al., 1998; Tien et al., 2005; Cui et al., 2021).

Interestingly, all extracted EPS samples exhibited comparable adsorption capacities for the tested REEs (with the exception of lanthanum, see Supplementary Material), whereas there were significant differences for untreated biomass. Similar adsorption capacities of EPS were observed despite variations in the monomeric EPS sugar composition. This might indicate an equally strong interaction of different sugar moieties with metal ions or the presence of other metal-interacting compounds in the EPS, such as proteins or lipids (Yadav et al., 2020). However, the content of proteins is mostly less than 10% in the EPS, and under N-limiting conditions—where higher adsorption capacities of separated EPS were found in this study—less proteins are produced arguing against an important role of proteins in REE adsorption, although special metal-binding proteins are synthesized by cyanobacteria such as metallothionein (Turner and Robinson, 1995). In this context, the analysis of FT-IR spectra indicated typical patterns for polysaccharide structures and indicated a dominant contribution of carbohydrate-associated hydroxyl and carboxyl groups during metal adsorption for all samples, which indicates a polysaccharide-driven mechanism. Metal adsorption by biological materials is often connected to the interaction of metal cations with hydroxyl and carboxyl groups (Ngah and Hanafiah, 2008; Javanbakht et al., 2014). EPS extracted from *Desmonostoc muscorum* 90.03 and *Komarekiella* sp. 89.12 comprised approximately 6%–10% glucuronic acids. Under standard environmental conditions, the carboxyl groups of uronic acids are partially ionized in aqueous solutions and contribute negative charges to the EPS polymers. These negative charges attract metal cations and support their sequestration.

In contrast, the EPS derived from *Nostoc* sp. 20.02 only contained small amounts of uronic acids. However, subsequent chemical hydrolysis released elevated amounts of acetic acid. The occurrence of acetic acid indicates the presence of acetylated sugar compounds in the EPS polymer. These building blocks can interact with metal ions in a same manner as uronic acids. This is in accordance with the FT-IR spectra, which indicated the involvement of carboxyl groups in metal adsorption for all strains tested in this study.

Compared to isolated EPS, the adsorption capacity for REE of biomass was significantly reduced if EPS were removed. Nevertheless, the EPS-extracted biomass still adsorbed metals from aqueous solutions. This indicates that REEs interact with components of the cyanobacterial cell wall. Compared to EPS, the cell wall might display fewer active binding sites or functional moieties and may exhibit a weaker REE affinity. For *Nostoc* sp. 20.02, the differences in metal adsorption capacity between EPS and untreated biomass were small. This suggests a major contribution of EPS to the overall metal adsorption in this cyanobacterium. Crude *Nostoc* sp. 20.02 biomass might have been fully encapsulated by EPS and, therefore, displayed similar adsorption properties to those of extracted EPS. On the other hand, differences in adsorption capacity between untreated biomass and EPS-extracted biomass for *Desmonostoc muscorum* 90.03 and *Komarekiella* sp. 89.12 indicate a supporting role of EPS in the total metal uptake.

Further investigations are required to determine the extent of the influence of EPS on the major mechanisms of overall adsorption. The differences between untreated and EPS-extracted biomass are mostly significant, but EPS-extracted biomass still had adsorption capacities of an average of 59.2% ± 2% (*Nostoc* sp. 20.02), 72.5% ± 12% (*Desmonostoc muscorum* 90.03), and 84.1% ± 11% (*Komarekiella* sp. 89.12) compared to untreated biomass. However, 16% (*Komarekiella* sp. 89.12)–41% (*Nostoc* sp. 20.02) of REE adsorption involves the extracellular passive binding of EPS (biosorption) caused by their chemical composition, especially that of polysaccharides. Moreover, separated EPS have even higher adsorption capacities than the intact biomass of the cyanobacteria assayed in this study.

In the context of a potential biosorption-based application for metal recovery, the continuous removal of EPS from a cyanobacterial culture during cultivation might be a feasible approach (Strieth et al., 2017). After metal adsorption, the separated EPS can be dried, and the resulting metal-enriched powder can be further processed for metal recovery. Cyanobacteria usually survive EPS extraction and can be reused for biomass and EPS production.

EPS extracted from cyanobacterial biomass demonstrated notable adsorption properties for REEs, suggesting their potential as an effective adsorbent for the separation and recovery of these valuable elements from wastewater or industrial effluents. The maximum adsorption capacity for REEs of the extracted EPS was higher than other adsorbents that have been investigated for metal recovery from aqueous solutions, including composite materials or untreated and modified biomass (see Table 1). Based on these

TABLE 1 Comparison of the maximum adsorption capacity for rare earth elements of various adsorbents.

Adsorbent	Metal studied	Q_{max} [mg/g]	Reference
Calothrix brevissima biomass and *Chlorella kessleri* biomass	Nd^{3+}	67.8	Heilmann et al. (2021)
	Eu^{3+}	50.1	
	Nd^{3+}	53.4	
	Eu^{3+}	16.7	
Nanocomposite of calcium alginate carrying poly (pyrimidine-thiophene-amide), CA-P(P-T-A)-NZFO	Nd^{3+}	72.5	Javadian et al. (2020a)
	Tb^{3+}	108.8	
	Dy^{3+}	113.1	
Nanocomposite of calcium alginate/carboxymethyl chitosan, CA/CMC/$Ni_{0.2}Zn_{0.2}Fe_{2.6}O_4$	Nd^{3+}	73.4	Javadian et al. (2020b)
	Tb^{3+}	101.6	
	Dy^{3+}	114.7	
Magnetic alginate–chitosan gel beads	La^{3+}	97.1	Wu et al. (2011)
Chitosan–manganese–ferrite beads	Nd^{3+}	44.3	Durán et al. (2020)
Alginate–lignin composite	Ce^{3+}	98.0	Fila et al. (2022)
	Nd^{3+}	98.0	
	Pr^{3+}	98.7	
	La^{3+}	109.6	
Escherichia coli biomass	Nd^{3+}	30.9	Hosomomi et al. (2013)
	Dy^{3+}	32.7	
	Lu^{3+}	42.7	
Calcium-loaded *Sargassum polycystum* biomass	La^{3+}	40.3	Diniz and Volesky (2005)
	Eu^{3+}	62.3	
	Yb^{3+}	48.4	
EPS of *Nostoc* sp. 20.02, EPS of *Desmonostoc muscorum* 90.03, and EPS of *Komarekiella* sp. 89.12	Ce^{3+}	129.3 ± 2.7	This study
	Nd^{3+}	112.9 ± 7.6	
	Tb^{3+}	109.5 ± 8.2	
	La^{3+}	103.5 ± 3.7	
	Ce^{3+}	134.8 ± 0.7	
	Nd^{3+}	136.7 ± 1.3	
	Tb^{3+}	133.1 ± 0.2	
	La^{3+}	137.4 ± 1.3	
	Ce^{3+}	132.4 ± 0.5	
	Nd^{3+}	123.9 ± 1.3	
	Tb^{3+}	138.2 ± 1.9	
	La^{3+}	128.5 ± 0.4	

promising results, further research and optimization are necessary to determine the feasibility and efficiency of EPS in an adsorption-based metal recovery process.

For process development, important parameters and adsorption characteristics have to be examined, including adsorption kinetics, isotherms, and the influence of the pH value on metal uptake. Furthermore, adsorption–desorption cycles are commonly employed in the recovery of valuable materials, and the reversibility of the adsorption process is a key factor for environmentally friendly and cost-effective process implementation. Most important is probably the evaluation of additional and different cyanobacterial strains in terms of EPS

and adsorption of REEs to determine the efficiency of the process and to further untangle strain-specific and general properties of the overall process. The desorption characteristics of REEs from EPS and biomass long-term stability have to be investigated to assess the viability of using EPS in practical applications.

Data availability statement

The original contributions presented in the study are included in the article/Supplementary Material; further inquiries can be directed to the corresponding author.

Author contributions

MP: Conceptualization, Data curation, Formal Analysis, Investigation, Methodology, Validation, Visualization, and Writing–original draft. PJ: Investigation, Resources, Visualization, Writing–original draft, and Writing–review and editing. MK: Data curation, Formal Analysis, Investigation, Methodology, and Writing–review and editing. ML: Conceptualization, Funding acquisition, Project administration, Resources, Supervision, Validation, and Writing–review and editing. TN: Conceptualization, Funding acquisition, Project administration, Resources, Supervision, Validation, and Writing–review and editing. TB: Conceptualization, Funding acquisition, Project administration, Resources, Supervision, Validation, and Writing–review and editing.

Funding

The author(s) declare financial support was received for the research, authorship, and/or publication of this article. This project was funded by the Bavarian State Ministry of the Environment and Consumer Protection within the framework of the ForCYCLE II Project Group. ML was supported by the Ministry of Science and Health Rhineland-Palatinate (PhytoBioTech, 724–0116#2021 and 004–1501 15405), the Federal Ministry of Education and Research (W2V-Strategy2Value, 03WIR4502A, and Technology2Value 03WIR4504B), and the EU-HORIZON (Waste2BioComp ID: 101058654). PJ was funded by the German Research Council (DFG; Grit Life; JU 3228, 1–1).

Acknowledgments

The authors would like to thank Lina Werner and Andreas Wruck for their help during laboratory work as well as Dorina Strieth for her help during the modification of the EPS extraction.

Conflict of interest

The authors declare that the research was conducted in the absence of any commercial or financial relationships that could be construed as a potential conflict of interest.

Publisher's note

Supplementary material

The Supplementary Material for this article can be found online at: https://www.frontiersin.org/articles/10.3389/fbioe.2023.1299349/full#supplementary-material

References

Abdelnour, S. A., Abd El-Hack, M. E., Khafaga, A. F., Noreldin, A. E., Arif, M., Chaudhry, M. T., et al. (2019). Impacts of rare earth elements on animal health and production: highlights of cerium and lanthanum. *Sci. Total Environ.* 672, 1021–1032. doi:10.1016/j.scitotenv.2019.02.270

Acharya, C., Chandwadkar, P., and Apte, S. K. (2012). Interaction of uranium with a filamentous, heterocystous, nitrogen-fixing cyanobacterium, *Anabaena torulosa*. *Bioresour. Technol.* 116, 290–294. doi:10.1016/j.biortech.2012.03.068

Al-Amin, A., Parvin, F., Chakraborty, J., and Kim, Y. I. (2021). Cyanobacteria mediated heavy metal removal: a review on mechanism, biosynthesis, and removal capability. *Environ. Technol. Rev.* 10 (1), 44–57. doi:10.1080/21622515.2020.1869323

Bilal, M., Rasheed, T., Sosa-Hernández, J. E., Raza, A., Nabeel, F., and Iqbal, H. M. (2018). Biosorption: an interplay between marine algae and potentially toxic elements—a review. *Mar. drugs* 16 (2), 65. doi:10.3390/md16020065

Brown, R. M., Mirkouei, A., Reed, D., and Thompson, V. (2023). Current nature-based biological practices for rare earth elements extraction and recovery: bioleaching and biosorption. *Renew. Sustain. Energy Rev.* 173, 113099. doi:10.1016/j.rser.2022.113099

Chen, L., Wu, Y., Dong, H., Meng, M., Li, C., Yan, Y., et al. (2018). An overview on membrane strategies for rare earths extraction and separation. *Sep. Purif. Technol.* 197, 70–85. doi:10.1016/j.seppur.2017.12.053

Cho, D. H., and Kim, E. Y. (2003). Characterization of Pb 2+ biosorption from aqueous solution by *Rhodotorula glutinis*. *Bioprocess Biosyst. Eng.* 25, 271–277. doi:10.1007/s00449-002-0315-8

Cui, L., Fan, L., Li, Z., Wang, J., Chen, R., Zhang, Y., et al. (2021). Characterization of extracellular polymeric substances from *Synechocystis* sp. PCC6803 under Cd (II), Pb (II) and Cr (VI) stress. *J. Environ. Chem. Eng.* 9 (4), 105347. doi:10.1016/j.jece.2021.105347

da Costa, T. B., da Silva, M. G. C., and Vieira, M. G. A. (2020). Recovery of rare-earth metals from aqueous solutions by bio/adsorption using non-conventional materials: a review with recent studies and promising approaches in column applications. *J. Rare Earths* 38 (4), 339–355. doi:10.1016/j.jre.2019.06.001

De Philippis, R., Colica, G., and Micheletti, E. (2011). Exopolysaccharide-producing cyanobacteria in heavy metal removal from water: molecular basis and practical applicability of the biosorption process. *Appl. Microbiol. Biotechnol.* 92, 697–708. doi:10.1007/s00253-011-3601-z

De Philippis, R., Margheri, M. C., Materassi, R., and Vincenzini, M. (1998). Potential of unicellular cyanobacteria from saline environments as exopolysaccharide producers. *Appl. Environ. Microbiol.* 64 (3), 1130–1132. doi:10.1128/aem.64.3.1130-1132.1998

De Philippis, R., and Vincenzini, M. (1998). Exocellular polysaccharides from cyanobacteria and their possible applications. *FEMS Microbiol. Rev.* 22, 151–175. doi:10.1016/s0168-6445(98)00012-6

Dev, S., Sachan, A., Dehghani, F., Ghosh, T., Briggs, B. R., and Aggarwal, S. (2020). Mechanisms of biological recovery of rare-earth elements from industrial and electronic wastes: a review. *Chem. Eng. J.* 397, 124596. doi:10.1016/j.cej.2020.124596

Diniz, V., and Volesky, B. (2005). Biosorption of La, Eu and Yb using *Sargassum* biomass. *Water Res.* 39 (1), 239–247. doi:10.1016/j.watres.2004.09.009

Dixit, S., and Singh, D. P. (2013). Phycoremediation of lead and cadmium by employing *Nostoc muscorum* as biosorbent and optimization of its biosorption potential. *Int. J. phytoremediation* 15 (8), 801–813. doi:10.1080/15226514.2012.735290

DuChanois, R. M., Cooper, N. J., Lee, B., Patel, S. K., Mazurowski, L., Graedel, T. E., et al. (2023). Prospects of metal recovery from wastewater and brine. *Nat. Water* 1 (1), 37–46. doi:10.1038/s44221-022-00006-z

Durán, S. V., Lapo, B., Meneses, M., and Sastre, A. M. (2020). Recovery of neodymium (III) from aqueous phase by chitosan-manganese-ferrite magnetic beads. *Nanomaterials* 10 (6), 1204. doi:10.3390/nano10061204

Fila, D., Hubicki, Z., and Kołodyńska, D. (2022). Fabrication, characterization and evaluation of an alginate–lignin composite for rare-earth elements recovery. *Materials* 15 (3), 944. doi:10.3390/ma15030944

Fischer, C. B., Körsten, S., Rösken, L. M., Cappel, F., Beresko, C., Ankerhold, G., et al. (2019). Cyanobacterial promoted enrichment of rare earth elements europium, samarium and neodymium and intracellular europium particle formation. *RSC Adv.* 9 (56), 32581–32593. doi:10.1039/c9ra06570a

Flaibani, A., Olsen, Y., and Painter, T. J. (1989). Polysaccharides in desert reclamation: compositions of exocellular proteoglycan complexes produced by filamentous blue-green and unicellular green edaphic algae. *Carbohydr. Res.* 190 (2), 235–248. doi:10.1016/0008-6215(89)84128-x

Giese, E. C. (2020). Biosorption as green technology for the recovery and separation of rare earth elements. *World J. Microbiol. Biotechnol.* 36 (4), 52–11. doi:10.1007/s11274-020-02821-6

Gupta, R., Ahuja, P., Khan, S., Saxena, R. K., and Mohapatra, H. (2000). Microbial biosorbents: meeting challenges of heavy metal pollution in aqueous solutions. *Curr. Sci.*, 967–973.

Hammer, Ø., Harper, D. A. T., and Ryan, P. D. (2001). PAST: paleontological statistics software package for education and data analysis. *Palaeontol. Electron.* 4 (1), 9pp. (Øyvind Hammer).

Heilmann, M., Breiter, R., and Becker, A. M. (2021). Towards rare earth element recovery from wastewaters: biosorption using phototrophic organisms. *Appl. Microbiol. Biotechnol.* 105 (12), 5229–5239. doi:10.1007/s00253-021-11386-9

Heilmann, M., Jurkowski, W., Buchholz, R., Brueck, T., and Becker, A. M. (2015). Biosorption of neodymium by selected photoautotrophic and heterotrophic species. *J. Chem. Eng. Process Technol.* 6 (4), 1. doi:10.4172/2157-7048.1000241

Hosomomi, Y., Baba, Y., Kubota, F., Kamiya, N., and Goto, M. (2013). Biosorption of rare earth elements by *Escherichia coli*. *J. Chem. Eng. Jpn.* 46 (7), 450–454. doi:10.1252/jcej.13we031

Hrouzek, P., Lukešová, A., Mareš, J., and Ventura, S. (2013). Description of the cyanobacterial genus *Desmonostoc* gen. nov. including *D. muscorum* comb. nov. as a distinct, phylogenetically coherent taxon related to the genus *Nostoc*. *Fottea* 13 (2), 201–213. doi:10.5507/fot.2013.016

Huang, Z., Liu, Y., Paulsen, B. S., and Klaveness, D. (1998). Studies on polysaccharides from three edible species of *Nostoc* (Cyanobacteria) with different colony morphologies: comparison of monosaccharide compositions and viscosities of polysaccharides from field colonies and suspension cultures. *J. Phycol.* 34, 962–968. doi:10.1046/j.1529-8817.1998.340962.x

Javadian, H., Ruiz, M., Saleh, T. A., and Sastre, A. M. (2020b). Ca-alginate/carboxymethyl chitosan/Ni0. 2Zn0. 2Fe2. 6O4 magnetic bionanocomposite: synthesis, characterization and application for single adsorption of Nd+ 3, Tb+ 3, and Dy+ 3 rare earth elements from aqueous media. *J. Mol. Liq.* 306, 112760. doi:10.1016/j.molliq.2020.112760

Javadian, H., Ruiz, M., Taghvai, M., and Sastre, A. M. (2020a). Novel magnetic nanocomposite of calcium alginate carrying poly (pyrimidine-thiophene-amide) as a novel green synthesized polyamide for adsorption study of neodymium, terbium, and dysprosium rare-earth ions. *Colloids Surfaces A Physicochem. Eng. Aspects* 603, 125252. doi:10.1016/j.colsurfa.2020.125252

Javanbakht, V., Alavi, S. A., and Zilouei, H. (2014). Mechanisms of heavy metal removal using microorganisms as biosorbent. *Water Sci. Technol.* 69 (9), 1775–1787. doi:10.2166/wst.2013.718

Johansen, J. R., Hentschke, G. S., Pietrasiak, N., Rigonato, J., Fiore, M. F., and Sant'Anna, C. L. (2017). *Komarekiella atlantica gen. et sp. nov. (Nostocaceae, Cyanobacteria): a new subaerial taxon from the Atlantic Rainforest and Kauai*. Hawaii: Fottea.

Joly, N., Ghemati, D., Aliouche, D., and Martin, P. (2020). Interaction of metal ions with mono-and polysaccharides for wastewater treatment: a Review. *Nat. Prod. Chem. Res.* 8 (3). doi:10.35248/2329-6836.20.8.373

Jurkowski, W., Paper, M., and Brück, T. B. (2022). Isolation and investigation of natural rare earth metal chelating agents from *Calothrix brevissima* - a step towards unraveling the mechanisms of metal biosorption. *Front. Bioeng. Biotechnol.* 10, 833122. doi:10.3389/fbioe.2022.833122

Jyothi, R. K., Thenepalli, T., Ahn, J. W., Parhi, P. K., Chung, K. W., and Lee, J. Y. (2020). Review of rare earth elements recovery from secondary resources for clean energy technologies: grand opportunities to create wealth from waste. *J. Clean. Prod.* 267, 122048. doi:10.1016/j.jclepro.2020.122048

Khattar, J. I. S., Singh, D. P., Jindal, N., Kaur, N., Singh, Y., Rahi, P., et al. (2010). Isolation and characterization of exopolysaccharides produced by the cyanobacterium *Limnothrix redekei* PUPCCC 116. *Appl. Biochem. Biotechnol.* 162 (5), 1327–1338. doi:10.1007/s12010-010-8922-3

Klingelhöfer, D., Braun, M., Dröge, J., Fischer, A., Brüggmann, D., and Groneberg, D. A. (2022). Environmental and health-related research on application and production of rare earth elements under scrutiny. *Glob. Health* 18 (1), 86. doi:10.1186/s12992-022-00879-5

Klock, J. H., Wieland, A., Seifert, R., and Michaelis, W. (2007). Extracellular polymeric substances (EPS) from cyanobacterial mats: characterisation and isolation method optimisation. *Mar. Biol.* 152, 1077–1085. doi:10.1007/s00227-007-0754-5

Lakatos, M., and Strieth, D. (2018): Terrestrial microalgae: novel concepts for Biotechnology and applications. In: F. M. Cánovas, *Ulrich Lüttge und Rainer Matyssek* (eds. Vol. 79, No. 79. China, Springer International Publishing , 269–312.

Lama, L., Nicolaus, B., Calandrelli, V., Manca, M. C., Romano, I., and Gambacorta, A. (1996). Effect of growth conditions on endo- and exopolymer biosynthesis in Anabaena cylindrica 10 C. *Phytochemistry* 42, 655–659. doi:10.1016/0031-9422(95)00985-x

Lerat-Hardy, A., Coynel, A., Dutruch, L., Pereto, C., Bossy, C., Gil-Diaz, T., et al. (2019). Rare Earth Element fluxes over 15 years into a major European Estuary (Garonne-Gironde, SW France): hospital effluents as a source of increasing gadolinium anomalies. *Sci. Total Environ.* 656, 409–420. doi:10.1016/j.scitotenv.2018.11.343

Liang, C. Y., and Marchessault, R. H. (1959). Infrared spectra of crystalline polysaccharides. I. Hydrogen bonds in native celluloses. *J. Polym. Sci.* 37 (132), 385–395. doi:10.1002/pol.1959.1203713209

Makhalanyane, T. P., Valverde, A., Velázquez, D., Gunnigle, E., Van Goethem, M. W., Quesada, A., et al. (2015). Ecology and biogeochemistry of cyanobacteria in soils, permafrost, aquatic and cryptic polar habitats. *Biodivers. Conservation* 24 (4), 819–840. doi:10.1007/s10531-015-0902-z

Mitic-Stojanovic, D. L., Zarubica, A., Purenovic, M., Bojic, D., Andjelkovic, T., and Bojic, À. L. (2011). Biosorptive removal of Pb^{2+}, Cd^{2+} and Zn^{2+} ions from water by *Agenaria vulgaris* shell. *Water sa.* 37 (3). doi:10.4314/wsa.v37i3.68481

Mollenhauer, D., Büdel, B., and Mollenhauer, R. (1994). Approaches to species delimitations in the genus *Nostoc* Vaucher 1803 ex Bornet et Flahault 1888. *Arch. für Hydrobiol.* 105, 189–209. doi:10.1127/algol_stud/75/1995/189

Moore, D., O'Donohue, H., Garnett, C., Critchley, C., and Shaw, G. (2005). Factors affecting akinete differentiation in *Cylindrospermopsis raciborskii* (Nostocales, Cyanobacteria). *Freshw. Biol.* 50 (2), 345–352. doi:10.1111/j.1365-2427.2004.01324.x

Mota, R., Flores, C., and Tamagnini, P. (2022). "Cyanobacterial extracellular polymeric substances (EPS)," in *Polysaccharides of microbial origin: biomedical applications* (Cham: Springer International Publishing), 139–165.

Mota, R., Rossi, F., Andrenelli, L., Pereira, S. B., De Philippis, R., and Tamagnini, P. (2016). Released polysaccharides (RPS) from *Cyanothece* sp. CCY 0110 as biosorbent for heavy metals bioremediation: interactions between metals and RPS binding sites. *Appl. Microbiol. Biotechnol.* 100, 7765–7775. doi:10.1007/s00253-016-7602-9

Myklestad, S. M. (1995). Release of extracellular products by phytoplankton with special emphasis on polysaccharides. *Sci. Total Environ.* 165, 155–164. doi:10.1016/0048-9697(95)04549-g

Nakamoto, K. (2009). *Infrared and Raman spectra of inorganic and coordination compounds, Part B. Applications in coordination, organometallic, and bioinorganic Chemistry*. John Wiley and Sons.

Ngah, W. W., and Hanafiah, M. A. K. M. (2008). Biosorption of copper ions from dilute aqueous solutions on base treatedrubber (*Hevea brasiliensis*) leaves powder: kinetics, isotherm, and biosorption mechanisms. *J. Environ. Sci.* 20 (10), 1168–1176. doi:10.1016/s1001-0742(08)62205-6

Nicolaus, B., Panico, A., Lama, L., Romano, I., Manca, M. C., De Giulio, A., et al. (1999). Chemical composition and production of exopolysaccharides from representative members of heterocystous and non-heterocystous cyanobacteria. *Phytochemistry* 52 (4), 639–647. doi:10.1016/s0031-9422(99)00202-2

Ojima, Y., Kosako, S., Kihara, M., Miyoshi, N., Igarashi, K., and Azuma, M. (2019). Recovering metals from aqueous solutions by biosorption onto phosphorylated dry baker's yeast. *Sci. Rep.* 9 (1), 225–229. doi:10.1038/s41598-018-36306-2

Okajima, M. K., Nakamura, M., Mitsumata, T., and Kaneko, T. (2010). Cyanobacterial polysaccharide gels with efficient rare-earth-metal sorption. *Biomacromolecules* 11 (7), 1773–1778. doi:10.1021/bm100231q

Olguín, E. J., and Sánchez-Galván, G. (2012). Heavy metal removal in phytofiltration and phycoremediation: the need to differentiate between bioadsorption and bioaccumulation. *New Biotechnol.* 30 (1), 3–8. doi:10.1016/j.nbt.2012.05.020

Pannard, A., Pedrono, J., Bormans, M., Briand, E., Claquin, P., and Lagadeuc, Y. (2016). Production of exopolymers (EPS) by cyanobacteria: impact on the carbon-to-nutrient ratio of the particulate organic matter. *Aquat. Ecol.* 50 (1), 29–44. doi:10.1007/s10452-015-9550-3

Paper, M., Koch, M., Jung, P., Lakatos, M., Nilges, T., and Brück, T. B. (2023). Rare earths stick to rare cyanobacteria: future potential for bioremediation and recovery of rare earth elements. *Front. Bioeng. Biotechnol.* 11, 1130939. doi:10.3389/fbioe.2023.1130939

Park, D., Middleton, A., Smith, R., Deblonde, G., Laudal, D., Theaker, N., et al. (2020). A biosorption-based approach for selective extraction of rare earth elements from coal byproducts. *Sep. Purif. Technol.* 241, 116726. doi:10.1016/j.seppur.2020.116726

Passow, U., and Alldredge, A. L. (1995). Aggregation of a diatom bloom in a mesocosm: the role of transparent exopolymer particles (TEP). *Deep Sea Res. II* 42, 99–109. doi:10.1016/0967-0645(95)00006-c

Pereao, O., Bode-Aluko, C., Fatoba, O., Laatikainen, K., and Petrik, L. (2018). Rare earth elements removal techniques from water/wastewater: a review. *Desalin. Water Treat.* 130, 71–86. doi:10.5004/dwt.2018.22844

Pereira, S., Micheletti, E., Zille, A., Santos, A., Moradas-Ferreira, P., Tamagnini, P., et al. (2011). Using extracellular polymeric substances (EPS)-producing cyanobacteria for the bioremediation of heavy metals: do cations compete for the EPS functional groups and also accumulate inside the cell? *Microbiology* 157 (2), 451–458. doi:10.1099/mic.0.041038-0

Pereira, S., Zille, A., Micheletti, E., Moradas-Ferreira, P., De Philippis, R., and Tamagnini, P. (2009). Complexity of cyanobacterial exopolysaccharides: composition, structures, inducing factors and putative genes involved in their biosynthesis and assembly. *FEMS Microbiol. Rev.* 33 (5), 917–941. doi:10.1111/j.1574-6976.2009.00183.x

Pramanik, B. K., Nghiem, L. D., and Hai, F. I. (2020). Extraction of strategically important elements from brines: constraints and opportunities. *Water Res.* 168, 115149. doi:10.1016/j.watres.2019.115149

Qian, J. Y., Chen, W., Zhang, W. M., and Zhang, H. (2009). Adulteration identification of some fungal polysaccharides with SEM, XRD, IR and optical rotation: a primary approach. *Carbohydr. Polym.* 78 (3), 620–625. doi:10.1016/j.carbpol.2009.05.025

Qian, L., Ye, X., Xiao, J., Lin, S., Wang, H., Liu, Z., et al. (2022). Nitrogen concentration acting as an environmental signal regulates cyanobacterial EPS excretion. *Chemosphere* 291, 132878. doi:10.1016/j.chemosphere.2021.132878

A. N. Rai, B. Bergman, and U. Rasmussen (Editors) (2002). *Cyanobacteria in symbiosis* (Kluwer Academic Pub).

Reynolds, C. S. (2007). Variability in the provision and function of mucilage in phytoplankton: facultative responses to the environment. *Hydrobiologia* 578, 37–45. doi:10.1007/s10750-006-0431-6

Romera, E., Gonzalez, F., Ballester, A., Blázquez, M. L., and Munoz, J. A. (2006). Biosorption with algae: a statistical review. *Crit. Rev. Biotechnol.* 26 (4), 223–235. doi:10.1080/07388550600972153

Rzymski, P., Niedzielski, P., Karczewski, J., and Poniedziałek, B. (2014). Biosorption of toxic metals using freely suspended *Microcystis aeruginosa* biomass. *Open Chem.* 12 (12), 1232–1238. doi:10.2478/s11532-014-0576-5

Sánchez-Baracaldo, P., and Cardona, T. (2020). On the origin of oxygenic photosynthesis and Cyanobacteria. *New Phytol.* 225 (4), 1440–1446. doi:10.1111/nph.16249

Shaw, E., Hill, D. R., Brittain, N., Wright, D. J., Tauber, U., Marand, H., et al. (2003). Unusual water flux in the extracellular polysaccharide of the cyanobacterium *Nostoc commune*. *Appl. Environ. Microbiol.* 69 (9), 5679–5684. doi:10.1128/aem.69.9.5679-5684.2003

Singh, S. (2020). Biosorption of heavy metals by cyanobacteria: potential of live and dead cells in bioremediation. *Microb. bioremediation Biodegrad.*, 409–423. doi:10.1007/978-981-15-1812-6_15

Singh, S., Pradhan, S., and Rai, L. C. (1998). Comparative assessment of Fe3+ and Cu2+ biosorption by field and laboratory-grown *Microcystis*. *Process Biochem.* 33 (5), 495–504. doi:10.1016/s0032-9592(97)00094-0

Strieth, D., Schwing, J., Kuhne, S., Lakatos, M., Muffler, K., and Ulber, R. (2017). A semi-continuous process based on an ePBR for the production of EPS using *Trichocoleus sociatus*. *J. Biotechnol.* 256, 6–12. doi:10.1016/j.jbiotec.2017.06.1205

Strieth, D., Stiefelmaier, J., Wrabl, B., Schwing, J., Schmeckebier, A., Di Nonno, S., et al. (2020). A new strategy for a combined isolation of EPS and pigments from cyanobacteria. *J. Appl. Phycol.* 32, 1729–1740. doi:10.1007/s10811-020-02063-x

Sukenik, A., Kaplan-Levy, R. N., Viner-Mozzini, Y., Quesada, A., and Hadas, O. (2013). Potassium deficiency triggers the development of dormant cells (akinetes) in *Aphanizomenon ovalisporum* (Nostocales, Cyanoprokaryota). *J. Phycol.* 49 (3), 580–587. doi:10.1111/jpy.12069

Tamaru, Y., Takani, Y., Yoshida, T., and Sakamoto, T. (2005). Crucial role of extracellular polysaccharides in desiccation and freezing tolerance in the terrestrial cyanobacterium *Nostoc commune*. *Appl. Environ. Microbiol.* 71 (11), 7327–7333. doi:10.1128/aem.71.11.7327-7333.2005

Tien, C. J., Sigee, D. C., and White, K. N. (2005). Copper adsorption kinetics of cultured algal cells and freshwater phytoplankton with emphasis on cell surface characteristics. *J. Appl. Phycol.* 17, 379–389. doi:10.1007/s10811-005-5555-y

Trivedi, M. K., Dahryn, T., and Alice, B. (2015). Spectroscopic characterization of disodium hydrogen orthophosphate and sodium nitrate after biofield treatment. *J. Chromatogr. Sep. Tech.* 06 (05). doi:10.4172/2157-7064.1000282

Turner, J. S., and Robinson, N. J. (1995). Cyanobacterial metallothioneins: biochemistry and molecular genetics. *J. industrial Microbiol.* 14 (2), 119–125. doi:10.1007/bf01569893

Underwood, G., Paterson, D. M., and Parkes, R. J. (1995). The measurement of microbial carbohydrate exopolymers from intertidal sediments. *Limnol. Oceanogr.* 40, 1243–1253. doi:10.4319/lo.1995.40.7.1243

Vincenzini, M., De Philippis, R., Sili, C., and Materassi, R. (1990). Studies on exopolysaccharide release by diazotrophic batch cultures of *Cyanospira capsulata*. *Appl. Microbiol. Biotechnol.* 34 (3), 392–396. doi:10.1007/bf00170066

Wilke, A., Buchholz, R., and Bunke, G. (2006). Selective biosorption of heavy metals by algae. *Environ. Biotechnol.* 2 (2), 47–56.

Wu, D., Zhang, L., Wang, L., Zhu, B., and Fan, L. (2011). Adsorption of lanthanum by magnetic alginate-chitosan gel beads. *J. Chem. Technol. Biotechnol.* 86 (3), 345–352. doi:10.1002/jctb.2522

Yadav, A. P. S., Dwivedi, V., Kumar, S., Kushwaha, A., Goswami, L., and Reddy, B. S. (2020). Cyanobacterial extracellular polymeric substances for heavy metal removal: a mini review. *J. Compos. Sci.* 5 (1), 1. doi:10.3390/jcs5010001

Yushin, N., Zinicovscaia, I., Cepoi, L., Chiriac, T., Rudi, L., and Grozdov, D. (2022). Application of cyanobacteria *Arthospira platensis* for bioremediation of erbium-contaminated wastewater. *Materials* 15 (17), 6101. doi:10.3390/ma15176101

Supplementary Material

1 Supplementary Data

Supplementary Table S1. Sugar composition of isolated cyanobacterial EPS

Sugars / organic acids	***Nostoc* sp. 20.02**		***Desmonostoc muscorum* 90.03**		***Komarekiella* sp. 89.12**	
	concentration [mg/g]	relative concentration [%]	concentration [mg/g]	relative concentration [%]	concentration [mg/g]	relative concentration [%]
Formic Acid	11.4 ± 14.8	3.6	16.9 ± 15.8	4.7	1.1 ± 0.5	0.4
Acetic acid	32.4 ± 34.9	10.1	9.0 ± 7.8	2.5	6.2 ± 6.2	2.3
Glucuronic acid	2.6 ± 2.9	0.8	36.8 ± 13.8	10.3	16.7 ± 1.7	6.3
Galacturonic acid	1.1 ± 0.4	0.3	4.7 ± 2.6	1.3	1.1 ± 1.0	0.4
Arabinose	n.d.	0.0	n.d.	0.0	9.0 ± 0.7	3.4
Fucose	4.9 ± 5.4	1.5	16.7 ± 10.5	4.7	44.4 ± 2.1	16.9
Glucose	136.7 ± 3.22	42.7	54.0 ± 9.6	15.0	78.2 ± 1.2	29.8
Mannitol	n.d.	0.0	0.2 ± 0.3	0.1	0.2 ± 0.3	0.1
Rhamnose	63.9 ± 8.8	20.0	93.0 ± 23.2	26.0	17.3 ± 0.3	6.6
Xylose, mannose, galactose, fructose	67.3 ± 4.8	21.0	127.6 ± 15.7	36.0	88.5 ± 1.3	33.7

Supplementary Table S2. (A) Two-way ANOVA tests (multivariate treatment conditions) of Cerium adsorption capacities depending on the species (*Nostoc* sp. 20.02 = Nost; *Desmonostoc muscorum* 90.03 = Desmo; *Komarekiella* sp. 89.12 = Koma) and treatments (Treat: separated EPS = EPS; EPS separated biomass = Bio-EPS; untreated biomass = Bio+EPS) and (B) checked for interactions by Tukey's post-hoc test ($p < 0.05$).

FIXED-EFFECTS TWO-WAY ANOVA					
Cerium	**Sum of sqrs**	**df**	**Mean square**	**F**	**p (same)**
Species:	1.520	2	760,4	93,38	3,14E-10
Treat:	22.402	2	11.201	1375	2,07E-20
Interaction:	2.187	4	546,9	67,16	1,43E-10
Within:	146	18	8,143		
Total:	26.257	26			

INTERACTION			
Cerium		**Q**	**p**
Nost-EPS	Nost-Bio-EPS	37,79	3,95E-14
Nost-EPS	Nost-Bio+EPS	5,577	0,01364
Nost-EPS	Koma-EPS	1,867	0,834
Nost-EPS	Desmo-EPS	3,344	0,2684
Nost-Bio-EPS	Nost-Bio+EPS	32,21	2,64E-13
Nost-Bio-EPS	Koma-Bio-EPS	6,248	0,005048
Nost-Bio-EPS	Desmo-Bio-EPS	3,516	0,2213
Nost-Bio+EPS	Koma-Bio+EPS	29,05	1,15E-12
Nost-Bio+EPS	Desmo-Bio+EPS	18,04	3,50E-09
Koma-EPS	Koma-Bio-EPS	45,91	2,55E-14
Koma-EPS	Koma-Bio+EPS	36,49	5,37E-14
Koma-EPS	Desmo-EPS	1,477	0,9363
Koma-Bio-EPS	Koma-Bio+EPS	9,415	5,25E-05
Koma-Bio-EPS	Desmo-Bio-EPS	2,732	0,4864
Koma-Bio+EPS	Desmo-Bio+EPS	11,01	6,45E-06
Desmo-EPS	Desmo-Bio-EPS	44,65	2,55E-14
Desmo-EPS	Desmo-Bio+EPS	26,96	3,75E-12
Desmo-Bio-EPS	Desmo-Bio+EPS	17,69	4,80E-09

Supplementary Table S3. (A) Two-way ANOVA tests (multivariate treatment conditions) of Neodymium adsorption capacities depending on the species (*Nostoc* sp. 20.02 = Nost; *Desmonostoc muscorum* 90.03 = Desmo; *Komarekiella* sp. 89.12 = Koma) and treatments (Treat: separated EPS = EPS; EPS separated biomass = Bio-EPS; untreated biomass = Bio+EPS) and (B) checked for interactions by Tukey's post-hoc test ($p < 0.05$).

FIXED-EFFECTS TWO-WAY ANOVA					
Neodymium	**Sum of sqrs**	**df**	**Mean square**	**F**	**p (same)**
Species:	1372,8	2	686,402	13,18	0,0002978
Treat:	20492,2	2	10246,1	196,8	5,85E-13
Interaction:	4947,34	4	1236,83	23,76	5,65E-07
Within:	937,166	18	52,0648		
Total:	27749,5	26			

INTERACTION			
Neodymium		**Q**	**p**
Nost-EPS	Nost-Bio-EPS	10,63	1,04E-05
Nost-EPS	Nost-Bio+EPS	0,0947	1
Nost-EPS	Koma-EPS	2,63	0,5284
Nost-EPS	Desmo-EPS	5,712	0,01118
Nost-Bio-EPS	Nost-Bio+EPS	10,54	1,18E-05
Nost-Bio-EPS	Koma-Bio-EPS	1,744	0,8721
Nost-Bio-EPS	Desmo-Bio-EPS	5,954	0,007811
Nost-Bio+EPS	Koma-Bio+EPS	12,51	1,04E-06
Nost-Bio+EPS	Desmo-Bio+EPS	9,736	3,40E-05
Koma-EPS	Koma-Bio-EPS	15,01	6,57E-08
Koma-EPS	Koma-Bio+EPS	15,23	5,20E-08
Koma-EPS	Desmo-EPS	3,082	0,3526
Koma-Bio-EPS	Koma-Bio+EPS	0,2259	1
Koma-Bio-EPS	Desmo-Bio-EPS	4,21	0,09372
Koma-Bio+EPS	Desmo-Bio+EPS	2,772	0,47
Desmo-EPS	Desmo-Bio-EPS	22,3	1,06E-10
Desmo-EPS	Desmo-Bio+EPS	15,54	3,79E-08
Desmo-Bio-EPS	Desmo-Bio+EPS	6,756	0,002372

Supplementary Table S4. (A) Two-way ANOVA tests (multivariate treatment conditions) of Terbium adsorption capacities depending on the species (*Nostoc* sp. 20.02 = Nost; *Desmonostoc muscorum* 90.03 = Desmo; *Komarekiella* sp. 89.12 = Koma) and treatments (Treat: separated EPS = EPS; EPS separated biomass = Bio-EPS; untreated biomass = Bio+EPS) and (B) checked for interactions by Tukey's post-hoc test ($p < 0.05$).

FIXED-EFFECTS TWO-WAY ANOVA					
Terbium	**Sum of sqrs**	**df**	**Mean square**	**F**	**p (same)**
Species:	131,639	2	65,8195	0,6279	0,545
Treat:	17529,4	2	8764,7	83,62	7,73E-10
Interaction:	2993,16	4	748,291	7,139	0,001259
Within:	1886,73	18	104,818		
Total:	22540,9	26			

INTERACTION			
Terbium		**Q**	**p**
Nost-EPS	Nost-Bio-EPS	7,277	0,001099
Nost-EPS	Nost-Bio+EPS	0,3398	1
Nost-EPS	Koma-EPS	4,847	0,03918
Nost-EPS	Desmo-EPS	3,992	0,1243
Nost-Bio-EPS	Nost-Bio+EPS	7,617	0,0006677
Nost-Bio-EPS	Koma-Bio-EPS	1,108	0,9837
Nost-Bio-EPS	Desmo-Bio-EPS	0,1135	1
Nost-Bio+EPS	Koma-Bio+EPS	5,546	0,01427
Nost-Bio+EPS	Desmo-Bio+EPS	3,22	0,3062
Koma-EPS	Koma-Bio-EPS	13,23	4,49E-07
Koma-EPS	Koma-Bio+EPS	10,05	2,22E-05
Koma-EPS	Desmo-EPS	0,8549	0,9958
Koma-Bio-EPS	Koma-Bio+EPS	3,179	0,3195
Koma-Bio-EPS	Desmo-Bio-EPS	1,222	0,9736
Koma-Bio+EPS	Desmo-Bio+EPS	2,326	0,6577
Desmo-EPS	Desmo-Bio-EPS	11,16	5,36E-06
Desmo-EPS	Desmo-Bio+EPS	6,873	0,001996
Desmo-Bio-EPS	Desmo-Bio+EPS	4,283	0,08512

Supplementary Table S5. (A) Two-way ANOVA tests (multivariate treatment conditions) of Lanthanum adsorption capacities depending on the species (*Nostoc* sp. 20.02 = Nost; *Desmonostoc muscorum* 90.03 = Desmo; *Komarekiella* sp. 89.12 = Koma) and treatments (Treat: separated EPS = EPS; EPS separated biomass = Bio-EPS; untreated biomass = Bio+EPS) and (B) checked for interactions by Tukey's post-hoc test ($p < 0.05$).

FIXED-EFFECTS TWO-WAY ANOVA					
lanthanum	Sum of sqrs	df	Mean square	F	p (same)
Species:	344,852	2	172,426	15,92	0,0001047
Treat:	21542	2	10771	994,2	3,76E-19
Interaction:	4513,77	4	1128,44	104,2	3,45E-12
Within:	195,008	18	10,8338		
Total:	26595,6	26			

INTERACTION			
lanthanum		Q	p
Nost-EPS	Nost-Bio-EPS	22,59	8,47E-11
Nost-EPS	Nost-Bio+EPS	1,516	0,9286
Nost-EPS	Koma-EPS	13,14	4,97E-07
Nost-EPS	Desmo-EPS	17,86	4,13E-09
Nost-Bio-EPS	Nost-Bio+EPS	21,08	2,76E-10
Nost-Bio-EPS	Koma-Bio-EPS	5,826	0,009447
Nost-Bio-EPS	Desmo-Bio-EPS	1,69	0,8872
Nost-Bio+EPS	Koma-Bio+EPS	20,43	4,64E-10
Nost-Bio+EPS	Desmo-Bio+EPS	18,93	1,61E-09
Koma-EPS	Koma-Bio-EPS	41,56	2,71E-14
Koma-EPS	Koma-Bio+EPS	35,09	8,39E-14
Koma-EPS	Desmo-EPS	4,712	0,04738
Koma-Bio-EPS	Koma-Bio+EPS	6,479	0,003582
Koma-Bio-EPS	Desmo-Bio-EPS	4,136	0,1033
Koma-Bio+EPS	Desmo-Bio+EPS	1,499	0,9319
Desmo-EPS	Desmo-Bio-EPS	42,14	2,67E-14
Desmo-EPS	Desmo-Bio+EPS	38,3	3,62E-14
Desmo-Bio-EPS	Desmo-Bio+EPS	3,842	0,15

4 Conclusion

The main focus of this thesis was to investigate the recovery of REE from kaolinite minerals using a combined process of inorganic elution and microalgae-based biosorption. The objective was to develop an environmentally sustainable method for REE recovery by a combination of inorganic and biochemical processes.

In chapter 3.1, the investigation focused on the elution of Rare Earth Elements (REE) from 15 distinct kaolinite samples (Residual Kaolinites, RK) using various acids in a microwave-assisted elution process. Notably, RK1 and RK2 samples exhibited the highest REE yield. The elution efficiency for REE from RK2 samples followed the order: $HNO_3 < H_2SO_4 < HCl$. Although sulphuric acid had a slightly lower elution efficiency than hydrochloric acid, it did not release as many impurities. Therefore, it is preferred in the elution process. The study also aimed to develop an environmentally friendly REE recovery process using diluted acids. Diluted acid solutions exhibited a maximum elution potential of 0.8 g/kg REE weight proportion (32%) in a one-step elution process. A multiple-step process, particularly with diluted hydrochloric acid, enhanced the elution efficiency up to 69%. The use of diluted acids in the elution process offered advantages for subsequent steps, such as metal recovery by biosorption, which operates under pH 5–6 conditions, aligning with sustainability and cost-saving considerations The optimization of the elution process, transitioning from a batch to a semi-continuous method, poses a challenging yet crucial task for future studies, especially concerning large-scale industrial processes.

Furthermore, 12 cyanobacteria strains for their potential in REE enrichment through biosorption were investigated. In chapter 3.2, variations in metal uptake among strains were observed, with *Nostoc sp.* 20.02 exhibiting the highest maximum adsorption capacity. Interestingly, there was no apparent correlation between adsorption capacity and phylogenetic relationship or ecological environment. The variations in metal-interacting functional groups at the cell surface contribute to differences in metal uptake. Many cyanobacteria with high adsorption capacities produced extracellular polymeric substances (EPS), known to facilitate metal adsorption.

Further studies on the composition and influence of cyanobacterial EPS on REE adsorption were carried out. Chapter 3.3 explored the metal adsorption properties of biomass by varying the growth parameters during biomass production. With this approach, the formation of REE binding functional groups could be enhanced, thereby improving metal uptake.[131] In general, EPS production is triggered under unfavorable environmental conditions, offering new prospects for biosorption and biotechnological applications linked to cyanobacterial EPS. The isolated EPS surpassed the intact biomass in REE adsorption capacities, indicating the significant contribution of EPS to

metal uptake. Thus, extracted EPS from cyanobacterial biomass could be considered promising biosorbents for an effective separation and recovery of REE from wastewater or industrial effluents. It is advisable that EPS is continuously removed during the cultivation of cyanobacteria for potential applications based on biosorption and metal recovery. By highlighting the potential need for further research, optimization, and evaluation of different cyanobacterial strains to assess the efficiency and viability of EPS in practical applications for metal recovery processes.

In this work, various analytical methods for the characterization of mineral samples and the investigation of chemical elution of REE were applied, including inductively coupled plasma optical emission spectroscopy, scanning electron microscopy, X-ray fluorescence, and X-ray diffraction.
The practical applicability of elution and biosorption-based metal recovery was explored, with a focus on the potential economic feasibility of recovering valuable metals like REE from RK minerals. The growing demand for these Rare Earth Metals and their scarcity will become increasingly important for future applications through environmentally friendly extraction techniques.
Selective desorption of adsorbed metals and non-destructive biomass regeneration are crucial aspects for practical implementation. Different desorption agents and their effects on the reusability and long-term stability of biosorbents were evaluated in this study. The challenges associated with the selective desorption of a single target element in multi-element adsorption processes are emphasized.
This research showed the potential of the inorganic and biosorption-based metal recovery process. The optimization of the elution and biosorption processes was demonstrated and provided a roadmap for future research and development in this promising area. Despite advancements in understanding this complex procedure, optimization for commercial applications is still required to achieve practical relevance on a large scale.

5 List of Publications

Included publications that were used as contributed equally authorships for this thesis :

Rare earth element stripping from kaolin sands via mild acid treatment

Max Koch, Michael Paper, Thomas B. Brück, Tom Nilges
Asia-Pacific Journal of Chemical Engineering (2023), e3018.
https://doi.org/10.1002/apj.3018

Rare Earths stick to rare Microalgae: Bioremediation and Recovery of Rare Earth Elements by Cyanobacteria

Michael Paper, **Max Koch**, Patrick Jung, Michael Lakatos, Tom Nilges, Thomas B. Brück
Frontiers in Bioengineering and Biotechnology (2023), 11.
https://doi.org/10.3389/fbioe.2023.1130939

Stripped: contribution of cyanobacterial extracellular polymeric substances to the adsorption of rare earth elements from aqueous solutions

Michael Paper, Patrick Jung, **Max Koch**, Tom Nilges, Michael Lakatos, Thomas B. Brück
Frontiers in Bioengineering and Biotechnology (2023), 11.
https://doi.org/10.3389/fbioe.2023.1299349

Publications not included in the thesis that have a co-authorship:

Metamorphosis of Heterostructured Surface-Mounted Metal–Organic Frameworks Yielding Record Oxygen Evolution Mass Activities

Shujin Hou, Weijin Li, Sebastian Watzele, Regina M. Kluge, Song Xue, Shanshan Yin, Xinyu Jiang, Markus Döblinger, Alexander Welle, Batyr Garlyyev, **Max Koch**, Peter Müller-Buschbaum, Christof Wöll, Aliaksandr S. Bandarenka, Roland A. Fischer
Advanced Materials (2021), 33, 38, 2103218.
https://doi.org/10.1002/adma.202103218

Dual In Situ Laser Techniques Underpin the Role of Cations in Impacting Electrocatalysts

Shujin Hou, Lili Xu, Xing Ding, Dr. Regina M. Kluge, Theophilus Kobina Sarpey, Richard W. Haid, Dr. Batyr Garlyyev, Dr. Soumya Mukherjee, Dr. Julien Warnan, **Max Koch**, Prof. Shengli Zhang, Dr. Weijin Li, Prof. Aliaksandr S. Bandarenka, Prof. Roland A. Fischer
Angewandte Chemie International Edition (2022), 134, 24, e202201610.
https://doi.org/10.1002/ange.202201610

Porphyrinic MOF derived Single-atom electrocatalyst enables methanol oxidation

Zhenyu Zhou, Jing Zhang, Soumya Mukherjee, Shujin Hou, Rachit Khare, Markus Döblinger, Ondřej Tomanec, Michal Otyepka, **Max Koch**, Pan Gao, Liujiang Zhou, Weijin Li, Roland A. Fischer
Chemical Engineering Journal (2022), 449, 137888.
https://doi.org/10.1016/j.cej.2022.137888

Microscopic Bubble Accumulation: The Missing Factor in Evaluating Oxygen Evolution Catalyst Stability during Accelerated Stress Tests

Niklas Trogisch, **Max Koch**, Ehab N. El Sawy, Hany A. El-Sayed
ACS Catalysis (2022), 12, 21, 13715–13724.
https://doi.org/10.1021/acscatal.2c03881

Surface-stabilization of LMR-NCM by Washing with Aqueous Buffers to Reduce Gassing and Improve Cycle-Life

Louis Hartmann, Cheuck Hin Ching, Tim Kipfer, **Max Koch**, Hubert A. Gasteiger
Journal of The Electrochemical Society (2022), 169, 7.
https://iopscience.iop.org/article/10.1149/1945-7111/ac7ef0/meta

Structure–Activity Relationships in Ni- Carboxylate-Type Metal–Organic Frameworks' Metamorphosis for the Oxygen Evolution Reaction

Xiaoxin Ma, Daniel J. Zheng, Shujin Hou, Soumya Mukherjee, Rachit Khare, Guanhui Gao, Qing Ai, Batyr Garlyyev, Weijin Li, **Max Koch**, János Mink, Yang Shao-Horn, Julien Warnan, Aliaksandr S. Bandarenka, Roland A. Fischer
ACS Catalysis (2023), 13, 11, 7587–7596.
https://doi.org/10.1021/acscatal.3c00625

Heterogeneity of lithium distribution in the graphite anode of 21700-type cylindrical Li-ion cells during degradation

Dominik Petz, Volodymyr Baran, Juyeon Park, Alexander Schökel, Armin Kriele, Joana Rebelo-Kornmeier, Carsten Paulmann, **Max Koch**, Tom Nilges, Peter Müller-Buschbaum, Anatoliy Senyshyn
Batteries (2024), 10, 68.
https://doi.org/10.3390/batteries10030068

6 Reprint Permissions

John Wiley and Sons

JOHN WILEY AND SONS LICENSE
TERMS AND CONDITIONS

May 15, 2024

This Agreement between TU Munich – Max Koch ("You") and John Wiley and Sons ("John Wiley and Sons") consists of your license details and the terms and conditions provided by John Wiley and Sons and Copyright Clearance Center.

License Number	5790310755408
License date	May 15, 2024
Licensed Content Publisher	John Wiley and Sons
Licensed Content Publication	Asia-Pacific Journal of Chemical Engineering
Licensed Content Title	Rare earth element stripping from kaolin sands via mild acid treatment
Licensed Content Author	Max Koch, Michael Paper, Thomas B. Brück, et al
Licensed Content Date	Dec 21, 2023
Licensed Content Volume	19
Licensed Content Issue	2
Licensed Content Pages	13
Type of use	Dissertation/Thesis
Requestor type	Author of this Wiley article
Format	Print and electronic
Portion	Full article
Will you be translating?	No
Title of new work	A Novel Process for Rare Earth Metal Extraction from Kaolin by Elution and Biosorption
Institution name	TU Munich
Expected presentation date	Jun 2024
Requestor Location	TU Munich Lichtenbergstraße 4 Garching, 85748 Germany Attn: TU Munich
Publisher Tax ID	EU826007151
Total	0.00 USD

TERMS AND CONDITIONS

This copyrighted material is owned by or exclusively licensed to John Wiley & Sons, Inc. or one of its group companies (each a"Wiley Company") or handled on behalf of a society with which a Wiley Company has exclusive publishing rights in relation to a particular work (collectively "WILEY"). By clicking "accept" in connection with completing this licensing transaction, you agree that the following terms and conditions apply to this transaction (along with the billing and payment terms and conditions established by the Copyright Clearance Center Inc., ("CCC's Billing and Payment terms and conditions"), at the time that you opened your RightsLink account (these are available at any time at `http://myaccount.copyright.com)`.

Terms and Conditions

- The materials you have requested permission to reproduce or reuse (the "Wiley Materials") are protected by copyright.
- You are hereby granted a personal, non-exclusive, non-sub licensable (on a standalone basis), non-transferable, worldwide, limited license to reproduce the Wiley Materials for the purpose specified in the licensing process. This license, **and any CONTENT (PDF or image file) purchased as part of your order**, is for a onetime use only and limited to any maximum distribution number specified in the license. The first instance of republication or reuse granted by this license must be completed within two years of the date of the grant of this license (although copies prepared before the end date may be distributed thereafter). The Wiley Materials shall not be used in any other manner or for any other purpose, beyond what is granted in the license. Permission is granted subject to an appropriate acknowledgement given to the author, title of the material/book/journal and the publisher. You shall also duplicate the copyright notice that appears in the Wiley publication in your use of the Wiley Material. Permission is also granted on the understanding that nowhere in the text is a previously published source acknowledged for all or part of this Wiley Material. Any third party content is expressly excluded from this permission.
- With respect to the Wiley Materials, all rights are reserved. Except as expressly granted by the terms of the license, no part of the Wiley Materials may be copied,modified, adapted (except for minor reformatting required by the new Publication),translated, reproduced, transferred or distributed, in any form or

by any means, and no derivative works may be made based on the Wiley Materials without the prior permission of the respective copyright owner. **For STM Signatory Publishers clearing permission under the terms of the STM Permissions Guidelines only,the terms of the license are extended to include subsequent editions and for editions in other languages, provided such editions are for the work as a whole in situ and does not involve the separate exploitation of the permitted figures or extracts**, You may not alter, remove or suppress in any manner any copyright,trademark or other notices displayed by the Wiley Materials. You may not license,rent, sell, loan, lease, pledge, offer as security, transfer or assign the Wiley Materials on a stand-alone basis, or any of the rights granted to you hereunder to any other person.

- The Wiley Materials and all of the intellectual property rights therein shall at all times remain the exclusive property of John Wiley & Sons Inc, the Wiley Companies, or their respective licensors, and your interest therein is only that of having possession of and the right to reproduce the Wiley Materials pursuant to Section 2 herein during the continuance of this Agreement. You agree that you own no right, title or interest in or to the Wiley Materials or any of the intellectual property rights therein. You shall have no rights hereunder other than the license as provided for above in Section 2. No right, license or interest to any trademark, trade name, service mark or other branding ("Marks") of WILEY or its licensors is granted hereunder, and you agree that you shall not assert any such right, license or interest with respect thereto

- NEITHER WILEY NOR ITS LICENSORS MAKES ANY WARRANTY OR-REPRESENTATION OF ANY KIND TO YOU OR ANY THIRD PARTY, EXPRESS, IMPLIED OR STATUTORY, WITH RESPECT TO THE MATERIALSOR THE ACCURACY OF ANY INFORMATION CONTAINED IN THEMATERIALS, INCLUDING, WITHOUT LIMITATION, ANY IMPLIEDWARRANTY OF MERCHANTABILITY, ACCURACY, SATISFACTORYQUALITY, FITNESS FOR A PARTICULAR PURPOSE, USABILITY, INTEGRATION OR NON-INFRINGEMENT AND ALL SUCH WARRANTIESARE HEREBY EXCLUDED BY WILEY AND ITS LICENSORS AND WAIVEDBY YOU.

- WILEY shall have the right to terminate this Agreement immediately upon breach of this Agreement by you.

- You shall indemnify, defend and hold harmless WILEY, its Licensors and their respective directors, officers, agents and employees, from and against any actual or threatened claims, demands, causes of action or proceedings arising from any breach of this Agreement by you.

- IN NO EVENT SHALL WILEY OR ITS LICENSORS BE LIABLE TO YOU ORANY OTHER PARTY OR ANY OTHER PERSON OR ENTITY FOR ANY-SPECIAL, CONSEQUENTIAL, INCIDENTAL, INDIRECT, EXEMPLARY OR-PUNITIVE DAMAGES, HOWEVER CAUSED, ARISING OUT OF OR IN-CONNECTION WITH THE DOWNLOADING, PROVISIONING, VIEWING ORUSE OF THE MATERIALS REGARDLESS OF THE FORM OF ACTION, WHETHER FOR BREACH OF CONTRACT, BREACH OF WARRANTY, TORT, NEGLIGENCE, INFRINGEMENT OR OTHERWISE (INCLUDING, WITHOUTLIMITATION, DAMAGES BASED ON LOSS OF PROFITS, DATA, FILES, USE,BUSINESS OPPORTUNITY OR CLAIMS OF THIRD PARTIES), ANDWHETHER OR NOT THE PARTY HAS BEEN ADVISED OF THE-POSSIBILITY OF SUCH DAMAGES. THIS LIMITATION SHALL APPLY-NOTWITHSTANDING ANY FAILURE OF ESSENTIAL PURPOSE OF ANY-LIMITED REMEDY PROVIDED HEREIN.

- Should any provision of this Agreement be held by a court of competent jurisdiction to be illegal, invalid, or unenforceable, that provision shall be deemed amended to achieve as nearly as possible the same economic effect as the original provision,and the legality, validity and enforceability of the remaining provisions of this Agreement shall not be affected or impaired thereby.

- The failure of either party to enforce any term or condition of this Agreement shall not constitute a waiver of either party's right to enforce each and every term and condition of this Agreement. No breach under this agreement shall be deemed waived or excused by either party unless such waiver or consent is in writing signed by the party granting such waiver or consent. The waiver by or consent of a party to a breach of any provision of this Agreement shall not operate or be construed as a waiver of or consent to any other or subsequent breach by such other party.

- This Agreement may not be assigned (including by operation of law or otherwise)by you without WILEY's prior written consent.

- Any fee required for this permission shall be non-refundable after thirty (30) days from receipt by the CCC.

- These terms and conditions together with CCC's Billing and Payment terms and conditions (which are incorporated herein) form the entire agreement between you and WILEY concerning this licensing transaction and (in the absence of fraud)supersedes all prior agreements and representations of the parties, oral or written. This Agreement may not be amended except in writing signed by both parties. This Agreement shall be binding upon and inure to the benefit of the parties' successors,legal representatives, and authorized assigns.

- In the event of any conflict between your obligations established by these terms and conditions and those established by CCC's Billing and Payment terms and conditions, these terms and conditions shall prevail.

- WILEY expressly reserves all rights not specifically granted in the combination of(i) the license details provided by you and accepted in the course of this licensing transaction, (ii) these terms and conditions and (iii) CCC's Billing and Payment terms and conditions.

- This Agreement will be void if the Type of Use, Format, Circulation, or Requestor Type was misrepresented during the licensing process.

- This Agreement shall be governed by and construed in accordance with the laws of the State of New York, USA, without regards to such state's conflict of law rules. Any legal action, suit or proceeding arising out of or relating to these Terms and Conditions or the breach thereof shall be instituted in a court of competent jurisdiction in New York County in the State of New York in the United States of America and each party hereby consents and submits to the personal jurisdiction of such court, waives any objection to venue in such court and consents to service of process by registered or certified mail, return receipt requested, at the last known address of such party.

WILEY OPEN ACCESS TERMS AND CONDITIONS

Wiley Publishes Open Access Articles in fully Open Access Journals and in Subscription journals offering Online Open. Although most of the fully Open Access journals publish open access articles under the terms of the Creative Commons Attribution (CC BY)License only, the subscription journals and a few of the Open Access Journals offer a choice of Creative Commons Licenses. The license type is clearly identified on the article.

The Creative Commons Attribution License

The Creative Commons Attribution License (CC-BY) allows users to copy, distribute and transmit an article, adapt the article and make commercial use of the article. The CC-BYlicense permits commercial and non-

Creative Commons Attribution Non-Commercial License

The Creative Commons Attribution Non-Commercial (CC-BY-NC)License permits use, distribution and reproduction in any medium, provided the original work is properly citedand is not used for commercial purposes.(see below)

Creative Commons Attribution-Non-Commercial-NoDerivs License

The Creative Commons Attribution Non-Commercial-NoDerivs License (CC-BY-NC-ND) permits use, distribution and reproduction in any medium, provided the original work is properly cited, is not used for commercial purposes and no modifications or adaptations are made. (see below)

Use by commercial "for-profit" organizations

Use of Wiley Open Access articles for commercial, promotional, or marketing purposes requires further explicit permission from Wiley and will be subject to a fee.

Further details can be found on Wiley Online Library
http://olabout.wiley.com/WileyCDA/Section/id-410895.html

Other Terms and Conditions:

v1.10 Last updated September 2015

Questions? customercare@copyright.com.

Frontiers

Frontiers Copyright Statement available on web page at on January 18, 2024, at 4:42 p.m. (`https://www.frontiersin.org/legal/copyright-statement`) "Frontiers Copyright Statement" Frontiers publishes its own journals (referred to here as Frontiers Journals) and journals owned by third parties (referred to here as Hosted Journals). When we refer to Journals, we include both Frontiers Journals and Hosted Journals.

In this Copyright Statement, Websites (with a capitalised W) refers to all Frontiers websites, including those of Hosted Journals. An Owner means Frontiers as owner of all Frontiers Journals, or the respective owner of a Hosted Journal. All content included on these Websites (including Loop), such as text, graphics, logos, button icons, images, video/audio clips, downloads, data compilations and software, is the property of the person or entity who or which owned it prior to submission to Frontiers or to a Hosted Journal. If not owned by Frontiers or an Owner of a Hosted Journal, it is licensed to Frontiers Media SA ("Frontiers"), such Owner or its or their licensees and/or subcontractors.

The ownership of copyright in the text of individual articles (including research articles, opinion articles, book reviews, conference proceedings and abstracts) is not affected by its submission to or publication by Frontiers, whether for itself or for a Hosted Journal. Frontiers benefits from a general licence over all content submitted. Hosted Journal Owners benefit from a general licence over all content submitted to their respective Hosted Journals. Frontiers, Hosted Journal Owners and all their users benefit from a Creative Commons CC-BY licence over all content, as specified below.

Images and graphics not forming part of user-contributed materials are the property of or are licensed to Frontiers and may not be downloaded or copied without Frontiers' explicit and specific permission or in accordance with any specific copyright notice attached to that material.

The combination of all content on Frontiers websites, and the look and feel of the Frontiers websites, is the property of Frontiers Media SA.

As an author or contributor you grant permission to others to reproduce your articles, including any graphics and third-party materials supplied by you, in accordance with the Frontiers Terms and Conditions. The licence granted to third parties over all contents of each article, including third-party elements, is a Creative Commons Attribution ("CC BY") licence. The current version is CC-BY, version 4.0

(http://creativecommons.org/licenses/by/4.0/), and the licence will automatically be updated as and when updated by the Creative Commons organisation.

You may include a requirement to reproduce copyright notices but you may not restrict the right to reproduce the entire article, including third-party graphics. This means that you must obtain any necessary third-party consents and permissions to reproduce third-party materials in your articles submitted to Frontiers.

E-books are subject to the same licensing conditions as the articles within them.

Articles published prior to 25th May 2018: Please note that reproduction of third-party graphics and other third-party materials contained in articles published prior to 25th May 2018 may be subject to third-party notices prohibiting their reproduction without permission. You must comply with those notices.

Articles published prior to July 2012: The licence granted for these articles may be different and you should check the pdf version of any article to establish what licence was granted. If an article carries only a non-commercial licence and you wish to obtain a commercial licence, please contact Frontiers at editorial.office@frontiersin.org.

Article metadata, as defined in Frontiers' terms and conditions, are the property of Frontiers or the Owner of the respective Hosted Journal, and are licensed under Creative Commons CC0 terms.

All software used on this site, and the copyright in the code constituting such software, and all intellectual property in all such elements, is the property of or is licensed to Frontiers and its use is restricted in accordance with the Frontiers Terms and Conditions. All copyright, and all rights therein, are protected by national and international copyright laws.

Please also see the Frontiers Terms and Conditions.

Copyright Statement updated with effect from 16th December 2020.

7 Figures and Tables

List of Figures

List of Tables

References

[1] Seltene Erden - Rohstoff für die Technologien der Zukunft. Available at https://www.steine-und-minerale.de/artikel.php?topic=5&ID=181, 24.07.2023.

[2] Nils Wiberg, Arnold F. Holleman, Egon Wiberg, and Gerd Fischer. *Inorganic Chemistry*. De Gruyter, Inc, Berlin/Boston, 102th ed. edition, 1995.

[3] S. R. Taylor and S. M. McLennan. The composition and evolution of the continental crust: rare earth element evidence from sedimentary rocks. *Philosophical Transactions of the Royal Society of London. Series A, Mathematical and Physical Sciences*, 301(1461):381–399, 1981.

[4] Seltene Erden. – Seltene Erden Infoseite. Available at https://selteneerden.de/, 05.07.2023.

[5] Encyclopedia Britannica. Rare-earth element - Properties, Metals, Uses. Available at https://www.britannica.com/science/rare-earth-element/Properties-of-the-metals, 22.02.2024.

[6] Christopher M. Sims, Russell A. Maier, Aaron C. Johnston-Peck, Justin M. Gorham, Vincent A. Hackley, and Bryant C. Nelson. Approaches for the quantitative analysis of oxidation state in cerium oxide nanomaterials. *Nanotechnology*, 30(8):085703, 2019.

[7] A. D. Burnham, A. J. Berry, H. R. Halse, P. F. Schofield, G. Cibin, and J.F.W. Mosselmans. The oxidation state of europium in silicate melts as a function of oxygen fugacity, composition and temperature. *Chemical Geology*, 411:248–259, 2015.

[8] Bernhard Adler and Ralf Müller. *Seltene Erdmetalle: Gewinnung, Verwendung und Recycling*, volume Bd. 10 of *Berichte aus der Biomechatronik*. Univ.-Verl., Ilmenau, 2014.

[9] Gordon Haxel. *Rare Earth Elements: Critical Resources for High Technology*. U.S. Department of the Interior, U.S. Geological Survey, 2002.

[10] Dylan T. Buechler, Nadezhda N. Zyaykina, Cole A. Spencer, Emily Lawson, Natasha M. Ploss, and Inez Hua. Comprehensive elemental analysis of consumer electronic devices: Rare earth, precious, and critical elements. *Waste management (New York, N.Y.)*, 103:67–75, 2020.

[11] Simon Cotton. *Lanthanide and Actinide Chemistry*. Inorganic Chemistry: A Textbook Series. John Wiley & Sons, New York, NY, 2013.

[12] J. H. L. Voncken. Physical and Chemical Properties of the Rare Earths. In *The Rare Earth Elements*, pages 53–72. Springer, Cham, 2016.

[13] Marino Gergoric, Antonin Barrier, and Teodora Retegan. Recovery of Rare-Earth Elements from Neodymium Magnet Waste Using Glycolic, Maleic, and Ascorbic Acids Followed by Solvent Extraction. *Journal of Sustainable Metallurgy*, 5(1):85–96, 2019.

[14] Jessica T. Dahle and Yuji Arai. Environmental geochemistry of cerium: applications and toxicology of cerium oxide nanoparticles. *International journal of environmental research and public health*, 12(2):1253–1278, 2015.

[15] Mihail Nazarov and Do Young Noh. *New generation of europium and terbium activated phosphors: From syntheses to applications.* CRC Press, Boca Raton, Fla., 2012.

[16] S. S. Syamchand and G. Sony. Europium enabled luminescent nanoparticles for biomedical applications. *Journal of Luminescence*, 165:190–215, 2015.

[17] David R. Lide, editor. *CRC handbook of chemistry and physics: A ready-reference book of chemical and physical data : 2005-2006.* CRC Press, Boca Raton, 86th ed. edition, op. 2005.

[18] Alexander Schmid, Martin Krammer, and Jürgen Fleig. Rechargeable Oxide Ion Batteries Based on Mixed Conducting Oxide Electrodes. *Advanced Energy Materials*, 13(11):2203789, 2023.

[19] Yasuo Kanazawa and Masaharu Kamitani. Rare earth minerals and resources in the world. *Journal of Alloys and Compounds*, 408-412:1339–1343, 2006.

[20] Der Spiegel. Wichtige Hightech-Metalle: China erklärt Erden-Export zu Staatsgeheimnis. Available at `https://www.spiegel.de/wirtschaft/soziales/wichtige-hightech-metalle-china-erklaert-erden-export-zu\-staatsgeheimnis-a-737301.html`. 10.08.2023.

[21] European Commission. Directorate General for Internal Market, Industry, Entrepreneurship and SMEs. *Study on the EU's list of critical raw materials (2020): final report.* Publications Office, 2020.

[22] U.S. Geological Survey. Mineral commodity summaries 2023: US; 2023, 21p. Available at `https://doi.org/10.3133/mcs2023`, 09.08.2023.

[23] Sebastiaan Peelman, Zhi H.I. Sun, Jilt Sietsma, and Yongxiang Yang. Leaching of Rare Earth Elements. *Rare Earths Industry*, pages 319–334, 2016.

[24] F. Habashi. Extractive metallurgy of rare earths. *Canadian Metallurgical Quarterly*, 52(3):224–233, 2013.

[25] B. Ramachandra Reddy, B. Nagaphani Kumar, and S. Radhika. Solid–Liquid Extraction of Terbium from Phosphoric Acid Medium using Bifunctional Phosphinic Acid Resin, Tulsion CH–96. *Solvent Extraction and Ion Exchange*, 27(5-6):695–711, 2009.

[26] Xavier Hérès, Vincent Blet, Patricia Di Natale, Abla Ouaattou, Hamid Mazouz, Driss Dhiba, and Frederic Cuer. Selective Extraction of Rare Earth Elements from Phosphoric Acid by Ion Exchange Resins. *Metals*, 8(9):682, 2018.

[27] Feng Xie, Ting an Zhang, David Dreisinger, and Fiona Doyle. A critical review on solvent extraction of rare earths from aqueous solutions. *Minerals Engineering*, 56:10–28, 2014.

[28] V. V. Belova. Development of solvent extraction methods for recovering rare earth metals. *Theoretical Foundations of Chemical Engineering*, 51(4):599–609, 2017.

[29] Mineralienatlas - Fossilienatlas. Available at `https://www.mineralienatlas.de/lexikon/index.php/Mineralienportrait/Seltene%20Erden/Gewinnung`, 11.08.2023.

[30] Yusheng Yang, Chaoqun Lan, Lingyun Guo, Zhuoqing An, Zengwu Zhao, and Baowei Li. Recovery of rare-earth element from rare-earth permanent magnet waste by electro-refining in molten fluorides. *Separation and Purification Technology*, 233:116030, 2020.

[31] Wenjie Zhang, Xian Xie, Xiong Tong, Yunpeng Du, Qiang Song, and Dongxia Feng. Study on the Effect and Mechanism of Impurity Aluminum on the Solvent Extraction of Rare Earth Elements (Nd, Pr, La) by P204-P350 in Chloride Solution. *Minerals*, 11(1):61, 2021.

[32] Critical Loads - LfU Bayern. Available at `https://www.lfu.bayern.de/luft/schadstoffe_luft/eutrophierung_versauerung/critical_loads/index.htm`, 22.01.2024.

[33] Umweltbundesamt. Critical Loads für Schwermetalle. Available at `https://www.umweltbundesamt.de/themen/luft/wirkungen-von-luftschadstoffen/wirkungen-auf-oekosysteme/critical-loads-fuer-schwermetalle#wie-werden-critical-loads-fur-schwermetalle-und-ihre-\uberschreitung-berechnet`, 16.08.2023.

[34] J. Baby, J. S. Raj, E. T. Biby, P. Sankarganesh, M. V. Jeevitha, S. U. Ajisha, and S. S. Rajan. Toxic effect of heavy metals on aquatic environment. *International Journal of Biological and Chemical Sciences*, 4(4), 2011.

[35] Paul B. Tchounwou, Clement G. Yedjou, Anita K. Patlolla, and Dwayne J. Sutton. Heavy Metal Toxicity and the Environment. In *Molecular, Clinical and Environmental Toxicology*, pages 133–164. Springer, Basel, 2012.

[36] In-Chul Kong, Gabriel Bitton, Ben Koopman, and Keum-Hee Jung. Heavy Metal Toxicity Testing in Environmental Samples. In *Reviews of Environmental Contamination and Toxicology*, pages 119–147. Springer, New York, NY, 1995.

[37] Petra Zapp, Andrea Schreiber, Josefine Marx, and Wilhelm Kuckshinrichs. Environmental impacts of rare earth production. *MRS bulletin*, 47(3):267–275, 2022.

[38] Serkan Kulaksız and Michael Bau. Anthropogenic dissolved and colloid/nanoparticle-bound samarium, lanthanum and gadolinium in the Rhine River and the impending destruction of the natural rare earth element distribution in rivers. *Earth and Planetary Science Letters*, 362:43–50, 2013.

[39] Kerstin Redling. *Rare Earth Elements in Agriculture with Emphasis on Animal Husbandry*. PhD thesis, Ludwig-Maximilians-Universität München, 2006.

[40] E. C. Giese. Rare Earth Elements: therapeutic and diagnostic applications in modern medicine. *Clinical and Medical Reports*, 2(1), 2018.

[41] P. Ascenzi, M. Bettinelli, A. Boffi, M. Botta, G. de Simone, C. Luchinat, E. Marengo, H. Mei, and S. Aime. Rare earth elements (ree) in biology and medicine. *Rendiconti Lincei. Scienze Fisiche e Naturali*, 31(3):821–833, 2020.

[42] Kyung-Taek Rim. Effects of rare earth elements on the environment and human health: A literature review. *Toxicology and Environmental Health Sciences*, 8(3):189–200, 2016.

[43] Silvia Gonçalves Egler, Júlia Carina Niemeyer, Fábio Veríssimo Correia, and Enrico Mendes Saggioro. Effects of rare earth elements (REE) on terrestrial organisms: current status and future directions. *Ecotoxicology (London, England)*, 31(5):689–699, 2022.

[44] Kyung Taek Rim, Kwon Ho Koo, and Jung Sun Park. Toxicological evaluations of rare earths and their health impacts to workers: a literature review. *Safety and Health at Work*, 4(1):12–26, 2013.

[45] Doris Klingelhöfer, Markus Braun, Janis Dröge, Axel Fischer, Dörthe Brüggmann, and David A. Groneberg. Environmental and health-related research on application and production of rare earth elements under scrutiny. *Globalization and health*, 18(1):86, 2022.

[46] Luca Ciacci, E. M. Harper, N. T. Nassar, Barbara K. Reck, and T. E. Graedel. Metal Dissipation and Inefficient Recycling Intensify Climate Forcing. *Environmental science & technology*, 50(20):11394–11402, 2016.

[47] Zhenzhen Zhao, Shichao Feng, Chunyan Xiao, Jianquan Luo, Weijie Song, Yinhua Wan, and Shaohua Li. Exploring ions selectivity of nanofiltration membranes for rare earth wastewater treatment. *Separation and Purification Technology*, 289:120748, 2022.

[48] Li Chen, Yilin Wu, Hongjun Dong, Minjia Meng, Chunxiang Li, Yongsheng Yan, and Ji Chen. An overview on membrane strategies for rare earths extraction and separation. *Separation and Purification Technology*, 197:70–85, 2018.

[49] Vidya Dhar Pandey. Cyanobacteria-mediated heavy metal remediation. In *Agro-Environmental Sustainability*, pages 105–121. Springer, Cham, 2017.

[50] Meijun Yang, Xiaoliang Liang, Lingya Ma, Jian Huang, Hongping He, and Jianxi Zhu. Adsorption of REEs on kaolinite and halloysite: A link to the REE distribution on clays in the weathering crust of granite. *Chemical Geology*, 525:210–217, 2019.

[51] Fabian Pienkoß, Cristina Ochoa-Hernández, Nils Theyssen, and Walter Leitner. Kaolin: A Natural Low-Cost Material as Catalyst for Isomerization of Glucose to Fructose. *ACS Sustainable Chemistry & Engineering*, 6(7):8782–8789, 2018.

[52] Jorge C. Miranda-Trevino and Cynthia A. Coles. Kaolinite properties, structure and influence of metal retention on pH. *Applied Clay Science*, 23(1-4):133–139, 2003.

[53] Chi Ma and Richard A. Eggleton. Surface Layer Types of Kaolinite: A High-Resolution Transmission Electron Microscope Study. *Clays and Clay Minerals*, 47(2):181–191, 1999.

[54] R. B. Neder. Refinement of the Kaolinite Structure from Single-Crystal Synchrotron Data. *Clays and Clay Minerals*, 47(4):487–494, 1999.

[55] Ray L. Frost. Hydroxyl Deformation in Kaolins. *Clays and Clay Minerals*, 46(3):280–289, 1998.

[56] Christian Detellier. Functional Kaolinite. *Chemical record (New York, N.Y.)*, 18(7-8):868–877, 2018.

[57] Haydn H. Murray, editor. *Developments in Clay Science : Applied Clay Mineralogy*. Elsevier, 2006.

[58] Gustave Kenne Dedzo and Christian Detellier. Functional nanohybrid materials derived from kaolinite. *Applied Clay Science*, 130:33–39, 2016.

[59] Mahmoud E. Awad, Alberto López-Galindo, Massimo Setti, Mahmoud M. El-Rahmany, and César Viseras Iborra. Kaolinite in pharmaceutics and biomedicine. *International Journal of Pharmaceutics*, 533(1):34–48, 2017.

[60] César Viseras, Rita Sánchez-Espejo, Rosanna Palumbo, Ninfa Liccardi, Fátima García-Villén, Ana Borrego-Sánchez, Marina Massaro, Serena Riela, and Alberto López-Galindo. Clays in cosmetics and personal-care products. *Clays and Clay Minerals*, 69(5):561–575, 2021.

[61] Georgiana A. Moldoveanu and Vladimiros G. Papangelakis. Recovery of rare earth elements adsorbed on clay minerals: I. Desorption mechanism. *Hydrometallurgy*, 117-118:71–78, 2012.

[62] Brian J. Teppen and David M. Miller. Hydration Energy Determines Isovalent Cation Exchange Selectivity by Clay Minerals. *Soil Science Society of America Journal*, 70(1):31–40, 2006.

[63] J. L. Ferracane. Elution of leachable components from composites. *Journal of Oral Rehabilitation*, 21(4):441–452, 1994.

[64] Yukun HUANG, Ting'an ZHANG, Jiang LIU, Zhihe DOU, and Junhang TIAN. Decomposition of the mixed rare earth concentrate by microwave-assisted method. *Journal of Rare Earths*, 34(5):529–535, 2016.

[65] Carlos Ayora, Francisco Macías, Ester Torres, Alba Lozano, Sergio Carrero, José-Miguel Nieto, Rafael Pérez-López, Alejandro Fernández-Martínez, and Hiram Castillo-Michel. Recovery of rare earth elements and yttrium from passive-remediation systems of acid mine drainage. *Environmental science & technology*, 50(15):8255–8262, 2016.

[66] Xiuchuan Ran, Zijie Ren, Huimin Gao, Renji Zheng, and Junxun Jin. Kinetics of Rare Earth and Aluminum Leaching from Kaolin. *Minerals*, 7(9):152, 2017.

[67] M. Hermassi, M. Granados, C. Valderrama, N. Skoglund, C. Ayora, and J. L. Cortina. Impact of functional group types in ion exchange resins on rare earth element recovery from treated acid mine waters. *Journal of Cleaner Production*, 379:134742, 2022.

[68] Adam Jordens, Ying Ping Cheng, and Kristian E. Waters. A review of the beneficiation of rare earth element bearing minerals. *Minerals Engineering*, 41:97–114, 2013.

[69] Marcel Pourbaix. *Atlas of electrochemical equilibria in aqueous solutions*. National Association of Corrosion Engineers, Houston, Tex., 2d english ed. edition, 1974.

[70] Nilanjana Das and Devlina Das. Recovery of rare earth metals through biosorption: An overview. *Journal of Rare Earths*, 31(10):933–943, 2013.

[71] Kenneth N. Han, Jon J. Kellar, William M. Cross, and Sadegh Safarzadeh. Opportunities and challenges for treating rare-earth elements. *Geosystem Engineering*, 17(3):178–194, 2014.

[72] Georgiana A. Moldoveanu and Vladimiros G. Papangelakis. Recovery of rare earth elements adsorbed on clay minerals: II. Leaching with ammonium sulfate. *Hydrometallurgy*, 131-132:158–166, 2013.

[73] Xing-liang FENG, Zhi-qi LONG, Da-li CUI, Liang-shi WANG, Xiao-wei HUANG, and Guo-cheng ZHANG. Kinetics of rare earth leaching from roasted ore of bastnaesite with sulfuric acid. *Transactions of Nonferrous Metals Society of China*, 23(3):849–854, 2013.

[74] Walaa A. Kassab, Gawad, Ebrahim A.: Salah, Shimaa, and Salem Amany R. *Modeling and simulation studies for leaching of some valuable metals from Southwestern Sinai, Egypt.* ournal of Research in Environmental and Earth Sciences, 2023.

[75] Wei-Sheng Chen and Hsing-Jung Ho. Recovery of Valuable Metals from Lithium-Ion Batteries NMC Cathode Waste Materials by Hydrometallurgical Methods. *Metals*, 8(5):321, 2018.

[76] Xiaohong Zheng, Zewen Zhu, Xiao Lin, Yi Zhang, Yi He, Hongbin Cao, and Zhi Sun. A Mini-Review on Metal Recycling from Spent Lithium Ion Batteries. *Engineering*, 4(3):361–370, 2018.

[77] A. A. Nayl, R. A. Elkhashab, Sayed M. Badawy, and M. A. El-Khateeb. Acid leaching of mixed spent Li-ion batteries. *Arabian Journal of Chemistry*, 10:S3632–S3639, 2017.

[78] Xuejiao Zhou, Yongli Chen, Jianguo Yin, Wentang Xia, Xiaoli Yuan, and Xiaoyan Xiang. Leaching kinetics of cobalt from the scraps of spent aerospace magnetic materials. *Waste management (New York, N.Y.)*, 76:663–670, 2018.

[79] Manis Kumar Jha, Pankaj Kumar Choubey, Amrita Kumari Jha, Archana Kumari, Jae-chun Lee, Vinay Kumar, and Jinki Jeong. Leaching studies for tin recovery from waste e-scrap. *Waste management (New York, N.Y.)*, 32(10):1919–1925, 2012.

[80] Shuang Qiu, Chang Wei, Minting Li, Xuejiao Zhou, Chunxiong Li, and Zhigan Deng. Dissolution kinetics of vanadium trioxide at high pressure in sodium hydroxide–oxygen systems. *Hydrometallurgy*, 105(3-4):350–354, 2011.

[81] Wei Luo, Qiming Feng, Leming Ou, Guofan Zhang, and Yun Chen. Kinetics of saprolitic laterite leaching by sulphuric acid at atmospheric pressure. *Minerals Engineering*, 23(6):458–462, 2010.

[82] Xue BIAN, Shao-hua YIN, Yao LUO, and Wen-yuan WU. Leaching kinetics of bastnaesite concentrate in HCl solution. *Transactions of Nonferrous Metals Society of China*, 21(10):2306–2310, 2011.

[83] Thomas B. Reed. Induction-Coupled Plasma Torch. *Journal of Applied Physics*, 32(5):821–824, 1961.

[84] Sebastian Groh. *Absolute Elementbestimmung von Nanopartikeln durch ICP-Spektrometrie und Untersuchung der Plasma-Partikel-Wechselwirkung*. PhD thesis, Technische Universität Dortmund, 2012.

[85] Agilent Technologies. Dedicated axial or radial plasma view for superior speed and performance. Available at `https://www.agilent.com/cs/library/technicaloverviews/Public/5991-0842EN_TechOview_700_OneView.pdf`, 23.08.2023.

[86] Jeneé L. Jacobs. *Diagnostic studies of ion beam formation in inductively coupled plasma mass spectrometry with the collision reaction interface*. Iowa State University, 2015.

[87] J. Mostaghimi, P. Proulx, M. I. Boulos, and R. M. Barnes. Computer modeling of the emission patterns for a spectrochemical ICP. *Spectrochimica Acta Part B: Atomic Spectroscopy*, 40(1-2):153–166, 1985.

[88] Ali Ali Redha. Removal of heavy metals from aqueous media by biosorption. *Arab Journal of Basic and Applied Sciences*, 27(1):183–193, 2020.

[89] Ellen Cristine Giese. Biosorption as green technology for the recovery and separation of rare earth elements. *World Journal of Microbiology and Biotechnology*, 36(4):52, 2020.

[90] Muhammad Bilal, Tahir Rasheed, Juan Eduardo Sosa-Hernández, Ali Raza, Faran Nabeel, and Hafiz M. N. Iqbal. Biosorption: An interplay between marine algae and potentially toxic elements-a review. *Marine drugs*, 16(2), 2018.

[91] Wojciech Jurkowski, Michael Paper, and Thomas B. Brück. Isolation and Investigation of Natural Rare Earth Metal Chelating Agents From Calothrix brevissima - A Step Towards Unraveling the Mechanisms of Metal Biosorption. *Frontiers in bioengineering and biotechnology*, 10:833122, 2022.

[92] Arti Hansda, Vipin Kumar, and Anshumali. A comparative review towards potential of microbial cells for heavy metal removal with emphasis on biosorption and bioaccumulation. *World Journal of Microbiology and Biotechnology*, 32(10):170, 2016.

[93] B. Volesky. Biosorbents for metal recovery. *Trends in Biotechnology*, 5(4):96–101, 1987.

[94] Elisangela Heiderscheidt, Heini Postila, and Tiina Leiviskä. Removal of metals from wastewaters by mineral and biomass-based sorbents applied in continuous-flow continuous stirred tank reactors followed by sedimentation. *The Science of the total environment*, 700:135079, 2020.

[95] Edyta Kordialik-Bogacka. Surface properties of yeast cells during heavy metal biosorption. *Open Chemistry*, 9(2):348–351, 2011.

[96] Ahmed M. Yousif. Rapid and Selective Adsorption of Rh(III) from its Solutions Using Cellulose-Based Biosorbent Containing Iminodiacetate Functionality. *Separation Science and Technology*, 46(15):2341–2347, 2011.

[97] Abdolkarim Abbaspour, Masoud A. Mehrgardi, Abolhasan Noori, Mohammad Ali Kamyabi, Ali Khalafi-Nezhad, and Mohammad Navid Soltani Rad. Speciation of iron(II), iron(III) and full-range pH monitoring using paptode: A simple colorimetric method as an appropriate alternative for optodes. *Sensors and Actuators B: Chemical*, 113(2):857–865, 2006.

[98] Luísa P. Cruz-Lopes, Morgana Macena, Bruno Esteves, and Raquel P. F. Guiné. Ideal pH for the adsorption of metal ions Cr^{6+} , Ni^{2+} , Pb^{2+} in aqueous solution with different adsorbent materials. *Open Agriculture*, 6(1):115–123, 2021.

[99] E. Romera, F. González, A. Ballester, M. L. Blázquez, and J. A. Muñoz. Comparative study of biosorption of heavy metals using different types of algae. *Bioresource Technology*, 98(17):3344–3353, 2007.

[100] Aridane G. González, Oleg S. Pokrovsky, J. Magdalena Santana-Casiano, and Melchor González-Dávila. Bioadsorption of Heavy Metals. In Bhumi Nath Tripathi and Dhananjay Kumar, editors, *Prospects and challenges in algal biotechnology*, pages 233–255. Springer Nature Singapore, Singapore, 2017.

[101] S. Klimmek, H. J. Stan, A. Wilke, G. Bunke, and R. Buchholz. Comparative analysis of the biosorption of cadmium, lead, nickel, and zinc by algae. *Environmental science & technology*, 35(21):4283–4288, 2001.

[102] Emmanuel D. Revellame, Dhan Fortela, Wayne Sharp, Rafael Hernandez, and Mark E. Zappi. Adsorption kinetic modeling using pseudo-first order and pseudo-second order rate laws: A review. *Cleaner Engineering and Technology*, 1:100032, 2020.

[103] Courtie Mahamadi. On the dominance of Pb during competitive biosorption from multi-metal systems: A review. *Cogent Environmental Science*, 5(1):1635335, 2019.

[104] Ayla Ozer and Dursun Ozer. Comparative study of the biosorption of Pb(ii), Ni(ii) and Cr(vi) ions onto s. cerevisiae: determination of biosorption heats. *Journal of Hazardous Materials*, 100(1-3):219–229, 2003.

[105] Y. Sag and T. Kutsal. Determination of the biosorption heats of heavy metal ions on Zoogloea ramigera and Rhizopus arrhizus. *Biochemical Engineering Journal*, 6(2):145–151, 2000.

[106] Jianlong Wang and Can Chen. Biosorption of heavy metals by Saccharomyces cerevisiae: a review. *Biotechnology Advances*, 24(5):427–451, 2006.

[107] Yesim Sag and Tülin Kutsal. Recent trends in the biosorption of heavy metals: A review. *Biotechnology and Bioprocess Engineering*, 6(6):376–385, 2001.

[108] Y. Andrès, A. C. Texier, and P. Le Cloirec. Rare earth elements removal by microbial biosorption: a review. *Environmental Technology*, 24(11):1367–1375, 2003.

[109] Pablo H. Pacheco, Raúl A. Gil, Soledad E. Cerutti, Patricia Smichowski, and Luis D. Martinez. Biosorption: a new rise for elemental solid phase extraction methods. *Talanta*, 85(5):2290–2300, 2011.

[110] William D. Bonificio and David R. Clarke. Rare-earth separation using bacteria. *Environmental Science & Technology Letters*, 3(4):180–184, 2016.

[111] Andrea Engl and Benno Kunz. Biosorption of heavy metals by Saccharomyces cerevisiae : Effects of nutrient conditions. *Journal of Chemical Technology & Biotechnology*, 63(3):257–261, 1995.

[112] Andres Abin-Bazaine, Alfredo Campos Trujillo, and Mario Olmos-Marquez. Adsorption Isotherms: Enlightenment of the Phenomenon of Adsorption. In *Wastewater Treatment*. IntechOpen, 2022.

[113] Dada A.O. Langmuir, Freundlich, Temkin and Dubinin–Radushkevich Isotherms Studies of Equilibrium Sorption of Zn^{2+} Unto Phosphoric Acid Modified Rice Husk. *IOSR Journal of Applied Chemistry*, 3(1):38–45, 2012.

[114] Christian Schulz, Tjasa Kumelj, Emil Karlsen, and Eivind Almaas. Genome-scale metabolic modelling when changes in environmental conditions affect biomass composition. *PLoS computational biology*, 17(5):e1008528, 2021.

[115] Qiang Hu. Environmental effects on cell composition. In Richmond, editor, *Handbook of Microalgal Culture*, pages 114–122. John Wiley & Sons, 2013.

[116] Robinson Soto-Ramírez, Maria-Gabriela Lobos, Olivia Córdova, Paola Poirrier, and Rolando Chamy. Effect of growth conditions on cell wall composition and cadmium adsorption in chlorella vulgaris: A new approach to biosorption research. *Journal of Hazardous Materials*, 411:125059, 2021.

[117] Gwonho Joo, Wooram Lee, and Yongju Choi. Heavy metal adsorption capacity of powdered chlorella vulgaris biosorbent: effect of chemical modification and growth media. *Environmental Science and Pollution Research*, 28(20):25390–25399, 2021.

[118] Zhipeng Duan, Xiao Tan, Lin Shi, Qingfei Zeng, Imran Ali, Rui Zhu, Huaimin Chen, and Keshab Parajuli. Phosphorus Accumulation in Extracellular Polymeric Substances (EPS) of Colony-Forming Cyanobacteria Challenges Imbalanced Nutrient Reduction Strategies in Eutrophic Lakes. *Environmental science & technology*, 57(4):1600–1612, 2023.

[119] Sara Pereira, Andrea Zille, Ernesto Micheletti, Pedro Moradas-Ferreira, Roberto de Philippis, and Paula Tamagnini. Complexity of cyanobacterial exopolysaccharides: composition, structures, inducing factors and putative genes involved in their biosynthesis and assembly. *FEMS microbiology reviews*, 33(5):917–941, 2009.

[120] Donna R. Hill, Thomas W. Keenan, Richard F. Helm, Malcolm Potts, Lois M. Crowe, and John H. Crowe. Extracellular polysaccharide of Nostoc commune (Cyanobacteria) inhibits fusion of membrane vesicles during desiccation. *Journal of Applied Phycology*, 9(3):237–248, 1997.

[121] R. Y. Stanier, R. Kunisawa, M. Mandel, and G. Cohen-Bazire. Purification and properties of unicellular blue-green algae (order Chroococcales). *Bacteriological Reviews*, 35(2):171–205, 1971.

[122] Robert A. Andersen. *Algal culturing techniques*. Elsevier Academic Press, Burlington, MA, 2005.

[123] Václav Petříček, Michal Dušek, and Lukáš Palatinus. Crystallographic Computing System JANA2006: General features. *Zeitschrift für Kristallographie - Crystalline Materials*, 229(5):345–352, 2014.

[124] Sytle M. Antao. Quartz: structural and thermodynamic analyses across the $\alpha \leftrightarrow \beta$ transition with origin of negative thermal expansion (NTE) in β quartz and calcite. *Acta Crystallographica Section B: Structural Science, Crystal Engineering and Materials*, 72(Pt 2):249–262, 2016.

[125] Hsin-Yi Tseng, PeterJ. Heaney, and T. C. Onstott. Characterization of lattice strain induced by neutron irradiation. *Physics and Chemistry of Minerals*, 22(6):399–405, 1995.

[126] K. Ishida and F. C. Hawthorne. Far-infrared spectra of synthetic dioctahedral muscovite and muscovite-tobelite series micas: Characterization and assignment of the interlayer I-Oinner and I-Oouter stretching bands. *American Mineralogist*, 98(10):1848–1859, 2013.

[127] T. J. Dzikowski, L. A. Groat, and J. L. Jambor. The symmetry and crystal structure of gorceixite, $BaAl_3[PO_3(O,OH)]_2(OH)_6$, a member of the alunite supergroup. *The Canadian Mineralogist*, 44(4):951–958, 2006.

[128] Marcus Heilmann Wojciech Jurkowski, Rainer Buchholz Thomas Brueck, and Anna Maria Becker. Biosorption of Neodymium by Selected Photoautotrophic and Heterotrophic Species. *Journal of Chemical Engineering & Process Technology*, 06(04), 2015.

[129] Marcus Heilmann, Roman Breiter, and Anna Maria Becker. Towards rare earth element recovery from wastewaters: biosorption using phototrophic organisms. *Applied Microbiology and Biotechnology*, 105(12):5229–5239, 2021.

[130] Cristian Tunsu, Martina Petranikova, Marino Gergorić, Christian Ekberg, and Teodora Retegan. Reclaiming rare earth elements from end-of-life products: A review of the perspectives for urban mining using hydrometallurgical unit operations. *Hydrometallurgy*, 156:239–258, 2015.

[131] Giorgos Markou, Dimitris Mitrogiannis, Abuzer Çelekli, Hüseyin Bozkurt, Dimitris Georgakakis, and Constantinos V. Chrysikopoulos. Biosorption of Cu^{2+} and Ni^{2+} by Arthrospira platensis with different biochemical compositions. *Chemical Engineering Journal*, 259:806–813, 2015.